Centre for Geo-Information

Thesis Report GIRS-2013-07

A MULTI-SENSOR ANALYSIS OF VEGETATION INDICES FOR LEAF AREA INDEX RETRIEVAL IN PRECISION AGRICULTURE

Asefa Areda

April 2013

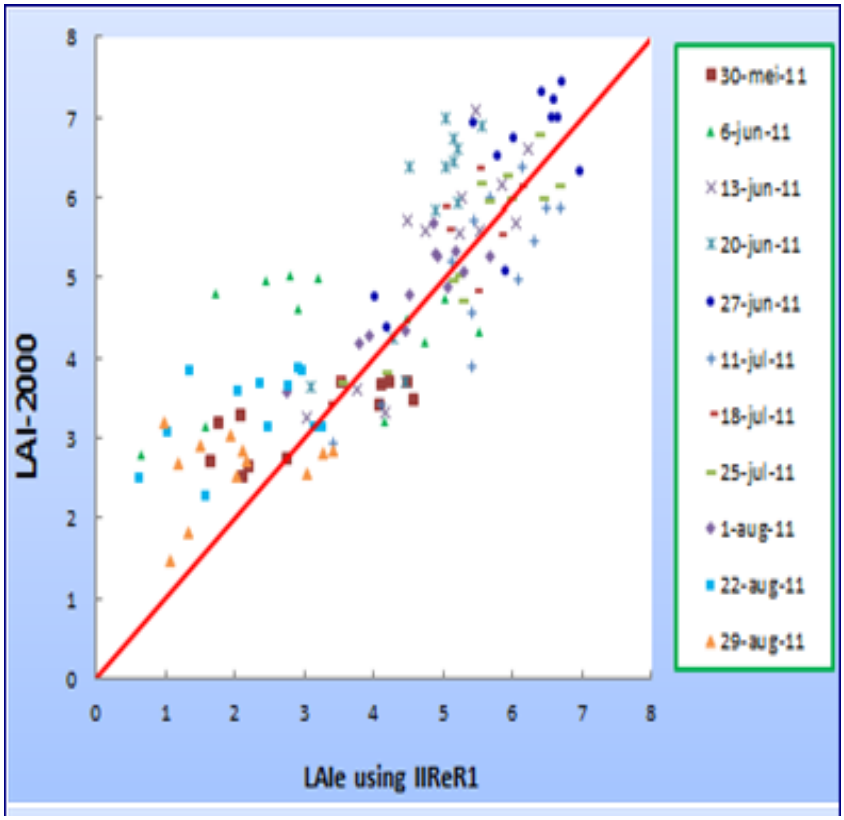

WAGENINGEN UNIVERSITY
WAGENINGEN UR

A MULTI-SENSOR ANALYSIS OF VEGETATION INDICES FOR LEAF AREA INDEX RETRIEVAL IN PRECISION AGRICULTURE

Asefa Teferi Areda

Registration number: 82 01 05 017 030

Supervisors:

Dr. ir. Jan Clevers
Dr. ir. Lammert Kooistra

A thesis submitted in partial fulfillment of the degree of Master of Science at
Wageningen University and Research Centre,
The Netherlands

April 2013
Wageningen, the Netherlands

Thesis code number: GRS-80436
Thesis Report: GIRS-2013-07
Wageningen University and Research Centre
Laboratory of Geo-Information Science and Remote Sensing

Foreword

This research work has given me valuable knowledge and understanding about the subject matter. It also enabled me to gain useful skills in dealing with huge datasets and its subsequent analysis. At the very inception of the research idea, I thought that the research topic was too narrow in scope to tackle for MSc thesis. In due course of time I, together with my supervisors, discovered a lot of possibilities to be investigated as part of my research work. There comes the idea of tackling the entire research undertaking in two phases which I would say broadened my perspectives. Eventually, although it started with the analysis of SVIs for LAI retrieval based on multi-sensor data, I investigated possibilities for improving the existing SVIs by devising new indices. Moreover, I had to work with different statistical methods assisted by different software packages mainly for performing the sensitivity analysis which all positively affected my capabilities. Nevertheless, I also have to admit that I had difficult moments owing to my personal and family situations which have made the entire undertaking of this MSc research as well as the whole MSc programme much tougher than it would have been otherwise. Finally, I am very pleased with the results and having seen the final product, I am convinced that I can always materialize my own ideas.

Acknowledgements

Prior to all, thanks to the almighty God for His unspeakable help to overcome all the challenges. The successful completion of this research manuscript would not be a reality without the contribution of many people behind it. I would not imagine being here to pursue my studies in my field of interest without Nuffic scholarship. I am therefore very grateful to the government of the Netherlands for giving me this novel opportunity towards the fulfilment of my dreams. The support and encouragement I have received from my MSc Thesis supervisors was beyond imagination. My deepest gratitude therefore goes to my academic supervisors Dr. Ir. Jan Clevers and Dr. Ir. Lammert Kooistra for their invaluable support and comfortable guidance through the entire undertaking. They have always been on board to help me with any difficulties. Their support was never bounded even to the working week days and hours as I often get feedbacks from Lammert Kooistra even on the weekends. It has always been a surprise to me when I think of their commitment as they often approach me to ask on my progresses regularly. So, they were really caring and encouraging since the very date we met to discuss on the inception of the research idea. Their great personalities have affected me positively in many ways beyond the critical thinking in research. I wish to thank all the MGI staffs for equipping me with a lot of knowledge and skills in the field. Their great lectures and well organized instructions in every course have given me the courage and passion to quickly take-off with this new discipline as I lacked the experience at the start.

In addition, I am very grateful to my parents, who though uneducated, sent me to school from a rural village where chances for attending schools was rare at least by then. Even today, by the time they deserves my support, are supporting and encouraging me in all walks of my life. My special thanks also go to my wife, Tigist Shiferaw, for her understanding and encouragement throughout the study period.

Finally, I take this opportunity to thank all my MGI fellow students for the great moments we shared while studying together as well as for the friendly atmosphere I ever had as a student.

To my little hero, Moybon Asefa

Abstract

Precision agriculture (PA), a site specific timely intervention, has seen a growing importance over the past few years with widening practical application of remote sensing. This can mainly be attributed to advances in sensor technologies approaching the required temporal, spectral as well as spatial resolutions. PA could be implemented through the monitoring of crop biophysical and biochemical parameters. Leaf Area Index (LAI) is one of the key biophysical parameters for monitoring the crop condition. Although the use of spectral vegetation indices (SVIs) has been a common retrieval method for crucial information on crop condition from the huge stream of remote sensing data, the use of those indices has been constrained either by their lack of sensitivity to LAI or sensitivity to leaf, soil and canopy parameters. The objective of this research was therefore to explore the possibility to improve the sensitivity of SVIs using Radiative Transfer Modelling and assessing the performance of the existing SVIs across broad and narrow band sensors thereby evaluating the performance of European Space Agency (ESA's) upcoming multispectral space systems like Sentinel-2 (S-2) and VENµS. Another aim of the study was performing SVIs sensitivity analysis with varying leaf, soil and canopy parameters using a sensitivity function (*S*) and finally with different management practices and crop phenologies based on empirical data. To this end, PROSAIL model based simulated data as well as empirical field data measured for a potato (*Solanum tuberosum L.*) crop using a Cropscan MSR16R radiometer and LAI-2000 for the 2011 and 2012 growing seasons were used. In addition, a hyperspectral airborne prism experiment (APEX) image acquired on 27 June 2011 was used for evaluating the SVIs for image level application across multiple sensors. The sensitivity of each spectral region to LAI was assessed to explore possibilities for improving the sensitivity of SVIs by devising new indices. Based on the result obtained, the shortwave infrared (SWIR) bands followed by Red-edge showed better sensitivity to LAI for different soil moisture levels than the red bands. This implies that the former two spectral regions can provide complementary information for the improvement of NIR based SVI-LAI relationships. The evaluation of SVIs showed consistent performance across broad bands of TM and narrow bands of MSR16R, APEX, S-2 and VENµS. It was found that most of the considered SVIs showed high sensitivity to leaf chlorophyll concentration (C_{ab}) levels and leaf angle distributions (LADs). However, the SVIs showed less sensitivity to canopy background effects as simulated by the varying soil moisture levels. The use of the sensitivity function also showed a similar pattern for greenness indices such as the normalized difference vegetation index (NDVI), NDII, NDRE and ISR with a high sensitivity at low LAI (LAI < 3). On the other hand, Simple Ratio (SR) and Integrated Infrared Red edge Ratio ($IIReR_1$and $IIReR_2$) showed high sensitivity at higher vegetation densities. It was also found that the sensitivity function could not maintain consistent performance for all the SVIs as seen from their sensitivity record and the coefficient of determination (R^2) and root mean square error (RMSE) values. The validation of the SVI-LAI relationship also confirmed that $IIReR_1$, $IIReR_2$ and SR were among the most suitable indices for LAI prediction based on both the PROSAIL and empirical field data. The validation based on empirical data obtained for a potato field with MSR16R also confirmed superior performance for $IIReR_1$ (R^2 = 0.81) and SR (R^2= 0.79). Furthermore, the SVIs revealed consistent performance based on the validation using the APEX image with IIReR1, SR and WDVI being among the best predictors of LAI (all R^2=0.86). The performance of those SVIs, however, did not show consistency for the 2011 and 2012 growing seasons where many of the SVIs had inferior performance for the 2012 growing season. Exception to these include the SWIR based indices, NDII and ISR, which either maintained the same level of performance or showed improvement over the 2011 site. Hence, the choice of an index for crop monitoring in precision agriculture could be specific to site and crop conditions.

Keywords: Precision agriculture, Spectral vegetation indices, PROSAIL Model, Sensitivity, Leaf area index

Table of contents

List of Figures

List of Tables

Acronyms

ANOVA	Analysis of variance
APEX	Airborne Prism Experiment
EVI	Enhanced Vegetation Index
IIReR	Integrated Infrared Red-edge Ratio
ISR	Infrared Simple Ratio
LADs	Leaf Angle Distributions
LAI	Leaf Area Index
LSD	Least Significant Difference
MSR	Modified Simple Ratio
MSR16R	Multispectral 16 bands Radiometer
NDII	Normalized Difference Infrared Index
NDRE	Normalized Difference Red edge
NDVI	Normalized Difference Vegetation Index
S-2	Sentinel-2
SR	Simple Ratio
SVIs	Spectral vegetation indices
SWIR	Short wave infrared ratio
VENμS	Vegetation and Environmental New micro Spacecraft
WDVI	Weighted Difference Vegetation Index

CHAPTER ONE: INTRODUCTION

1.1 Background

The advancement in sensor technologies over the last decades has led to the application of near real time information to enhance farm management practices (Schellberg, Hill et al. 2008). This has resulted in a move towards unlocking the potentials of sensor technologies to enhance farming practices in precision agriculture (PA). The development of airborne and space borne satellites for remote sensing of land surface features in the 1960s and 70s was in use for crop biomass and soil sensing based on spectral analysis (Cox 2002). Over the years, different remote sensing models have been developed (Beeri and Peled 2009) to map vegetation factors that affect agricultural field crop monitoring such as water stress, nitrogen content, biomass, diseases, etc.

The factual basis of precision agriculture, which is the spatial and temporal variability of soil and crop factors within a field, has been appreciated for a few decades (Zhang, Wang et al. 2002) which allowed farmers to vary treatments manually. According to Seelan, Laguette et al. (2003) precision agriculture is a production system that promotes variable management practices within a field depending on site conditions. This implies PA being treated as system approach to re-organize the total system of agriculture towards a low-input, high-efficiency, sustainable agriculture. This approach depends on the use of efficient amount of data derived from several technologies. Agricultural industry is now capable of gathering more comprehensive data on production variability in both space and time although methods and tools for analysis remain limited. The desire to respond to such variability on a fine-scale has become the goal of PA. According to Zhang, Wang et al. (2002) United States of America, Canada and Western Europe have been pioneers in initiating PA research in the 1980s though its application was mainly focused on the utilization of existing farm machineries. Nowadays the trend is towards operational application due to standard availability of GPS tracking fitted on tractors as well as advancing sensor technologies and lowering costs of sensors and equipment and product-services.

Of the different biochemical and biophysical parameters of vegetation, the Leaf Area Index (LAI) is an important characteristic of vegetation canopies. LAI can be defined as a dimensionless ratio between the total one side leaf surface of a plant and the surface area of the land on which the plant grows (Wu, Niu et al. 2008; Zheng and Moskal 2009; Herrmann, Karnieli et al. 2010). This biophysical parameter is used to quantitatively characterize the radiation regime within and under the canopy, and simulates leaf controlled ecological processes (Zheng and Moskal 2009). As such LAI is directly linked to production and the accurate measurement of it is essential for monitoring crop growth (Xiao, Liang et al. 2011), ecosystem carbon fluxes and ecosystem changes (Canisius, Fernandes et al. 2010; Brantley, Zinnert et al. 2011). It is also an essential parameter to describe the geometric structure of plant canopies and an important input parameter for modelling earth-atmosphere interaction (Xu, Fan et al. 2009). LAI is also a variable of primary importance for crop monitoring though it is often measured with labour intensive destructive methods (Stroppiana, Boschetti et al. 2006). This direct measurement of LAI is however not only labour intensive but also virtually impractical at larger scales (Brantley, Zinnert et al. 2011) and is often unfeasible for remote locations. To overcome this an integrative use of remote sensing techniques could be used as it is able to provide spatially and temporally distributed information on vegetation cover as well as on state variables such as biomass and LAI (Dente, Satalino et al. 2008).

1.2 Problem definition

A variety of vegetation indices have been used to retrieve leaf characteristics from the complex vegetation spectra as a function of a multitude of parameters (Baret and Guyot 1991; Haboudane, Miller et al. 2002; Ji and Peters 2007; Clevers and Kooistra 2012; Gonsamo and Pellikka 2012). Currently, a variety of techniques has been used for the detection of early-stage vegetation stress in multispectral airborne and satellite imagery (Clevers and Kooistra 2012). These techniques include a number of different spectral vegetation indices (SVIs), "red edge" detection techniques, band absorption analysis, spectral mixture analysis, wavelet transform and neural networks (Shafri, Salleh et al. 2006). However, the widely used broad band vegetation indices such as NDVI, which is widely used to characterize vegetation growth and leaf area index, suffer from quick saturation effect. The saturation effect limits the power of existing indices with a slight increase in leaf chlorophyll and LAI particularly in dense vegetation.

Moreover, attempts to fine tune the existing SVIs has been constrained by the spectral band settings as well as the spectral, spatial and/or temporal resolutions of the existing operational satellites. For instance, more recently the application of remote sensing for precision agriculture has shown progress as it relies on the high spatial resolution of operational satellites, namely Ikonos, QuickBird, RapidEye, GeoEye, Worldview-2 etc., among others. However, their spectral ability, being characterized by a small number of broad spectral bands in the visible and Near Infrared (NIR) bands, is limited to broad band vegetation indices (Herrmann, Karnieli et al. 2010). On the other hand high spectral resolution systems such as MERIS are also constrained by its coarser spatial resolution of 300m at best making it hardly suitable for most applications related to precision agriculture.

Nevertheless, several methods are employed to estimate LAI from the available remote sensing data mainly by utilizing the statistical relationship between LAI and spectral vegetation indices (SVIs) (Wang, Huang et al. 2007). Those vegetation indices have been developed to estimate plant biophysical parameters using remote sensing images and many of these were designed mainly with efforts to reduce interference from canopy background (Wang, Huang et al. 2007; Zhao, Yang et al. 2012). However, the relationship between LAI and SVIs is affected by several factors such as soil background reflectance, leaf angle distribution (LAD) and aggregation of leaf elements, and difference in chlorophyll concentrations among others. Furthermore, only few studies have examined those effects on the estimation of leaf area index (LAI) using remote sensing techniques for crops in general and potato in particular. Such background effects as well as canopy specific features need to be identified by integrating the empirical remote sensing data with situations on the ground that is typical to specific arable crops such as potato.

Remote sensing of vegetation characteristics has used these indices to determine various plant parameters such as LAI, leaf chlorophyll, biomass and ground cover (Hatfield and Prueger 2010). LAI is widely used in production ecology as a measure of crop growth. However, the measure of crop parameters such as LAI is affected by several disturbances. Several studies conducted to predict LAI focused either on establishing a statistical relationship between LAI and SVIs or using bidirectional reflectance distribution function (BRDF) (Wang, Huang et al. 2007). However, many of these vegetation indices are computed by averaging the spectral values over broad bands which might underestimate the typical crop spectral characteristics. The application of such relationship is not only sensor and crop specific but also insensitive after moderately high LAI values. Most SVIs such as NDVI, though widely used, are insensitive to higher LAI values which limit their application for precision agriculture apart

from ecological level inventories such as biomass estimation and detecting vegetation phenologies.

Contrary to the limitations of broad band based vegetation indices, the application of narrow bands around the red edge and red-edge inflection point for characterizing plant bio-chemical and biophysical parameters (Gitelson and Merzlyak 2003; Clevers and Kooistra 2012; Zhao, Yang et al. 2012) showed better results. This region of the electromagnetic spectrum as a transition between the visible and NIR bands shifts towards shorter wavelength as the vegetation comes under stress (Clevers and Kooistra 2012). Many studies are, however, not only limited to the use of vegetation indices derived over several bands from the massive spectrum for the characterization of canopy parameters but also limited to the use of statistical techniques such as regression analysis. This technique does not only suffer from the effect of multicollinearity (Darvishzadeh, Skidmore et al. 2008) but also ends up with an aggregate single value lacking the capacity to characterize the sensitivities of SVIs across the LAI ranges (Ji and Peters 2007). Meanwhile, the evolution of next generation satellites, namely Sentinel-2 and Vegetation and Environmental New Micro Spacecraft (VENμS) as well as the European Airborne Prism Experiment (APEX) with additional bands in the red-edge region of the spectrum is expected to have added values. These upcoming super-spectral space borne systems as well as the airborne APEX sensor need to be evaluated using physically based radiative transfer based models such as the PRO-SAIL model.

For these reasons this study analysed SVIs based on broad and narrow spectral band data (both empirical and physically-based) acquired with different sensors with the intention to explore methods for better prediction of key canopy parameters such as LAI for the potato crop with a possibility of upscaling the methods to other potential application areas. Therefore, further studies on the comparison as well as integration of different sensing techniques was required for better estimation of LAI to support PA. In addition, the upcoming next generation of satellites were also evaluated for their added values in this aspect. Moreover, this study proposed new SVIs, the performance of which was evaluated for LAI retrieval based on the band settings of those sensors. Finally, selected SVIs and the newly proposed ones were tested for their sensitivities to LAI and disturbances such as soil background effects, management practices and crop phenology to allow for adjustments to minimize such effects.

1.3 Objectives

The general objective of the study was to evaluate the performance of different SVIs across multiple sensors for LAI retrieval for agricultural crops with focus on potato.

This study intended to address the following specific objectives:

a) To explore the possibilities for improved LAI prediction by devising new SVIs.
b) To assess the suitability of different vegetation indices across different sensors (broad vs. narrow bands) for estimation of canopy bio-physical parameters such as LAI.
c) To analyse the sensitivity of SVIs to LAI under different leaf, soil and canopy parameters based on PROSAIL model.
d) To evaluate the performance of SVIs for LAI prediction under different management practices, crop phenology and soil background effects using empirical field data and APEX imagery.

1.4 Research questions

In order to achieve the above mentioned research objectives the study attempted to answer the following research questions.

a. What possibilities are there to improve the sensitivity of SVIs to LAI by devising new indices?
b. Which vegetation indices are suitable for LAI retrieval for a potato crop?
c. Do SVIs yield comparable prediction power across broad and narrow band sensors?
d. Could a sensitivity function be used to evaluate the suitability of SVIs for LAI mapping for arable crops?
e. Do SVIs yield comparable performance based on empirical data with different management practices and crop phenologies?

1.5 Set-up of the Report

This thesis report is organized in six chapters including this first chapter where the general background, problem statement, research objectives and research questions are presented while chapter two covers the review of literature related to the subject of this study. The third chapter addresses the materials and methods part which starts with the description of the study area; the data used; sensors analysed; and the pre-processing and data analysis methods employed at each stage of the analysis. The fourth chapter presents the results part. In this section the results on the SVI-LAI relationships based on both broad and narrow band sensors are presented using both the PROSAIL and empirical field data as well as APEX imagery. This section also covers the results of a sensitivity analysis as well as results on the validation of the SVI-LAI relationships. The last two chapters, chapter five and six discuss the results and draw concluding remarks, in that order.

CHAPTER TWO: LITERATURE REVIEW

2.1 Precision Agriculture: An Overview

Throughout the evolution of remote sensing several models have been developed for agricultural applications. These models have been developed with different purposes such as explaining the variability of crop yield as a function of physical factors such as topography, soil (Bishop and McBratney 2002) or meteorological data (Herrmann, Karnieli et al. 2010). There are also remote sensing models designed to map vegetation factors such as water stress, nitrogen, diseases and weeds.

From the precision agriculture perspectives, the role of remote sensing should go beyond mapping the crop parameters across different physical settings and crop factors to assist in site specific decision making at the right time. In this regard, there are some models that enable decision making based on soil component mapping (Palacios-Orueta and Ustin 1998; López-Granados, Jurado-Expósito et al. 2005) and the concept of management zones (Moreenthaler, Khatib et al. 2003). Such models, however, fail to provide the necessary information continuously over the growing season. As a result, the promise of precision agriculture is compromised.

The essence of precision agriculture is that it requires the integration of remote sensing into the monitoring and decision making process by shortening the time spent between data collection and decision making (Beeri and Peled 2009). According to Cox (2002) methods have been developed for the application of information to a broad range of decision making in agricultural production as well as extending our ability to control operations automatically. He grouped such techniques under precision agriculture or precision farming which include applications to livestock production as well as the spatially variable field operations aided by sensor technologies. Advances in the information technology has led to wider applications to precision farming, which is sustainable, environmentally sound and responsive to the welfare and safety needs of people and animals (Cox 2002). Moreenthaler et al. (2003) and Bishop and McBratney (2002) considered precision agriculture as a farming methodology that applies nutrients and moisture only where and when they are needed in the field. The rationale of precision farming is to increase farm profitability by identifying the additional treatments of chemical and water that increase revenues more than they increase costs and do not exceed pollution standards, i.e., constrained optimization.

Nevertheless, the growth of precision agriculture over the years has been below what most envisioned (Moreenthaler, Khatib et al. 2003; Seelan, Laguette et al. 2003; McBratney, Whelan et al. 2005) although the technology for successful remote sensing sensors as well as precision variable dispensing systems using GPS are now available and affordable. On the contrary, (Seelan, Laguette et al. 2003) mentioned that remote sensing has been widely used for large scale crop inventory though it has not made significant inroads to precision agriculture. The latter saw stunted progress because the application of remote sensing for PA was constrained mainly as: remote sensing is relatively new concept; precision farming requires frequent monitoring of crops at high spatial and temporal resolutions; sub optimality of existing satellites for PA; farmers as well as crop consultants and extension agents' lack of familiarity with imagery unlike the end users of large scale crop inventory. This is attributed mainly to the missing of a constrained optimization model which combines information from remote sensing and in-situ measurements with the farmer's tacit knowledge and experience of the farm.

2.2 Sensing techniques and data acquisition

2.2.1 Remote sensing and close-range sensing

The development of airborne and space borne systems for remote sensing of land surface features in the 1960s added a new edge to the well-established already functioning range of instruments for measuring variables. Since the 1970s a well-known Landsat series of satellites followed by other space borne platforms has been in use for biomass estimation and crop as well as soil moisture sensing (Cox 2002). With the improvement in sensors it has become possible to gather detailed information from the reflected spectra. Fast digital processing of the outputs coupled with data fusion techniques made it possible to produce powerful thematic mapping presentations (Cox 2002).

Moreover, Cox (2002) presented various applications of active sensors such as airborne laser-based systems (LIDAR) when combined with multi-spectral sensors operating in the visible and NIR bands can provide detailed three-dimensional information on ground cover. Furthermore, it can also simulate fluorescence which allows for the monitoring of plant condition. These days the monitoring of vegetation variables for different crops using SVIs is based on several high spatial resolution satellites such as Ikonos, QuickBird, RapidEye, and GeoEye with limited broad spectral bands in the visible and NIR bands (Herrmann, Karnieli et al. 2010). The limited spectral ability of these sensors is limited to broad band based SVIs and hence not suitable for PA. On the other hand, the super spectral space borne system, MERIS, has 15 bands within the VIS and NIR with programmable band widths ranging between 2.3nm and 30nm. The suitability of MERIS for most precision agricultural practices is however compromised by its coarse spatial resolution of 300m.

The European Space Agency's (ESA) next generation of super spectral satellites are marking the future of remote sensing with better prospects for its application in the field of precision agriculture. These space borne systems include Sentinel-2 and the Vegetation and Environmental New micro Space Craft (VENµS) space borne systems expected to be operational in 2014 (Herrmann, Karnieli et al. 2010; Clevers and Gitelson 2013). Sentinel-2 is aiming to serve missions related to environmental applications. The four red edge bands centred at 665, 705, 740, and 775nm with band widths of 30, 15, 15, and 20nm with the corresponding spatial resolution of 10 and 20m might give it an edge over the other operational sensors in precision agriculture.

VENµS, another super spectral space borne system, as its name indicates is meant for vegetation monitoring. It has characteristic features of high spatial (5.3m), spectral (with 12 bands in the VIS-NIR range) and temporal (a revisit time of two days with the same viewing angle) resolutions. Moreover, four of those bands are positioned across the red-edge at 667, 702, 742 and 782 nm with band widths of 30, 24, 16 and 16 nm in the same order. The system is flying in a near polar sun-synchronous orbit at an elevation of 720 km acquiring images across a swath of 27km. These unique combinations of capabilities of the upcoming ESA's space borne systems seem to be a significant contribution towards enhancing the application of remote sensing in precision agriculture.

Moreover, the revolution in the field of PA seems to be mainly driven by the integration of a range of close or in-situ sensing techniques with remote sensing data at broader scale. The use of global navigation satellite systems (GNSS), tractor based near sensing and in-situ wireless sensor networks provides a wealth of data while enhancing the subsequent benefit through improved efficiency which in fact demands the integration of the different streams of spectral data (Kooistra, Beza et al., 2012).

2.2.2 Empirical vs. physical approaches

Estimation of important crop parameters such as LAI using remote sensing techniques can be done based on two main approaches: empirical and physical (Darvishzadeh, Skidmore et al. 2008; Richter, Atzberger et al. 2009). The empirical approach involves the direct ground-based measurement which is however not only time consuming and costly but also constrained both spatially and temporally (Richter, Atzberger et al. 2009). Remote sensing data have been recognized as a remedy to those problems of traditional empirical methods and several studies have been carried out on the retrieval of vegetation and surface parameters using multi spectral as well as the newly developed hyper spectral VIs (Clevers and van Leeuwen 1996; Haboudane, Miller et al. 2002; Shafri, Salleh et al. 2006; Darvishzadeh, Skidmore et al. 2008; Darvishzadeh, Atzberger et al. 2009). This method uses statistical techniques to obtain a correlation between in situ measured crop parameter and spectral vegetation indices (Darvishzadeh, Skidmore et al. 2008). The derived relationships stands high chance of being sensor specific as well as dependent on site conditions and the employed sampling technique (Houborg and Boegh 2008). Yet, in situ calibration datasets need to be collected bearing high cost and labour-intensive measurement campaign to ensure that the different species, canopy conditions and view-sun constellations are taken care of (Richter, Atzberger et al. 2009).

These challenges have led several studies to use a more complex physically based approach of parameter estimation by means of radiative transfer modelling (RTM) (Jacquemoud and Baret 1990; Jacquemoud, Baret et al. 1995; Jacquemoud, Bacour et al. 2000; Herrmann, Pimstein et al. 2011). This approach assumes that the RTM accurately describes the spectral variation of canopy reflectance as a function of canopy, leaf and soil background characteristics, based on physical laws (Darvishzadeh, Skidmore et al. 2008). The RTM approach, apart from using the full spectrum acquired by hyper spectral sensors as opposed to the limited band usage by SVIs, also considers the directional signatures from multi-angle sensors (Richter, Atzberger et al. 2009). Nevertheless, the RTM has some limitations due to requirements for an extensive parameterization and high computational demand as well as the simplicity of some models which fail to suit complex canopies such as row crops (Yao, Liu et al. 2008). The model inversion involves determination of those parameters that minimize the difference between the measured and simulated spectra. Such an approach has been widely applied in remote sensing to infer properties of the atmosphere and targets on the ground such as soil, vegetation, or water areas (Jacquemoud, Baret et al. 1995).

2.3 An overview of next generation hyperspectral sensors: S-2 and VENµS

Among the European Space Agency's (ESA's) future space systems are Sentinel-2 and VENµS. The upcoming Sentinel-2 to be launched in 2014 includes a total of 13 bands from which the 4 red edge bands centred around 665, 705, 740 and 775 nm with spectral bandwidth varying between 15 and 30 nm and spatial resolution of 10, 20, 20, and 20 m, respectively (Clevers and Gitelson 2013). The spatial resolution of Sentinel which is 10 m at its best, however, is not large enough for precision agriculture depending on the monitoring purpose. The Vegetation and Environmental New micro Spacecraft (VENµS) represents another super spectral satellite characterized by high spatial, spectral and temporal resolutions. It also has 4 bands along the red-edge centred at 667, 702, 742, and 782 nm with spectral band widths of 30, 24, 16 and 16 m and spatial resolutions of 30, 24, 16 and 16, respectively (Herrmann, Karnieli et al. 2010). The added value of the narrowly positioned red-edge bands of the upcoming space systems should be evaluated against existing sensors regarding its performance in supporting PA in the years to come.

In addition, the Airborne Prism Experiment (APEX) imaging spectrometer developed by a Swiss-Belgian consortium on behalf of ESA constitutes a revolution to extending the scope of conventional remote sensing. This sensor is a dispersive push broom intended as a simulator, calibration and validation device for future spaceborne hyperspectral imagers recording hyperspectral data across 300 bands in the wavelength range between 400 nm and 2500 nm. The spectral band settings of the APEX sensor are believed to render opportunities for more precise identification of surface materials which is hardly possible with the conventional broadband multispectral sensors *(http://www.apex-esa.org/content/apex)*. The spatial resolution of this airborne sensor being as high as 2 m to 5 m makes the device particularly suitable for PA as well.

Contrary to the narrow band sensors, the Landsat Thematic Mapper (TM) is used as reference for broad band sensors as its band widths extend across wider ranges compared to the narrow bands of the upcoming ESA's space borne systems and APEX. The narrow spectral resolutions of the APEX bands offer opportunities to mimic the spectral settings of other systems such as S-2, VENμS and obviously that of Landsat TM. The detailed information on the spectral band settings of the different sensors analysed in this study will be provided in the methods section.

Some of the selected spectral bands were specifically meant for particular purposes of crop monitoring as the maximum chlorophyll absorption (665 nm), position of Red-edge (705 and 740 nm), LAI edge of NIR plateau (775 nm), LAI (842 nm) and NIR plateau being sensitive to total biomass and LAI as well as water vapour (865 nm) are centred at those bands (Richter, Atzberger et al. 2009). The integration of these specific bands could yield a better indicator of the vegetation density as well as the condition of a crop. Table 6 presents the summary of the five sensors and the corresponding band settings considered relevant for the purpose of LAI estimation as well as based on the requirements of the SVIs analysed in the study.

2.4 Monitoring crop biophysical characteristics: The Leaf Area Index (LAI)

The biophysical and biochemical parameters of plants are at the centre of any application based on remote sensing techniques to assist in the decision making process in the context of PA. According to Atzberger et al. (2009) the Leaf Area Index (LAI) is one of the most important biophysical surface parameter attracting interest in wider researches concerned with earth observation (EO) data. LAI, which could be defined as total one- sided area of photosynthetic tissue per unit of ground area (Asner, Scurlock et al. 2003; Tian, Dickinson et al. 2004; Demarty, Chevallier et al. 2007), has become a central and basic descriptor of vegetation condition in a wide variety of physiological, climatological and biogeochemical studies (Asner, Scurlock et al. 2003). However, the methods employed for the derivation of LAI from the massive spectral data to characterize the condition of crops over the growing season is not straight forward. The challenge lays not only in the limitations of the existing SVIs but also in integrating multi sensor data to arrive at the desired spatial and temporal resolutions.

By the same token LAI is the most important descriptor of crop condition (Xiao, Liang et al. 2009; Xiao, Liang et al. 2011). It is the basic quantity indicating crop growth condition and hence plays a significant role in agricultural, ecological and meteorological models at local, regional and global scale (Yao, Liu et al. 2008). With the growing concerns about efficient resource allocations in agricultural production systems knowledge of crop growth at early stage is important at farm level decision making and national as well as regional level agricultural planning and policy making (Clevers and van Leeuwen 1996). Under non-optimal conditions crop growth monitoring could be best done by employing remote sensing

techniques. According to Clevers, Büker et al. (1994) integration of remote sensing using spectral vegetation indices regularly through the growing season and subsequent calibration of the growth model based on periodic LAI estimates yielded a better result. Moreover, optical data could be complemented by microwave data to overcome constraints that arise from a cloudy weather. Nevertheless, the application of such a model at a regional scale is constrained as the empirical relationship between LAI and remote sensing data established locally may not be valid over a large spatial extent (Yuping, Shili et al. 2008).

2.5 Vegetation indices and sensitivity analysis

To date several SVIs have been developed in an attempt to improve the performance of the existing indices in terms of their sensitivity to biophysical variables such as LAI, green vegetation fraction (GVF), net primary productivity (NPP) and fraction of absorbed photo synthetically active radiation (fPAR) that are of wider application in vegetation studies (Ji and Peters 2007). The commonly applied SVIs include but are not limited to the ratio based indices such as normalized difference vegetation index (NDVI) (Rouse et al. 1974), simple ratio (SR) (Jordan, 1969), infrared simple ratio (ISR), normalized difference infrared index (NDII) (Hardisky, Klemas et al. 1983), normalized difference red edge index (NDRE) (Gitelson and Merzlyak 2003), soil adjusted vegetation index (SAVI) (Huete, 1988), transformed TSAVI (Baret & Guyot, 1991), enhanced vegetation index (EVI) (Huete et al., 1994), and the Weighted Difference Vegetation Index (WDVI) (Clevers, 1989).

Each of these and other SVIs have their own merits and demerits in various application areas. A very common limitation being their insensitivity to the vegetation biophysical parameters they are meant to explain. In addition, the degree of sensitivity of those indices to noises also varies. This is a widely felt problem when it comes to the estimation of biophysical parameters such as LAI to characterize the condition of vegetation as well as for monitoring crop condition in precision agriculture. The SVIs widely applied to date suffer from this saturation effect or lack of sensitivity to moderately high LAI values hence limiting their application for LAI mapping. The quality of the performance of the SVI in terms of their relationship with biophysical parameters such as LAI is evaluated on the basis of the degree of sensitivity to the parameters and relative insensitivity to disturbance factors such as canopy background and atmospheric effects (Ji and Peters 2007).

Previous studies widely employed regression analysis to evaluate the performance of SVIs in the estimation of biophysical parameters. The coefficients of determination (R^2), mean squared error (MSE) and the root mean squared error (RMSE) are among the widely used indicators of the sensitivity of any SVIs to biophysical parameter such as LAI (Ji and Peters 2007). While these approaches provide useful information regarding LAI-SVI relationships they all are single values summarizing the overall relationships across the range of biophysical parameters. The R^2 value in non-linear regression, commonly called Pseudo-R^2 (Ji and Peters 2007; Gonsamo and Pellikka 2012), represents the proportion of variability of SVIs explained by the changes in biophysical parameters (LAI) while performing a regression of SVI (y-axis) against LAI (x-axis). The interpretation of R^2 in nonlinear regression should however be treated with caution as it represents the goodness-of-fit of the model and not the proportion of variability in the dependent variable due to changes in the independent variable. This is because the proportion of variability explained by the model can vary within the model.

However, attempts to quantify SVI-LAI sensitivities with any single value such as R^2 is a gross simplification of the relationships as in reality the proportion of variability of SVIs across the LAI range changes substantially with a change in vegetation densities. The use of MSE and RMSE are even more precise methods to quantify sensitivity while these methods

are also constrained by differences in the unit or magnitude of measurements when it comes to cross-site comparisons (Ji and Peters 2007). As alternatives to these measures different statistical approaches have been developed to model the SVI-LAI relationships using sensitivity analysis. The earliest of these was the relative equivalent noise (REN) (Baret and Guyot 1991) descriptor ; vegetation equivalent noise (*VEN*) (Huete, Justice et al. 1994) and a relative sensitivity (*R*) (Becker and Choudhury 1988) based on two rescaled VIs, and more recently the relative sensitivity (S_r) (Gitelson 2004) as a means to compare two *VIs* based on the ratio of first derivatives and the ratio of ranges of value of both variables (Ji and Peters 2007). These methods failed to account for the estimation errors associated with the predicted variable. Moreover, the last two methods do not yield a function as they give a single value amenable for comparison of two SVIs under certain circumstances. On the other hand, a method developed by (Ji and Peters 2007) demonstrated a statistical technique for computing the sensitivity function (*S*) across the LAI range for both linear and non-linear models. This technique also accounted for the estimation error associated with the predicted values while LAI is estimated using any SVI of interest. This sensitivity function was adapted to evaluate the performances of different vegetation indices across the different vegetation densities.

Accordingly, some selected SVIs were assessed on their capacity to predict LAI. The selection of these indices was based partly on their extensive use in literature such as NDVI and SR and partly due to their performance, sensitivity or insensitivity to different parameters while predicting LAI. Limitations of multispectral remote sensing and problems related to specific band characteristics of crops, and the subsequent quick saturation of broad band based SVIs such as the NDVI, insensitivity after short growth stage while important growth stages still to come (Herrmann, Karnieli et al. 2010) were also reasons for including the narrow band red-edge indices for comparison. Yet, the high sensitivity of NIR to a range of LAI makes this spectral region a very important indicator of vegetation condition provided that an efficient correction for background effects is made (Houborg and Boegh 2008). This implies that proper correction for canopy background effect enhances LAI-NIR relationships more than other spectral regions due to high sensitivity of the NIR bands to vegetation densities.

Indices derived mainly based on the red edge region were included to examine whether they significantly contribute to overcoming the saturation effects of other SVIs as recommended by (Brantley, Zinnert et al. 2011). Other optimized SVIs such as the soil adjusted vegetation index (SAVI) and the enhanced vegetation index (EVI) were chosen for their adjustments to reduce soil background effects as well as their sensitivity to crop phenological changes, as SAVI is, for instance, responsive to changes in LAI at an early stage of the growing season whereas EVI is sensitive to seasonal changes in LAI (Hatfield and Prueger 2010). On the other hand, those indices which combine information from shortwave infrared (SWIR) such as Infrared Simple ratio (ISR) (Brown, Chen et al. 2000; Fernandes, Butson et al. 2003; Gonsamo and Pellikka 2012) and Normalized Difference Infrared Index (NDII) Hardisky, Klemas et al. (1983) and which was evaluated for biomass prediction in the Canadian forest (Gonsamo and Pellikka 2012) were chosen for further testing of their performance for field crop LAI estimation. A summary of the SVIs selected for analysis is presented in Table 6.

CHAPTER THREE: MATERIALS AND METHODS

3.1 Description of the experimental plots

The study was conducted using data generated from multiple sensors during the 2011 and 2012 growing seasons with the purpose of monitoring the growth of potato crops in agricultural field situated in the southern part of the Netherlands. Given the nature of cropping patterns in the Netherlands these potato fields needed to be shifted every year as potato is not grown on the same parcel every year. Accordingly these experimental parcels change every year with the chosen parcel being within different geographical area as shown in Figure 1 for the two growing seasons, for example.

The experimental set up was designed based on differential treatment of nitrogen for the different plots. To this end the agricultural farm was divided into 12 different treatment levels for 2011 growing season where a plot of 30 m*30 m was delineated in each of the different treatment levels. The 12 plots fall in four initial fertilization levels while each treatment level was comprised of three plots. Accordingly, plots C, D & K received no nitrogen (0 kg N/ha); plots A, B & L had 161 kg/ha; plots E,F & J had 242 kg N/ha and plots G, H & I had 322 kg N/ha initial nitrogen fertilizations. In addition, each of these plots were given different treatments throughout the growing season in such a way that they form three treatment classes. The first group consisted of plots C, A, E & G (CL) which received only initial fertilization before planting and no treatment afterwards. The second treatment group includes plots D, B, F & H (TTW) which received additional nitrogen application after planting based on sensor readings throughout the growing season. The third treatment group involves farm plots K, L, J & I (MB) which were given additional N application at a single point in time after the canopy closed based on the weighted difference vegetation index (WDVI) (table 1). A range of sensing techniques was employed to obtain data on basic crop characteristics such as LAI and

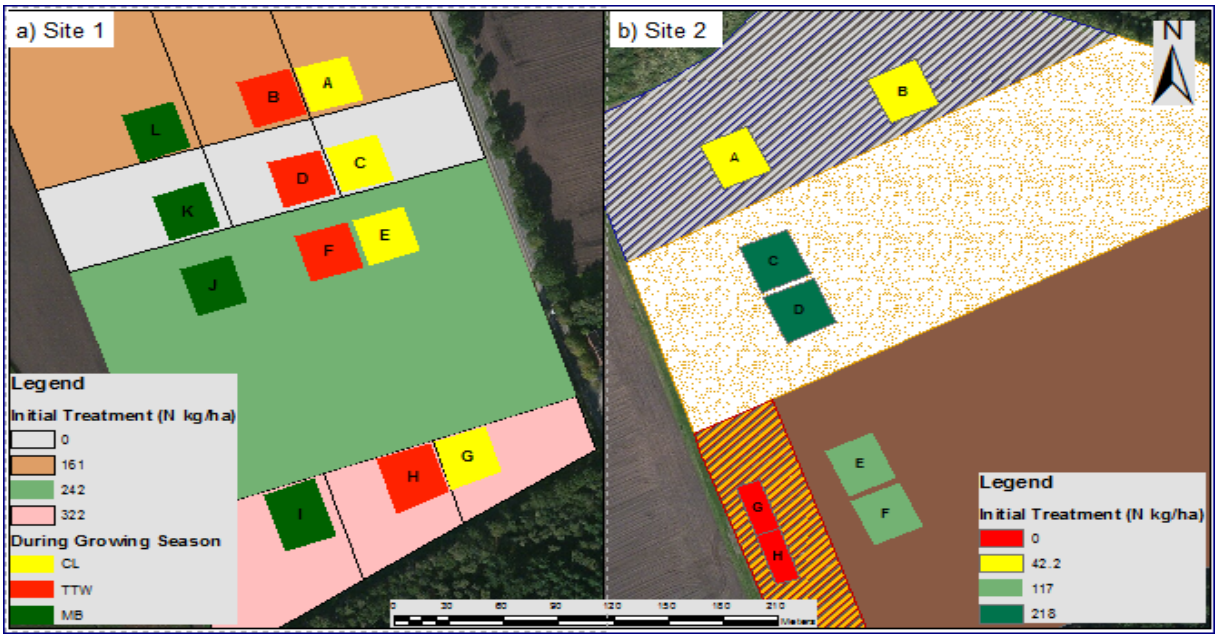

Figure 1. Farm sites for the potato experimental plots for 2011 (a) and 2012 (b) growing seasons

nitrogen status which was acquired weekly throughout the growing season. Basic crop characteristics were measured for which certain amount of treatment was applied or not.

Table 1. Plots by treatment levels for the 2011 experimental potato farm

N fertilization levels in $Kgha^{-1}$	CL	TTW	MB
0	C	D	K
161	A	B	L
242	E	F	J
322	G	H	I

A similar experimental set up was established for the 2012 growing season where eight plots were determined in such a way that four treatment classes were established i.e., a total of four nitrogen treatment levels consisted of two plots each. The first treatment class did not involve any initial fertilization whereas the second and third were subjected to different amounts of fertilization in two phases. The fourth class was however given no fertilization at all throughout the growth stages. Table 2 presents an overview of the experimental plots and the different treatment levels for the 2012 plots.

Table 2. The experimental set-up for 2012 growing season

Plots	Liquid Organic Fertilizer (m^3/ha)	Organic Fertilizer from Stable (m^3/ha)	N $kgha^{-1}$ Nmin
A & B	0	30	43.2
C & D	70	25	218
E & F	45	0	117
G & H	0	0	0

3.2 Data Sources and Acquisition Methods

3.2.1 Radiative Transfer Modelling: The PRO-SAIL model

To mimic the spectral settings of the different sensors, physically-based parameter estimation using the PRO-SAIL Radiative Transfer Model (RTM) inversion was used. These RTMs allow the use of the full spectrum acquired by the hyperspectral sensors in the waveband ranges of 400-2500 nm (Richter, Atzberger et al. 2009) as opposed to SVIs that are limited to few spectral bands. The PROSAIL, a widely used RTM, is a combined PROSPECT leaf optical properties model and SAIL canopy reflectance model (Verhoef 1985; Jacquemoud and Baret 1990) used to retrieve crop biophysical and biochemical properties such as the LAI, leaf and canopy chlorophyll contents. The coupled models allow for the estimation of both leaf and canopy parameters which is relatively simple and requires limited number of input parameters with reasonable computation time (Darvishzadeh, Skidmore et al. 2008).

The PROSPECT model (Jacquemoud, Bacour et al. 2000) computes the leaf hemispherical transmittance and reflectance as a function of four input parameters; namely, the leaf structural parameter, N (unit less), leaf chlorophyll a + b Concentration, C_{ab} (μgcm^{-2}), the dry matter content, C_m (gcm^{-2}), and the equivalent water thickness, C_w (gcm^{-2}) (Jacquemoud, Bacour et al. 2000). The SAIL model apart from the leaf reflectance and transmittance requires eight input parameters to yield top of canopy bidirectional reflectance. These include sun zenith angle, t_s *(deg)*; sensor viewing angle, t_o *(deg);* azimuth angle, *phi (deg),* fraction of diffuse incoming solar radiation, *skyl;* background reflectance (soil reflectance) for each wavelength, *rsl*; LAI *(m^2m^{-2}),* mean leaf inclination angle, *ALA (deg);* and hot spot size

parameter, *hot* (mm^{-1}), defined as the ratio between the average size of the leaves and the canopy height (Verhoef, 1985).

For the purpose of this study only selected parameters relevant to green leaf area estimation and sensitivity analysis were made varied. These parameters include LAI, C_{ab}, soil moisture (soil brightness), and leaf angle distributions (LIDFa and LIDFb) which were varied across a reasonable range to allow for the analysis of their disturbances while retrieving LAI from spectral data. The leaf structure parameter (N) was set at 1.8 based on previous literature where an N of 1.5 to 2.5 is often used (González-Sanpedro, Le Toan et al. 2008; Clevers and Kooistra 2012) suggesting the N value for potato to be around 1.8 on average. To allow for ease of distinction between the effects of those variables it was also deemed necessary to set the parameters which were once varied at certain fixed value and hence a value of 40 µg.cm^{-2} and 5%, were assigned to leaf C_{ab} and soil moisture, respectively. Spherical LAD was assumed as the default LAD whenever necessary. Moreover, the soil reflectance was fixed at 50% which means bright soil background to be able to model the robustness of indices to model LAI and their sensitivity to canopy background effects. The variability of soil background effect was instead modelled by varying soil moisture because these two soil parameters are interchangeable bearing similar effect on the spectra and hence it does not make sense to vary both simultaneously. The remaining PROSAIL model parameters were fixed at their soil leaf canopy (SLC) demo default values as summarized in table 3.

Table 3. Summary of nominal values for the PROSAIL model input parameters

No	PROSAIL parameters	Nominal values	Spectral signatures
1	Leaf type	*Green*	1
2	Chlorophyll concentration (Cab)*	*20/40/60 µg.cm^{-2}*	3
3	Equivalent water thickness (C_w)	*0,0137 g.cm^{-2}*	1
4	Leaf dry matter (C_{dm})	*0.008 g.cm^{-2}*	1
5	Leaf structure parameter (N)	*1.8*	1
6	Leaf area index (LAI)*	*(0.25, 8.0, 0.25) m^2m^{-2}*	32
	Hot-spot parameter	*0.05*	1
7	Leaf angle distribution (LAD)*	*Planophile/Spherical/Erectophile*	3
8	Soil Moisture	*5%/30%/55%*	3
9	Diffuse/direct radiation	*0*	1
10	Solar zenith angle (sza)	*45*	1
11	View zenith angle (vza)	*0*	1
12	Sun-view azimuth angle (azi)	*0*	1
	Total Combinations		288

3.2.2 Ground based LAI measurements

The LAI-2000 Plant Canopy Analyzer was used to measure LAI. The instrument uses an innovative technique for making rapid, non-destructive measurements of LAI and other plant attributes. The LAI-2000 calculates LAI and other attributes from radiation measurements made with a ''fish-eye'' optical sensor (148^0 field of view). Measurements made both above and below the canopy are used to determine canopy light interception at five angles, from which LAI is derived based on the radiative transfer model in vegetative canopies (Kooistra, Beza et al., 2012).

The monitoring of potato crop growth status in terms of biophysical and biochemical parameters was performed. LAI was measured on a weekly basis whereby two measurements were done above the canopy on each end of the row (one at each side) which would then be divided by the six LAI measurements performed inside the row to obtain an average LAI value for each row (Kooistra, Beza et al., 2012). In doing so radiation was measured both above and inside the canopy and this procedure was routinely performed for the 12 plots where four rows were measured per plot.

A Real Time Kinematic Global Positioning Satellite System (RTK-GPS) instrument was used to precisely geo-locate the horizontal position of the farm plots as well as the measurement sites to allow for time series analysis as well as validation of LAI predictions from different sensors against site specific measurements acquired with the LAI 2000.

3.2.3 MSR16R and APEX

In addition to the weekly acquired LAI measurements the spectral properties of the potato crop were measured using a Cropscan multispectral radiometer (MSR16R) which was carried alongside the LAI-2000 measurements for the corresponding experimental plots yielding a total of six measurement per row yielding an average LAI per row. These were routinely performed for four rows per plot. The instrument is a hand-held portable 16-band radiometer device which measures the incoming and outgoing radiance in narrow spectral bands. Reflectance is measured through a 28^0 field-of-view (FOV) aperture and incoming radiation is measured through a cosine-corrected sphere.

Next to the close sensing data, the Airborne Prism Experiment Spectrometer imagery (APEX) data was acquired during clear sky on the 27th June 2011. Even though such imagery data was available for a single flight, the fact that MSR16R data was also acquired on the same date allowed for the comparison of these sensors and for testing the capability of such sensor data for LAI retrieval as well as for the comparison of SVIs across sensors. Furthermore, this imagery allowed to simulate the performance of SVIs across multiple sensors including Sentinel-2 and VENµS for which actual data was not available. The high spectral and spatial resolution of the APEX sensor allows for testing the capability of ESA's upcoming super spectral space borne systems with empirical data. Hence, the value added by Sentinel-2 and VENµS due to their possession of narrow red edge bands could be evaluated. These hyper spectral next generation satellites are planned to be launched in 2014 and are expected to have added values because of those narrowly positioned red edge bands, which are lacking with most operational sensors. The same data was used to simulate the Landsat TM band setting in order to compare the performances of SVIs across broad and narrow sensors. These together constitute the remote sensing data for evaluating the potential of spectral data for LAI estimation as it would be measured through SVIs while at the same time evaluating the different SVIs including the newly proposed ones. Table 4 presents an overview of those sensors analysed in this study, the nature of datasets and the corresponding data acquisition methods.

Table 4. Overview of sensor types and the corresponding data analysed in this study

Sensor type	Description	Temporal resolution for data acquisition
LAI-2000	LAI-2000 plant canopy analyzer calculates LAI from radiation based on the model of radiative transfer in vegetative canopies. It measures in canopies ranging from forests to short grasses.	Field measurements made weekly for 2011 and 2012 growing season
CROPSCAN MSR16R SYSTEM	This device measures radiance/irradiance from a surface over 16 bands covering wide wavelengths ranging from 490nm to 1650nm with different spectral resolutions.	Field measurements undertaken weekly for 2011 and 2012 growing season. It is cloud insensitive allowing for regular data acquisition.
APEX (Airborne Prism Experiment) imaging spectrometer	The APEX dataset was acquired during an APEX flight campaign in June 2011. APEX was mounted on a Dornier DO-228 research aircraft operated by Flight Operation and Acquisition of DLR (German Space Agency) (M. E. Schaepman, M. Jehle et al. 2012) Image was acquired on a clear day from a flight height of about 4600m.	One time APEX flight data available (27 June 2011) and used to evaluate the performance of APEX, S-2 and VENµS as well as Landsat TM 7.
VENµS (Vegetation and Environmental New micro Spacecraft) and Sentinel-2, for assessing LAI in field crops.	These are the next generation satellites with super spectral red edge bands (Herrmann, Pimstein et al. 2011) Both VENµS and Sentinel-2 are multi spectral spaceborne systems which provide Multi-spectral information with 13 bands in the visible, near infra-red and shortwave infra-red part of the spectrum. They have narrowly positioned red-edge bands making them suitable for crop monitoring because of their 5 day re-visit time with spatial resolution of as high as 10m to 60m.	Simulated PRO-SAIL data was generated and used for the evaluation of the added value of red edge narrow bands. Field data acquired with APEX was also used for theses sensors.
Landsat Thematic Mapper (Landsat TM 7)	This is widely used NASA's Landsat space borne series which acquires imagery over broad spectral bands introduced in this study for the purpose of comparison with narrow band sensors.	The PROSAIL data was used to derive SVIs based on the broad bands.

The band settings of the hand held MSR16R radiometer, sensor, Landsat thematic mapper, the airborne hyperspectral APEX and ESA's upcoming multispectral spaceborne sensors are summarized in Table 5.

Table 5: Summary of sensors and their corresponding band settings used in this study

Sensor type	**Landsat TM***	**VENµS**		**Cropscan**		**Sentinel-2**		**APEX**
Band	width (**nm**)	Band position	Width (**nm**)	Band position	Width (**nm**)	Band position	Width (**nm**)	The band width ranges from 2.5 nm in the VIS and NIR to 8 nm in SWIR
1	450-520	490	40	490	7.3	490	65	
2	520-600	667	30	670	11	665	30	
3	630-690	702	24	700	12	705	15	
4	760-900	742	16	710	12	740	15	
5	1550-1750	782	16	740	13	775	20	
6	1040-1250	865	40	750	13	842	115	
7	2080-235	910	20	780	11	865	20	
				870	13	1610	90	
				1650	200			

*Denotes the complete listing of the sensor band settings

3.2.4 Biomass data

Biomass data was acquired destructively by harvesting one row of potato over one linear metre each time (0.75 m^2). Both fresh weight and the percentage of dry biomass was obtained after drying the harvested canopy for 24 hours at 70^oC (Clevers and Kooistra 2012). This same procedure was implemented for both 2011 and 2012 growing seasons. However, the biomass data was not acquired every week and hence available only for eight and seven weeks during the 2011 and 2012 growing seasons, respectively. For the purpose of this research, however, only the fresh above ground biomass was considered for the analysis of the LAI-biomass relationship.

3.2.5 Meteorological data

In addition to the remote sensing and biophysical data, meteorological data was also obtained from Eindhoven meteo-station as it was deemed important to consider variability in the weather parameters between the two growing seasons while performing a cross-site comparison. Weather parameters such as rainfall, temperature and total sun hours were considered, for these elements might affect agronomical practices. Hence, these weather parameters were used in the analysis as they might contribute to explaining the condition of the potato crop in addition to the level of nitrogen fertilization.

3.3 Selected SVIs for analysis

In addition to the indices introduced earlier (see section 2.4), newly developed indices are proposed in this study by integrating spectral information from the Red, Red-edge, Near Infrared (NIR) and Shortwave Infrared (SWIR) regions of the spectrum. This is mainly based on the differences in the sensitivities of these spectral regions to LAI as well as to canopy background effects. The SWIR remains sensitive to variations in soil moisture (Wang, Qu et al. 2008) compared to the red band, which saturates at relatively low LAI values. Hence the integration of these regions of the spectrum with the VIS and NIR could improve the sensitivity of SVIs to changes in the LAI. The incorporation of SWIR into the formulation of SVIs complement the information obtained from the NIR and VIS bands of the spectrum (Hardisky, Klemas et al. 1983; Brown, Chen et al. 2000; Gonsamo and Pellikka 2012). Moreover, Lee, Cohen et al. (Lee, Cohen et al. 2004) suggested that the red edge and SWIR bands of the electromagnetic spectrum contain more information relevant to LAI even compared to the conventionally used NIR bands. Table 6 presents a summary of the SVIs selected including the proposed ones for analysis in this study.

Table 6. Overview of selected SVIs for analysis by adapting their formulations to the specific band settings of different sensors

Index	Name	Sensor Specific Algorithms					
		Landsat TM5	**APEX**	**Sentinel-2**	**VENμs**	**Cropscan**	**References**
NDVI	Normalized Difference Vegetation Index	$[R_{(760:900)}-R_{(630:690)}]/[R_{(760:900)}+R_{(630:690)}]$	$(R_{782}-R_{669})/(R_{782}+R_{669})$	$(R_{783}-R_{665})/(R_{783}+R_{665})$	$(R_{782}-R_{667})/(R_{782}+R_{667})$	$(R_{870}-R_{670})/(R_{870}-R_{670})$	(Rouse Jr, Haas et al. 1974)
WDVI	Weighted Difference Vegetation Index	$R_{(760:900)}-R_{(630:690)}]$	$(R_{782}-C*R_{669})$	$(R_{783}-C*R_{665})$	$(R_{782}-C*R_{667})$	$(R_{870}-C*R_{670})$	(Clevers 1989)
			*Where C is a soil reflectance factor obtained as a ratio of NIR/red of pure soil spectra				
SR	Simple Ratio	$R_{(760:900)}/R_{(630:690)}$	R_{782}/R_{669}	(R_{783}/R_{665})	(R_{782}/R_{667})	(R_{870}/R_{670})	(Pearson and Miller 1972)
MSR	Modified Simple Ratio	-	(R_{741}/R_{705})-1/ Sqrt $[(R_{741}/R_{705})+1]$	(R_{740}/R_{705})-1/ Sqrt $[(R_{740}/R_{705})+1]$	(R_{742}/R_{702})-1/ Sqrt $[(R_{742}/R_{702})+1]$	(R_{740}/R_{710})-1/ Sqrt $[(R_{740}/R_{710})+1]$	(Si, Schlerf et al. 2012)
NDII	Normalized difference Infrared Index	$[R_{(760:900)}-R_{(1550-1750)}]/[R_{(760:900)}+(R_{1550-1750)}]$	$(R_{782}-R_{1646})/(R_{782+}R_{1646})$	$(R_{783}-R_{1610})/(R_{783}+R_{1610})$	-	$(R_{780}-R_{1650})/(R_{780}-R_{1650})$	(Hardisky, Klemas et al. 1983)
$NDRE_1$	Normalized Difference red Edge Index	-	$[(782-709)]/[(782+709)]$	$[R_{783}-R_{705})]/[(R_{783}+R_{705})]$	$[(R_{782}-R_{702})]/[(R_{782}+R_{702})]$	$[(R_{780}-R_{710})]/[(R_{780}+R_{710})]$	(Gitelson and Merzlyak 2003)
$NDRE_2$	Normalized Difference red Edge Index	-	$(741-705)/(741+705)$	$(R_{740}-R_{705})/(R_{740}+R_{705})$	$(R_{742}-R_{702})/(R_{742}+R_{702})$	$(740-700)/(740+700)$	
ISR	Infrared Simple ratio	$R_{(760:900)}/R_{(1550:1750)}$	R_{782}/R_{1646}	R_{783}/R_{1610}	-	R_{780}/R_{1650}	(Fernandes, Butson et al. 2003)
EVI	Enhanced Vegetation Index	$2.5(R_{NIR}-R_{RED})/(R_{NIR}+6R_{RED}-7.5R_{BLUE}+1)$	$2.5(R782-R669)/(R782+6R669-7.5R490+1)$	$2.5(R_{783}-R_{665})/(R_{783+}R_{665}-7.5R_{4490}+1)$	2.5(R782-R667)/(R782+R667-7.5*R490+1)	2.5(R780-R670)/(R780+R670-7.5*R490+1)	(Hatfield and Prueger 2010)
$IIReR_1$	Integrated Infrared Red-Edge Ratio	---------	$(R_{782}/R_{1646})*(R_{741}/R_{669})$	$(R_{783}/R_{1610})*(R_{740}/R_{665})$	------	$(R_{780}/R_{1650})*(R_{740}/R_{670})$	This study
IIR_eR_2	Integrated Infrared Red-Edge Ratio	---------	$(R_{782}/R_{1646})*(R_{710}/R_{669})$	$(R_{783}/R_{1610})*(R_{705}/R_{665})$	------	$(R_{780}/R_{1650})*(R_{710/R670})$	This study

3.4 Methodological overview

The schematic presentation of the logical flow of the research undertaking is organized in two phases as presented with the flow chart in Figure 2. The first phase of the research is concerned with the Radiative Transfer Modelling based on the PROSAIL Model. The simulation was performed using PROSPECT version 5 which yields spectral data at 1 nm spectral resolution over the broad range of the electromagnetic spectrum covering 400 nm to 2400 nm. This part mainly focusses on the evaluation of selected SVIs for LAI prediction. The analysis of the performance of selected SVIs was based on the simulated dataset where selected model parameters were either made variable or set to fixed values (table 3). It also involves the comparison of those indices for broad and narrow band sensors. Moreover, a sensitivity function was also tested for its ability to indicate the performance of the different SVIs. This part of the research was used as model calibration for the different SVIs including the newly proposed ones. The sensitivity analysis and the performance of SVIs across sensors as judged by the R^2 and RMSE values was used to screen out SVIs for further analysis based on empirical data.

The second phase of the research is devoted to further analysing those indices already evaluated based on the simulated data. In this part different remote sensing data as acquired with Cropscan MSR16R and LAI-2000 as well as the APEX imagery were analysed. The LAI-2000 measurements were compared for the different nitrogen treatment levels using different statistical analysis such as the analysis of variance (ANOVA) and least significant difference (LSD). The SVIs were also derived based on the MSR16R spectral information, which was then compared with the corresponding results from the simulation. The same procedure was applied to the APEX imagery. The APEX image was also used to evaluate the performances of ESA's upcoming spaceborne systems based on real data. The relationships for each of the analysed SVIs were judged based on the Pseudo-$R^{2.}$ The SVI-LAI relationships established based on MSR16R and APEX were also validated using the regression function already established based on the PROSAIL model. Furthermore, the sensitivity function used with the PROSAIL model was tested with empirical field data from MSR16R for the two growing seasons. This was used to examine if the sensitivity record of SVIs could be related to their LAI prediction power as measured by the R^2 and RMSE values. The overall undertaking of the research process was summarized as presented in Figure 2.

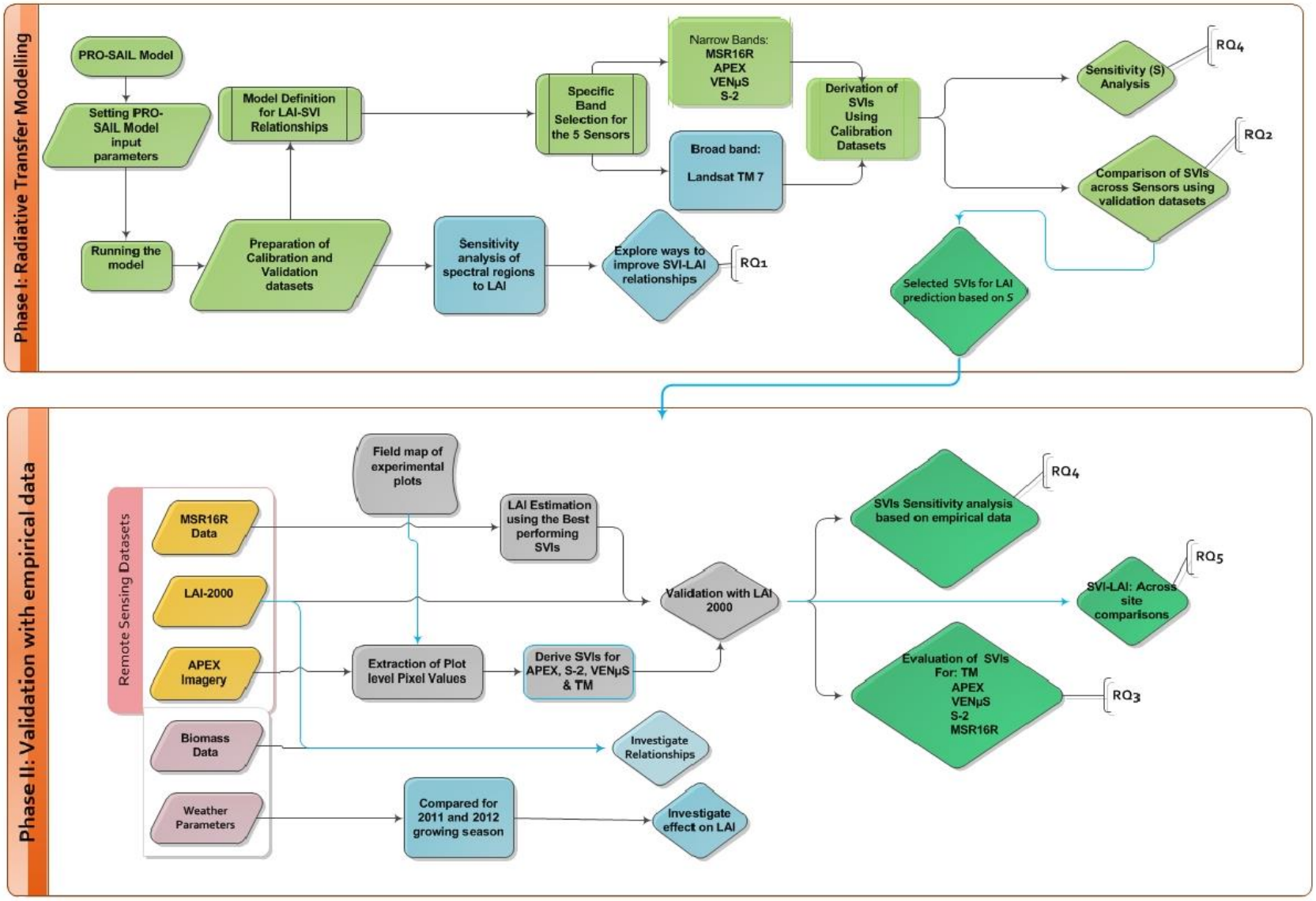

Figure 2. Datasets and processing steps to derive SVIs for LAI retrieval and sensitivity analysis. RQ stands for research question to be answered at each stage of the analysis

3.5 Data pre-processing

After the model parameters were set to the corresponding values as discussed earlier, the Python programming environment was used to run the PROSAIL simulations. The datasets obtained were systematically split into calibration and validation sets. In this case the simulated data were split into two equally sized datasets containing 112 spectral signatures each. The division was based on the LAI values involved in each of the simulations where all spectral signatures with LAI values of 0.5, 1.0, 1.5,...8.0 were allocated to the calibration datasets whereas those containing LAI values of 0.25, 0.75, 1.25,...and 7.75 were assigned to the validation set. Then the datasets obtained in each of the simulations contained at least one disturbance variable with 16 spectral signatures. The selected SVIs were calculated after the algorithms were adapted to the different band settings. Then the derived values for each of the computed SVIs were normalised to the same value ranges (see section 3.6.3 equation 3). This was done because the large differences in the SVI values was not feasible for comparison using the sensitivity function (see section 3.6.3) unless the values are normalized to similar magnitude ranges. The classification of the datasets into model calibration and validation sets was instead performed systematically.

The different datasets acquired using the aforementioned sensing techniques during 2011 and 2012 growing seasons were pre-processed. These include checking for "no data" and smoothing for outliers using appropriate algorithms. For instance, there were data gaps in the LAI-2000 field measurements for a few weeks which were filled using interpolation techniques. The LAI values for the plots on 20-07-12 was, for example, filled by taking the average value of the data acquired on the preceding and following week, 06-07-12 and 27-07-12, respectively. The LAI data was acquired at row level where six measurements were performed per row for four rows for every plot. The LAI value was therefore obtained as the average of all the four row values which was in turn the mean of six measurements acquired at every two meter interval in a row. These datasets were generated on a weekly basis which was combined into a time-stamped single dataset for analysis. The MSR16R data was acquired for the corresponding locations as where site the LAI was measured in similar time window. In addition, a pure soil spectra was also measured.

Moreover, the MSR16R spectral data was not without noises which were particularly noticeable with the soil spectra. In some of the MSR16R datasets the soil spectra contained spectral characteristic of green vegetation whereas it was presumed to exhibit the spectral characteristic of pure soil with possible variations in moisture levels. Moreover, there should not be such extreme values for reasonably similar soil types whose measurement was performed on the same date. The distortions in soil spectra could affect SVIs derived partly based on pure soil spectra while correcting for canopy background effects. These distortions were, therefore, corrected for by taking the average values using data acquired on the same date for a plot while excluding the outliers.

In addition to the LAI-2000 and MSR16R data, APEX imagery was also used which was not without noises. The imagery and the plots were available in different geographic projections. The APEX imagery was in WGS-84 which had to be transformed to the same projection as the plots that are in RD-New. The APEX imagery also had to be limited in extent matching the study area which in this case was the extent of the experimental plots for the 2011 growing season. Then, the experimental plots were used to define the extent of the imagery. Moreover, the APEX imagery also had pixels affected by noises that had to be excluded to avoid biases in the evaluation of SVIs across sensors based on the imagery. Hence, as the purpose of this study was partly to test the performance of APEX as well as ESA's upcoming hyperspectral sensors and not to map the LAI within the plot, those pixels with apparent noise

characterised by a black strip crossing over multiple plots as well as other grey line patterns were excluded to avoid systematic bias. To this end, new areas were digitized within each plot containing as many noise free pixels as possible while excluding noisy pixels within the experimental plots. Then the average pixel values for the entire APEX layers were extracted per plot using the R-statistical software from which the SVIs were derived not only for the APEX sensor but also simulating the band settings of S-2, VENµS and Landsat TM. This was done by adapting the band settings of those sensors to evaluate their performance based on the real data as well as to draw comparisons with the PROSAIL model.

The other dataset regards the dry biomass acquired along with the LAI and MSR16R spectral information. This biomass data was destructively acquired by measuring the dried weight of both above and below ground potato crop. The sampling was done per every 0.75m^2 for the rows for which the LAI and MSR16R data was already acquired. Like the other data measurements the biomass data was also taken every week coinciding with each other. However, this was not always the case as the date of biomass data measurement deviated from the date on which LAI and MSR16R were acquired. This was particularly the case for the 2012 growing season where the biomass data was acquired at a difference of a few days with the LAI as well as MSR16R data. In such cases the biomass data was compared with the other data measured on the closest possible date. Besides, there were weeks for which biomass data was not acquired at all and those weeks were excluded from the analysis of LAI-biomass relationships.

Given the fact that a differential nitrogen treatment might not be the only factor affecting crop growth particularly when variations in space and time were not accounted for. As a result, the

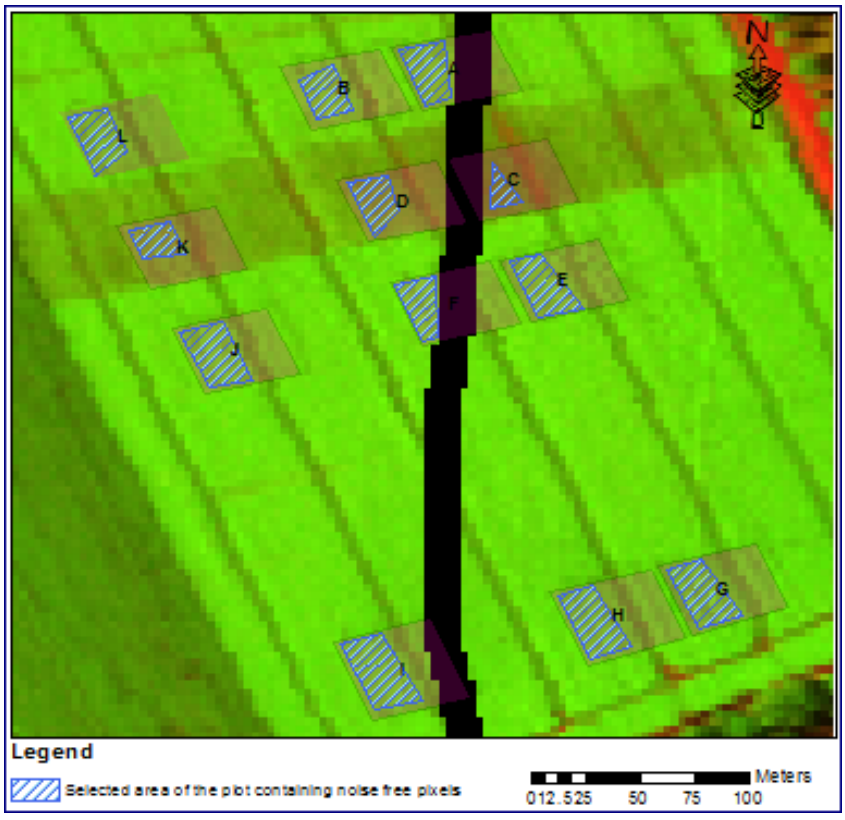

Figure 3.APEX Imagery acquired on 27 June 2011 indicating the areas selected within the 2011 plots by excluding noisy pixels.

inclusion of weather parameters was believed to at least partly explain the differences in crop growth condition in addition to the variable nitrogen application. To this end, the data on precipitation, temperature, and total sun hours were obtained from the nearest weather station via the Dutch National meteorology (www.knmi.nl). These data was available on daily basis as daily minimum and maximum temperature in degree Celsius, rainfall in mm and sun hour duration in hours. These datasets were organized in such a way that only those temporally covering the calendar years of the two growing seasons were considered for analysis. Furthermore, information regarding the soil conditions was taken into account as the two sites were located in different geographical locations.

3.6 Data analysis

3.6.1 Relationship between LAI and different spectral regions

The simulated data was used to test the sensitivity of the different spectral regions of the electromagnetic spectrum for LAI variation. Relationships were established between the selected spectral regions of relevance to LAI mapping such as NIR, Red, Red edge and SWIR regions with LAI to explore possibilities for devising new indices with improved sensitivity over a wide range of vegetation densities. The incorporation of SWIR in any SVI complements the information obtained from VIS and NIR bands as suggested by (Hardisky, Klemas et al. 1983; Brown, Chen et al. 2000; Gonsamo and Pellikka 2012). The SWIR remains sensitive to variations in soil moisture (Wang, Qu et al. 2008) compared to the red band, which saturates at relatively low LAI values. A sensitivity of these spectral regions to LAI ranges were analysed using simulated data based on the PROSAIL model to support the assertion that SWIR mainly remains sensitive to variations in soil moisture levels. Therefore, a test of sensitivity of those regions to LAI was performed for different canopy backgrounds as simulated with bright, intermediate and moist soils with soil moisture levels of 5%, 30% and 55%, respectively. Then a spectral band most sensitive to LAI was identified based on which the proposed indices were formulated.

3.6.2 SVI-LAI relationships based on PROSAIL model

The SVIs were derived from the simulated data after the algorithms for each of the indices were adapted to the band settings of the different sensors, namely, MSR16R, APEX, S-2, VENμS and Landsat TM. The SVI values were then normalized to equal value ranges to allow the comparison of sensitivities for different SVIs (see section 3.5.2). Then non-linear regression analysis was performed to establish SVI-LAI relationships across the five sensors. This was performed by regressing SVI against the corresponding LAI values as set in the PROSAIL model input parameters. The regression analysis was performed based on the exponential relation established following the Beer Lambert's law of light extinction from a canopy (see section 3.5.2 equation 5). The SVIs derived using the calibration dataset were used to empirically estimate the coefficients of light extinction (α) and the asymptotically limiting factor (SVI_∞) using the SPSS software (version 19.0). The non-linear regression analysis using SPSS was used to estimate model parameters to obtain the best fit model for estimation of LAI from spectral data by means of the derived spectral vegetation indices. Furthermore the best-fitting function was also used to define a SVI-LAI relationship which was later compared with the exponential function or Simplified Reflectance Model (SRM) (see section 3.6.3 for details).

The performance of SVIs based on narrow band sensors (APEX, S-2, VENμS, and MSR16R) was compared to those based on the broad bands of Landsat TM using the Pseudo R2 values. The band settings of APEX were dense enough to allow the simulation of S-2 and VENμS and hence were used to evaluate the performance of upcoming ESA's hyper spectral satellites

using empirical data. Then the SVIs were derived from the MSR16R and APEX datasets, which were then used for assessing the performance of those sensors. The selected SVIs were derived in each of those datasets and tested for their suitability to predict LAI for a potato crop.

3.6.3 Sensitivity analysis

As demonstrated by (Ji and Peters 2007) a statistical technique for computing the sensitivity function (*S*) across the LAI range for both linear and non-linear models was adapted for this study. The *S* function is defined based on a bivariate regression function where SVI is plotted as dependent variable on the Y-axis and LAI as independent variable on the X-axis which gives a fitted regression function as:

$$SVI = f(LAI) \quad \text{..... (1)}$$

In the non-linear regression, a change in the estimated SVI' as a function of LAI is approximated using a slope of the best fit regression line which indicates the change in SVI (Y) in response to a unit of change in LAI (X) given as:

$$SVI' = d(Y')/d(X) \quad \text{..... (2)}$$

Where SVI' is the slope of the estimated SVI (Y') and not SVI along the regression line and d(Y')/d(X) is the first order derivative of the estimated SVI in terms of LAI.

As this study involved a comparison of multiple SVIs with different value ranges and magnitudes a normalized sensitivity analysis was used as suggested by (Gonsamo 2011). Hence, the values for different SVIs were normalized by rescaling their values in such a way that they fall in a range of 1 to 10 for all the SVIs. To this end, the value range standardization technique adapted based on Vickers and Rees (2007) was used and is expressed as follows:

$$SVI_n = a + (SVI_i - SVI_{min})(b-a)/(SVI_{max} - SVI_{min}) \quad \text{.....(3)}$$

where SVI_n is the normalized SVI, *a and b* denote the minimum and maximum values of the normalized SVI_n data whereas SVI_{min} and SVI_{max} indicates the minimum and maximum values of the calculated SVI with SVI_i being the i^{th} value of the SVI values under consideration.

Many studies have shown that SVIs reach a point where they do not increase in response to increasing LAI values which is often called the saturation level. All SVIs exhibit similar patterns although there exist differences in their levels of sensitivity across LAI ranges and hence saturation levels. As a result, the relationship between LAI and SVIs can be fitted to an exponential equation as a function of LAI following the Beer Lambert's Law of light extinction from a canopy (Clevers 1988). This relationship can be expressed as:

$$SVI = SVI\infty + (SVIg - SVI\infty) * exp^{(-K*LAI)} \quad \text{..... (4)}$$

Where SVI is vegetation index, *SVIg* being vegetation index corresponding to that of bare soil, SVI_∞ is asymptotic value of SVI when the LAI value approaches to infinity and this value can be practically reached for LAI > 8.0 (Baret and Guyot 1991).

A simplified reflectance model for vegetation derived by (Clevers 1988) and also explained in (Baret and Guyot 1991) was used to get the best fit model using the simulated datasets. The requirements for such a model as discussed by (Clevers 1988) includes that a) it permits the estimation of LAI; b) relates LAI and reflectance as defined by physical parameters; c)allows

for multi temporal analysis by correcting for soil background effects and d) results in a meaningful vegetation index.

The model for LAI estimation based on SVIs using the relationship established between spectra and LAI can thus be expressed as follows:

$$LAI=-1/\alpha * Ln\ (1-SVI/SVI_{\infty+}) \quad \text{..... (5)}$$

where α is a complex combination of extinction and scattering coefficients and SVI_∞ being the asymptotically limiting value for the infrared reflectance developed by Clevers (1988) with a detailed derivation procedure. This model was used to compute LAI from the SVIs derived from simulated data using the SPSS Software (V.19.0) where the two parameters i.e., α and SVI_∞ are empirically estimated through an iterative process based on the simulated data. Moreover, the procedure yields a more realistic correlation coefficients (R^2) and residual values as opposed to the pseudo-R^2 values where the latter tells us only the goodness-of-fit of the model.

The non-linear regression was performed for estimating LAI based on the rescaled SVI values using the simplified reflectance model following Beer's law of light extinction from a canopy (Clevers 1988). Several studies confirmed the usefulness of this function (Wiegand, Maas et al. 1992; Broge and Mortensen 2002; Darvishzadeh, Atzberger et al. 2009; Gonsamo and Pellikka 2012)for retrieving LAI and hence applied in this study.

Once the non-linear regression was performed for the estimation of LAI based on the SVIs analysed the inverse of the local slope could be used to indicate the rate of change in SVI in response to a unit of change in LAI, simply an inverse of equation (2):

$$\mathbf{SVI' = [d\ (Y')/d(X)]\text{^}-1 \quad \text{..... (6)}}$$

More importantly, since the $\hat{Y}$ values are estimated, the associated estimation error should be considered to indicate the efficiency of the SVI-LAI relationships. This estimation error associated with the change in the local slope of SVI-LAI regression function is equated with the standard error of the estimate as predicted by the different SVIs for every point or LAI value along the X-axis. The standard error of the estimate is expressed as:

$$\sigma\hat{Y}i = \sqrt{\sigma^2 \hat{Y}'_i (\hat{Y}'\hat{Y})^{-1} \hat{Y}_i} \quad \text{..... (7)}$$

where $\sigma\hat{Y}i$ is the standard error of $\hat{Y}$ or asymptotic standard error of $\hat{Y}$ or standard error of the estimate; σ^2 is the mean squared error (MSE); $\hat{Y}$ is a matrix of the independent variables X; and $\hat{Y}i$ is the i^{th} row of $\hat{Y}$ and $\hat{Y}'$ stands for the matrix transpose. The statistical approach to calculating such estimation error is complicated to approach manually unless assisted by a statistical software package as proposed by (Ji and Peters 2007; Gonsamo 2011). The R-statistical software was used to compute the standard error of the estimate.

The *S* function, combining equations 6 and 7, can thus be expressed as the ratio of the first order derivatives of SVI' to the standard error of SVI ($\sigma\hat{Y}i'$). From the above formulations, the sensitivity function is given as:

$$\mathbf{(S) = SVI'/\sigma\hat{Y}i' \quad \text{..... (8)}}$$

where *S* of i^{th} observation equals t which is the Student's t-test statistic for a given P-value and degree of freedom because $t \cong \hat{Y}'_i / \sigma\hat{Y}_i$ (Ji and Peters 2007).

3.6.4 SVI-LAI relationships based on empirical data

The SVIs were computed from both the MSR16R and the APEX imagery. The computed indices were regressed against LAI-2000 measurements to judge the performance of those SVIs based on the Pseudo R^2. This procedure was performed for both MSR16R data and APEX imagery. The APEX imagery, on top of furnishing data for itself, was also used to model S-2, VENµS and Landsat TM and hence those SVIs were compared across all the five sensors. In doing so it was possible to evaluate the performance of SVIs across the broad bands of Landsat TM and the narrow band sensors. Moreover, the upcoming ESA's spaceborne sensors were evaluated for their narrowly positioned red edge bands based on the SVI-LAI relationships.

3.6.5 Relationships between LAI and nitrogen application

As described in the previous section, the experimental set-up was designed based on differential nitrogen application at the beginning of the growing season as well as variable rate of fertilization throughout the growing season. The effect of such differential nitrogen treatment was examined by plotting the LAI values acquired for the different plots through the growing season. This was performed for the two growing seasons to analyse the effect of the variable nitrogen application on the growth of the potato crop. Furthermore, an analysis of variance was conducted using SPSS to see the effect between treatment groups. The analysis of variance (ANOVA) was performed to see the treatment effects in terms of the average LAI values for treatment blocks as well as initial fertilizer application during the 2011 and 2012 growing seasons. In addition, a pairwise test of significance of the treatment effect between treatment groups as well as among plots was carried out using the Least Significant Difference (LSD) test.

3.6.6 Comparison of weather parameters for the 2011 and 2012 growing seasons

The data on weather parameters was also analysed for the two growing seasons. Daily temperature was computed by taking the average of daily minimum and maximum using a four (4^0C) accumulated day degrees (O'Brien, Allen et al. 1983; Allen and O'Brien 1986). Cumulative values were calculated for rainfall, temperature and sun hours for the entire calendar days starting with the planting dates for the two growing seasons. As the calendar days and the planting dates for the two years were closely matching being 10^{th} April 2011 and 12^{th} April 2012, the calendar dates for the computation of the parameters were set to 98 and 100, respectively. A paired t-test was also carried out to examine the mean difference of those parameters between the two growing seasons.

3.6.7 Relationships between biomass and LAI

A relationship between fresh biomass and LAI was studied to examine whether LAI could be used to predict the overall biomass for the potato crop. This was analysed using a linear regression function with the biomass data acquired for the two sites against the corresponding LAI. In addition, a comparison of the mean difference of biomass for the two sites was performed using a t-test. Furthermore, the analysis of variance was performed to see the effect of nitrogen treatment, whereas the test of significance of the difference was performed using the Least significant difference test (LSD).

3.6.8 Sensitivity analysis based on MSR16R and LAI-2000

The sensitivity function already explained (see section 3.6.3) was also implemented using the MSR16R data from the 2011 growing season. This was deemed necessary to compare the sensitivity function based on empirical data with those performed with the simulated datasets using the PROSAIL model, because the simulated dataset is supposed to be noise free as opposed to empirical data which is vulnerable to noise effects. Moreover, such sensitivity analysis was also used to test if there exists some degree of consistency in the performance of SVIs as judged by its LAI prediction power in terms of R^2 and RMSE values and the sensitivity record.

3.7 Validation

3.7.1 Validation of SVI-LAI relationships based on PROSAIL model

Different types of validation techniques can be used; namely, validation based on independent dataset, and a cross validation procedure also called the leave-one-out procedure (Darvishzadeh, Skidmore et al. 2008). The same study reported a comparable performance of both techniques. The validation method for the RTM modelling part of this study was based on an independent test dataset. The total of 224 spectral signatures with a particular LAI value under varying leaf and canopy parameters such as leaf Cab, LAD, and soil moisture levels were split into two independent datasets. The use of a completely independent dataset is often recommended to test the model's long term stability while at the same time an arbitrary division of datasets into calibration and validation samples may also lead to biased results (Darvishzadeh, Skidmore et al. 2008). The classification of the datasets into model calibration and validation sets was instead performed systematically as already described in the pre-processing part. In this case the simulated data were split into two equally sized datasets based on the LAI values involved in each of the simulations (see section 3.4)

The SVIs were derived from the validation datasets using the same algorithms applied for the calibration datasets. Moreover, to handle the variation in value range and magnitudes among the different SVIs analysed, the SVI values were normalized through rescaling. The regression equation established based on the calibration dataset was used for LAI prediction using the validation datasets. Then different statistical parameters such as the coefficient of determination (R^2) and Root Mean Square Error (RMSE) were computed to validate the performance of SVIs based on the established relationships.

$$\mathrm{RMSE} = \sqrt{\frac{\sum_{i=1}^{n}(\hat{y}_i - y_i)^2}{n}} \quad \textbf{.....(9)}$$

Where $\hat{y}_i$ is the value of predicted LAI, y_i is the measured LAI and n is the number of observations.

$$\mathrm{RPD} = \mathrm{St.Dv./RMSE} \quad \textbf{.....(10)}$$

where RPD is the relative percentage difference, St. Dv. is the standard deviation of the measured LAI and RMSE as obtained using eq. (9).

Then, a sensitivity analysis was performed using the sensitivity function to evaluate the relationship between the different SVIs and the LAI using (eq. 8).

3.7.2 Validation of SVI-LAI relationships using empirical field data and APEX imagery

Once the SVI-LAI relationships were established based on empirical field data as well as APEX imagery, validation was performed using the relationship defined based on PROSAIL data. The parameters coefficient of light extinction from a canopy and the asymptotically limiting factor (see section 3.5.3 equation 5) already estimated based on the PROSAIL calibration dataset were used to predict LAI based on the SRM (see section 3.6.3). These were applied to all SVIs derived from the MSR16R as well as the APEX imagery. In addition, the best fitting models from simulated datasets were also used for LAI prediction using the empirical data from MSR16R to compare the robustness of those models across different datasets. These same procedures were followed for the validation of SVI-LAI relationships based on APEX imagery. It includes validation of the consistency of the performance of those SVIs across the different sensors. This also allowed for comparing the performance of SVIs based on empirical field data as well as APEX imagery with apparent noise compared to the datasets simulated with PROSAIL modelling.

The predicted LAI was compared with the LAI-2000 measurement for every plot as the LAI-2000 data were available. Then statistical measures such as R^2, RMSE and the relative percentage difference (RPD) were computed to compare the performance of SVI for LAI prediction. The RPD was used to standardize for differences in the data value range across the two sites. This procedure was also meant to test the robustness of the LAI retrieval method for crop monitoring under varying management practices as well as throughout the growing season. The LAI datasets obtained using the LAI-2000 instrument were used for validation as well as to establish empirical relationships with the different spectral vegetation indices derived for the different sensing techniques. The same validation procedure was followed for LAI predictions made based on APEX imagery where the LAI-2000 data used for the validation of APEX imagery based LAI predictions were those acquired on the same date as the APEX flight (27-06-2011).

CHAPTER FOUR: RESULTS

4.1 Sensitivity analysis based on the PROSAIL Model

4.1.1 Sensitivity of selected spectral regions to LAI for different soil moisture levels

The selected spectral bands red (around 670 nm) and red-edge (around 705 nm, 710 nm and 740 nm), NIR (780 nm) and SWIR (1650 nm) were assessed based on their sensitivity to LAI for bright, intermediate and moist soil backgrounds. The sensitivity of those bands were evaluated using the simulated data. As demonstrated in Figure 4 the reflectance in the NIR (780 nm) showed high sensitivity not only to changes in LAI but also to canopy background effects. The background effect is most visible with the bright soil, because the reflectance curve for bright soil appears to be horizontal and not showing any change with LAI range. On the other hand, the corresponding reflectance for medium and moist soil increases with increasing LAI values (Figure 4a).

It can also be seen from the same figure 4 (b) that the reflectance at 670 nm is less sensitive to canopy background effects even at low LAI where the contrast between the three soil moisture levels is minimal compared to the other three band regions. The sensitivity of the red band also saturates earlier than the other three as it no longer distinguishes between bright and moist soil at LAI = 2.5 and onwards. As compared to the red band, the reflectance in the red-edge around 705 and 710 nm showed not only higher gap between bright, intermediate as well as moist soil conditions at low LAI but also showed improved sensitivity to LAI. This trend improves further with the red edge at 740 nm which follows a similar pattern with the NIR spectra at 780 nm showing higher sensitivity over wider LAI range while distinguishing between bright and moist soil backgrounds better than the red and other red edge bands. On the other hand, the result for SWIR (1650 nm) indicated higher sensitivity to soil moisture levels with the reflectance for bright soil being high at low LAI which continues to drop even at high LAI levels. This region also showed a better distinction even between intermediate and moist soil backgrounds where the reflectance for both soil moisture levels continues to drop up to moderately high LAI (LAI = 5). However, the reflectance for moist soil continues to increase at high vegetation density (LAI > 5) although this can hardly be witnessed from the graph (fig 4c).

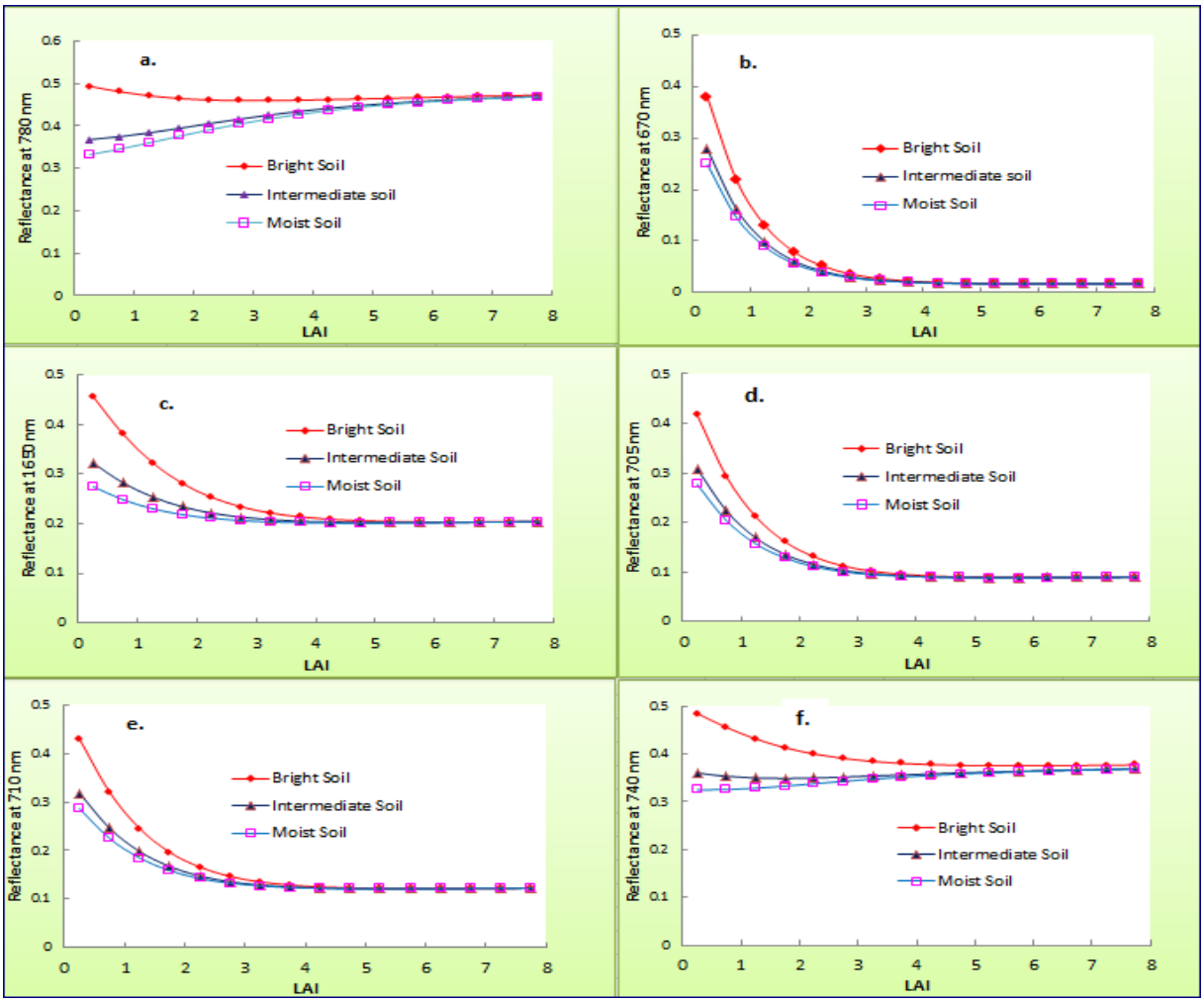

Figure 4. The effect of canopy background and LAI on the NIR (a), Red (b), SWIR (c) and Red-edge (d, e & f) reflectance for bright, intermediate and moist soil conditions.

4.1.2 Results on SVI-LAI relationships

The analysis of the SVI-LAI relationship was performed based on different soil, leaf and canopy parameters. The result of these relationships based on bright, intermediate and moist soil conditions is presented in the appendix 2. The effect of LADs based on planophile, shperical and erectophile LAD is found in appendix 3 whereas the effect of three C_{ab} levels (20, 40 and 60 µgcm^{-2}) can be found in appendix 4. The results showed that most of the SVIs were less sensitive to canopy background effects as the overlapping curves for the three soil moisture levels indicated homogeneity of the relationship. However, the WDVI, EVI, NDII and ISR showed relatively higher sensitivities to soil moisture levels at low LAI (LAI < 4) indicating the effect of soil moisture for open canopy (Appendix 2).

It was also found that most of the SVIs were sensitive to varying C_{ab} levels with relationship being the worst at low C_{ab} level (20 µgcm^{-2}). However, WDVI, NDVI and EVI showed similar relationships for all the three Cab levels. Other SVIs such as $IIReR_1$, NDII, NDII, EVI and ISR had similar relationships for Cab levels of 40 and 60 µgcm^{-2}, whereas their relationship with C_{ab} level of 20 µgcm^{-2} deviates from the other two (Appendix 3e, f, i & k). Other SVIs such as $NDRE_1$, $NDRE_2$, MSR, SR and $IIReR_2$ showed different relationships

with LAI based on the three C_{ab} levels. The effect of C_{ab} levels on SVI-LAI relationships increases at high LAI as indicated by the diverging curves corresponding to each C_{ab} level. Apart from showing higher sensitivity at higher LAI, all the SVIs had different sensitivities to LAI ranges. For instance EVI saturates earlier (LAI < 2) followed by WDVI , NDVI, $NDRE_1$ and $NDRE_2$ which appears to saturate at fairly low LAI (LAI < 3). Regardless of their sensitivity to varying C_{ab} levels $IIReR_1$, $IIReR_2$, NDII, ISR and SR had better sensitivity to LAI even at high vegetation density (see Appendix 3).

The analysis based on different LADs also reported differences in the sensitivities of the SVIs. The relationship was poor for most indices based on planophile LADs. The analysis also indicated higher sensitivities for such indices as SR, $IIReR_1$, $IIReR_2$ and NDVI for planophile LAD at lower LAI (LAI < 4) compared to the other LADs for the same SVI. For many of the SVIs the relationship with LAI showed a similar pattern for spherical and erectophile LADs. Except for WDVI and EVI the relationship based on an erectophile LAD was found to be more linear showing a better sensitivity of SVIs across a wider LAI ranges.

After the SVIs were derived based on the band settings of MSR16R, the regression analysis based both on the best fit model and SRM gave the results plotted in Figure 5. In addition to the simulated spectra at every LAI value SVIs were computed based on the SVI-LAI relationships established following Beer's Law (equation 5). The SRM based on non-linear regression model was used to empirically estimate the parameters of the model, namely, α and SVI_∞. The result of the regression analysis showed that most of the indices had exponential relations while regressing SVI (y-axis) against LAI (x-axis). This was the case with SVIs such as NDVI, NDII and $NDRE_2$ where the SVI-LAI relationships based on the two models were found to match more closely than for other SVIs.

Based on the best fit function $IIReR_1$, NDII, ISR, NDVI, $IIReR_2$ and SR had better relationships than other SVIs based on their Pseudo-R^2 value of 0.92, 0.90, 0.88, 0.86, 0.86 and 0.81, respectively. On the other hand, $NDRE_1$, $NDRE_2$, EVI, MSR and WDVI, which had a pseudo-R^2 value of 0.58, 0.79, 0.66, 0.67, 0.73, respectively, had worse relationships with LAI. However, the analysis based on the SRM (exponential function) indicated a more linear relationship for IIReR1, IIReR2, SR and MSR and the relation was also strong for the first three indices (R^2=0.82, 0.81 and 0.78). The other SVIs had logarithmic relations with SVI being a regressor (y-axis) and they had weaker relationships compared to the first three SVIs (Figure 5). In general, the use of exponential function showed weaker relationships as compared to the Pseudo-R^2 values obtained from the best fit functions.

Moreover, the point clouds in the scatter plots labelled in green colours showed different patterns. They represent the unique SVI values derived based on the spectra generated for the different disturbance factors, namely, soil, leaf and canopy parameters. Those points were quite dispersed from each other for MSR, SR, $NDRE_1$, and NDRE2 (Figure 5g, e, j and h) indicating higher sensitivity of these indices to leaf and canopy parameters, whereas NDVI, NDII, ISR, EVI and $IIReR_1$ showed less sensitivity to those parameters (Figure 5, a, b, c, f. i).

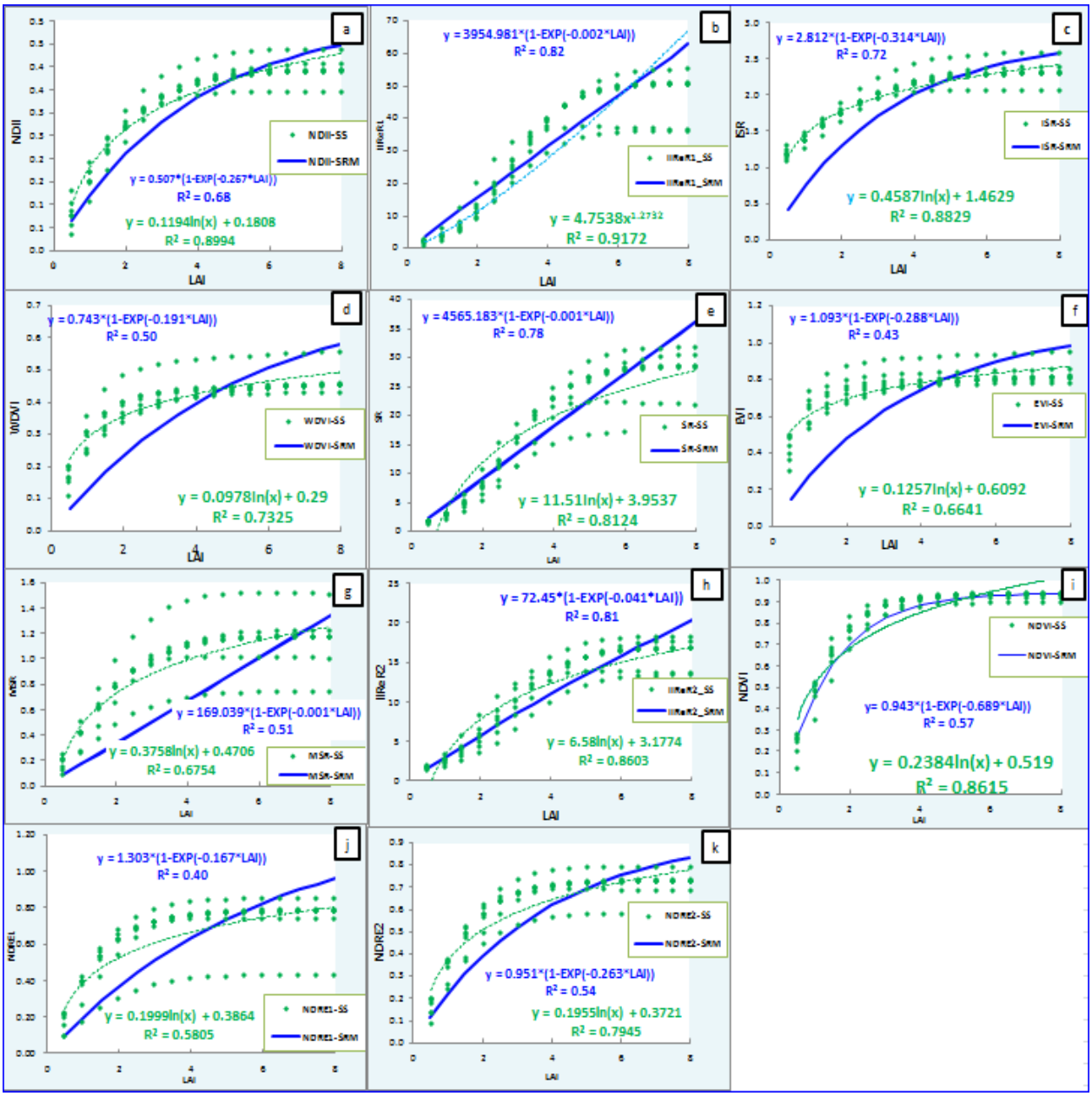

Figure 5. SVI-LAI relationships based on SRM and simulated spectra. NDII (a), IIReR1 (b), ISR (c), WDVI (d), SR (e), EVI (f), MSR (g), IIReR2 (h), NDVI (i), NDRE1 (j), and NDRE2 (k). The colours indicate the equations that match with the point cloud and the trend line with the same colour. SS stands for best fit function, SRM stands for fit with the simplified reflectance model (exponential function).

4.1.3 SVI-LAI Relationships based on Broad and Narrow Band sensors

SVIs that could be derived from broad bands were analysed across different sensors. This part presents a comparison of the relationships of those indices across the broad bands from Landsat TM with those derived based on narrow bands of MSR16R, APEX, S-2 and VENμS. The broad bands refer to the band settings of Landsat TM where a single band extends over 60 to 200 nm widths whereas the corresponding bands from other sensors are as narrow as 2.5 nm to 8 nm for APEX, 12 nm for MSR16R, and the band width extends up to 30 nm for S-2 and VENμS. Therefore, in this study, the Landsat TM bands were referred to as broad while the rest were treated as narrow bands.

Figure 6 depicts the relationships between six SVIs as derived from the band settings of different sensors. These indices are chosen for comparison because they could be derived from the broad bands of TM. The pattern of the relationships for all the SVIs, namely NDVI, SR, NDII, ISR, WDVI and EVI showed similar patterns with what was reported in Figure 5 for the SVI-LAI relationship based on MSR16R. The graphs indicate overlapping point clouds for those indices although the congestion or dispersion of the points vary depending on the sensitivity of each SVI to the leaf, soil and canopy parameters as simulated with the PROSAIL model. For instance, Figure 6 (a) which has similar patterns as Figure 5(i) illustrates the consistency of NDVI across the five sensors regardless of the band widths of those sensors. Similar comparisons could be made for the other indices with the relationship reported based on MSR16R (Figure 6) to gain an understanding on how consistent those SVIs derived from other sensors are.

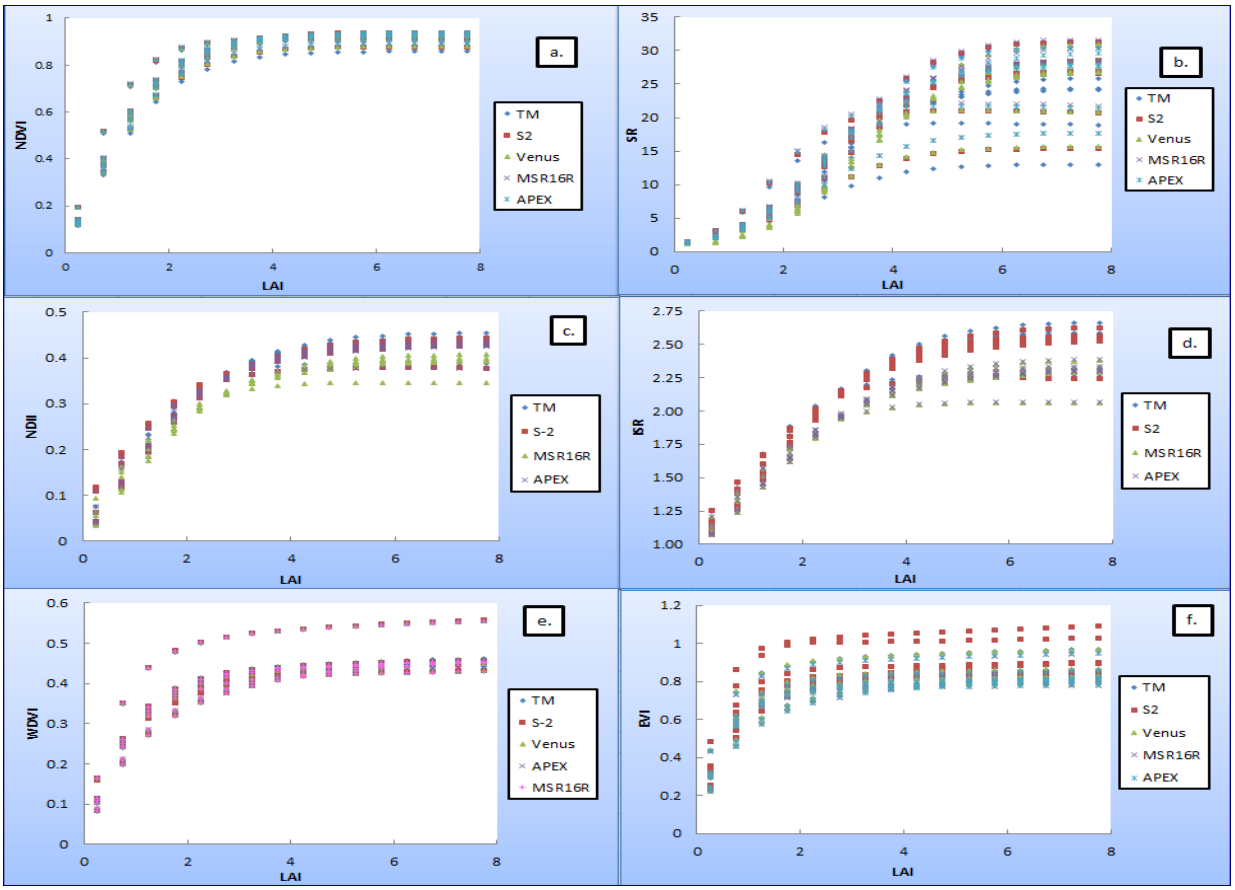

Figure 6. Relationships between LAI and NDVI (a), SR (b), NDII (c), ISR (d), WDVI (e) and EVI (f) for Broad and Narrow bands.

In addition, the validation datasets were used to predict LAI based on those different sensors to assess the degree of consistency of those SVIs. Then the predicted LAI for each SVI from narrow band sensors were plotted against the corresponding estimate (LAIe) from Landsat TM. The result in Figure 7 shows that the estimated LAI (LAIe) based on the different sensors could be compared. For instance, LAI estimated using the WDVI from the Landsat TM is more or less linearly correlated and fitted around a line through the origin with the LAIe from MSR16R, APEX, S-2 and VENµS. This of course follows from the consistency of the index which as a result estimates LAI at similar levels of accuracy. It can also be seen that LAI estimated based on NDVI and EVI appears to follow a linear pattern of relationship across sensors.

Similar to what has been reported for other SVIs, the NDII and ISR also showed consistency in predicting LAI for different band settings across TM, S-2, MSR16R and APEX sensors. Apart from the similar pattern of performance reported between NDII and ISR, it can be seen that the LAIe based on MSR16R with both indices deviates from S-2 and APEX at higher LAI values (Figure 7 d &f). The overlap is even more visible between S-2 and Landsat TM as well as between MSR16R and APEX. On the other hand, S-2 and APEX showed a more linear pattern with Landsat TM for both ISR and NDII. The WDVI showed particularly linear relationships due to overlapping patterns for all the five sensors confirming high degree of consistency of the performance of the index across different band widths. SR appeared to show the least consistency when compared to the other indices as the plot indicated dispersed point clouds around the line through the origin. The EVI also exhibited some degree of consistency for all the sensors considered except that S-2 based LAIe appeared to deviate from the LAIe from TM.

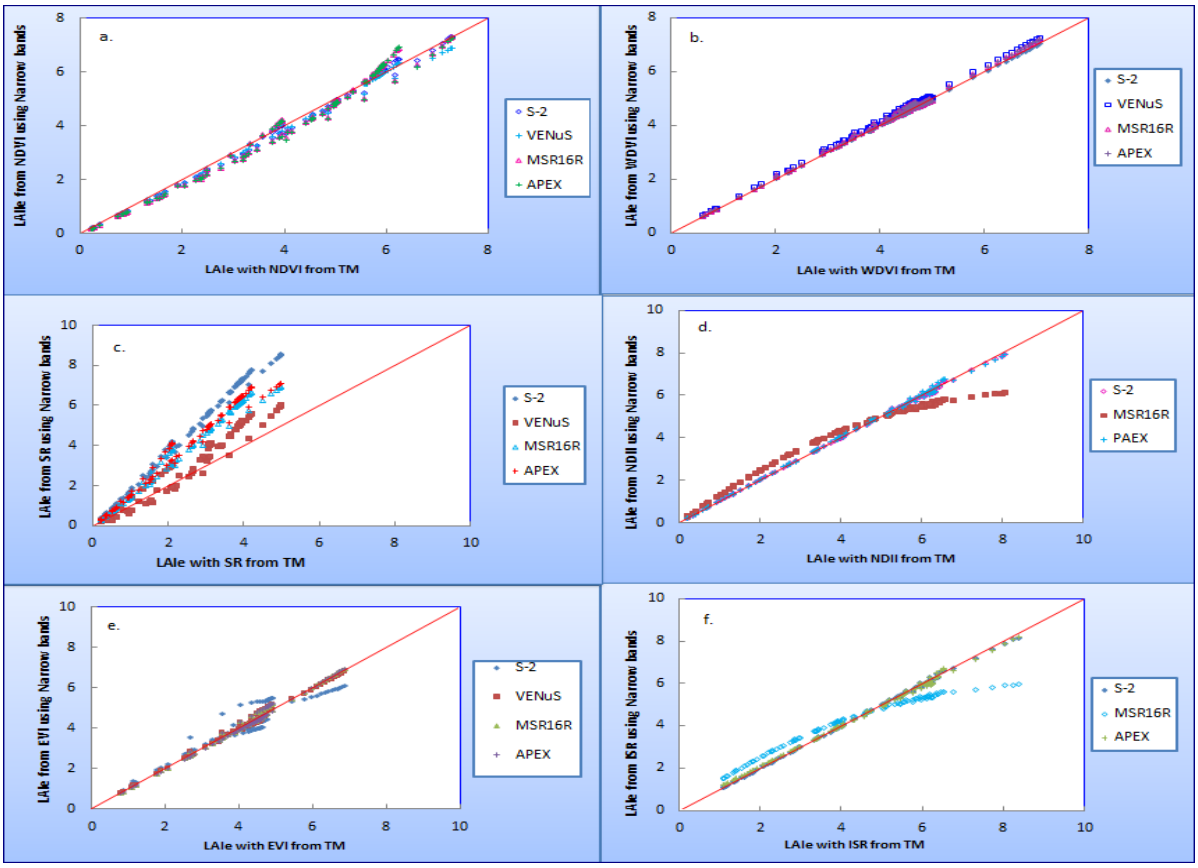

Figure 7. A comparison of LAI prediction power for SVIs based on broad and narrow band sensors. LAI estimated (LAIe) based on NDVI (a), WDVI (b), SR (c), NDII (d), EVI (e) and ISR (f) from Landsat TM was compared with LAIe based on the narrow band sensors.

Furthermore, a statistical analysis using correlation was performed to quantify the degree of consistency of the performance of those SVIs across sensors. The result of the correlation analysis of the LAIe from those SVIs was obtained for the Landsat TM and the other four narrow band sensors. The correlation (R) values indicated that the LAIe from broad band and narrow bands were significantly related for all the six SVIs analysed (Appendix 18). The relationship revealed strong correlation of the performance of SVIs across the broad and narrow band sensors. The correlation was also found to be statistically significant at 95% confidence level (P-value = 0.00) for all the indices (NDVI, WDVI, SR, NDII, ISR and EVI) based on Landsat TM and the other four sensors (S-2, MSR16R, APEX and VENμS). This confirms the consistency of those SVIs across different sensors regardless of the varying degree of consistency as well as sensitivity or insensitivity to different leaf and canopy parameters.

4.1.4 Results on the Validation of SVI-LAI Relationships

Relationships established using a regression analysis with both SRM and best fit function resulted in different relationships for the SVIs considered. As a preliminary assessment of the selected SVIs, the simulated data with all the disturbance parameters were combined and processed to derive the different SVIs from the specific band settings of the Landsat TM, MSR16R, APEX, S-2 and VENμS. After the LAI was estimated using the validation dataset statistical measures such as RMSE and R^2 values were computed. The procedure yielded the following statistics for the 11 SVIs considered (table 7).

Contrary to the SVI-LAI relationships introduced so far where the relationships were more or less defined exponentially, the IIReRs-LAI relationship follows a linear curve. As these indices demonstrated a better R^2 value and the smallest of all the RMSE values the linearity of the relationship is an indication of its better prediction power. The trend was similar for the different sensors (MSR16R, S-2, and APEX) where the band settings were similar. The results indicated that the SVIs considered best fitted to exponential functions defining their relations with the LAI values yielding better performances than others. The best fit functions for those indices were also found to be either linear or power functions instead of exponential relations (Figure 5). This was the case for a few indices such as SR, MSR and $IIReR_1$ and $IIReR_2$, whose relations with LAI were best explained linearly or as power functions. The validation results confirmed that the performance of the newly proposed indices, *$IIReR_2$ and $IIReR_1$* , hold as demonstrated by the smallest of all RMSE (i.e., 0.87 and 0.94) values based on MSR16R, for example, as well as the highest R^2 (0.81 and 0.82) values, respectively. They also showed consistently superior performance with R^2 values being 0.83 and 0.84 for IIReR1 and 0.84 and 0.83 for IIReR2 based on APEX and S-2, respectively.

On the other hand, $NDRE_1$, $NDRE_2$, WDVI, MSR and EVI had lower R^2 values. Yet, these indices showed consistency across the different sensors. It is also worth mentioning that NDVI, SR, ISR and NDII showed not only strong consistency but also better performance only next to IIReRs. NDVI showed strong consistency with R^2 value ranging between 0.72 and 0.79 for Landsat TM and MSR16R, respectively. The statistical analysis confirmed that the index is consistent across the five sensors as measured by the R^2 value being within the range of 0.72 (Landsat TM) and 0.79 (MSR16R). Moreover the RMSE value also confirmed the consistency of the index which for all the sensors was found to be between 1.0 (APEX) and 1.15 (Landsat TM). Similar result was reported for SR showing a consistent record across the narrow sensors with R^2 value ranges of 0.75 to 0.78, although its performance considerably dropped with TM (R^2 = 0.69). The SWIR based indices on the other hand saw a drop in performance for MSR16R with an R^2 of 0.65 and 0.72 for ISR and NDII where both had R^2 values of over 0.80 for other sensors (Table 7).

Table 7. Summary of statistical measures of the performance of SVIs across different sensors using the validation dataset (P-value < 0.01 for all SVIs).

Index	MSR16R		APEX		Landsat TM		Sentinel-2		VENμS	
	R^2	*RMSE*	R^2	*RMSE*	R^2	*RMSE*	R^2	*RMSE*	R^2	*RMSE*
IIReR2	0.82	0.87	0.84	0.86	-	-	0.83	0.88	-	-
IIReR$_1$	0.81	0.94	0.83	0.91	-	-	0.84	0.87	-	-
NDVI	0.79	1.01	0.78	1.00	0.72	1.15	0.77	1.07	0.75	1.07
SR	0.77	1.03	0.78	1.01	0.69	1.69	0.75	1.32	0.78	1.37
NDII	0.72	1.07	0.82	0.91	0.82	0.92	0.81	0.93		
ISR	0.65	1.24	0.79	1.01	0.80	1.00	0.80	1.00	-	-
NDRE2	0.56	1.46	0.52	1.51	-	-	0.53	1.50	0.53	1.47
MSR	0.51	2.12	0.54	1.49	-	-	0.53	1.51	0.54	1.46
WDVI	0.46	1.66	0.46	1.65	0.45	1.63	0.46	1.65	0.43	1.66
NDRE1	0.41	1.50	0.51	1.53	-	-	0.53	1.50	0.54	1.47
EVI	0.38	1.77	0.38	1.77	0.37	1.76	0.39	1.90	0.35	1.78

It is also interesting to note the variations in the sensitivity of those indices in response to varying leaf, soil and canopy parameters. The LAIe was obtained using the SRM model with the parameters already estimated with calibration dataset. The graphs in Figure 8 illustrate how the performance of those indices varies with varying parameters. It can be seen that many of the indices showed poor performance with low C_{ab} (20 μg.cm^{-2}) as well as with planophile LAD (Plano). This was particularly the case with NDVI, SR, IIReR$_1$, MSR, NDRE$_1$ and NDRE$_2$ where they all showed clearly distinguishable patterns, though to varying degrees. Exception to these were the SWIR based indices such as NDII, ISR and IIReR$_2$ as well as WDVI and EVI, which instead showed a different pattern in relation to the two parameters. For instance, the performance of ISR, NDII and IIReR$_2$ with C_{ab} level of 20μgcm^{-2} is comparable with their performance at higher C_{ab} levels. IIReR$_2$ instead showed high sensitivity to LAI at high C_{ab} level of 60 μgcm^{-2}. Moreover, IIReR$_1$, IIReR$_2$, ISR and NDII showed high sensitivity to LAI with erectophile LADs whereas the greenness indices such as NDVI, SR, MSR, NDRE$_1$ and NDRE$_2$ performed well with high leaf C_{ab} levels. For instance, NDVI showed high sensitivity to leaf C_{ab} levels with quick saturation effect with low level of C_{ab} where the LAI prediction hardly exceeded four (4). On the other hand, the index has performed well with high leaf C_{ab} levels where it showed a more linear pattern compared to its performance under other scenarios. It also showed considerable variation with varying LADs with the poorest performance being under planophile LAD, whereas it did well with an erectophile LAD.

On the other hand, the effect of canopy background as simulated by varying soil moisture levels did not have much effect on the performance of many of the SVIs. In fact, the overlapping curves for the three moisture levels confirms that many of the SVIs did show little or no sensitivity to the effects of variable soil moisture. This would be further discussed later under sensitivity analysis where a sensitivity function was used to test if the responsiveness of the different SVIs to LAI could be distinguished across LAI ranges. Analogous to the overlap observed with moisture levels is the consistency of the performance of ISR, NDII and IIReR$_2$ with varying C_{ab} levels.

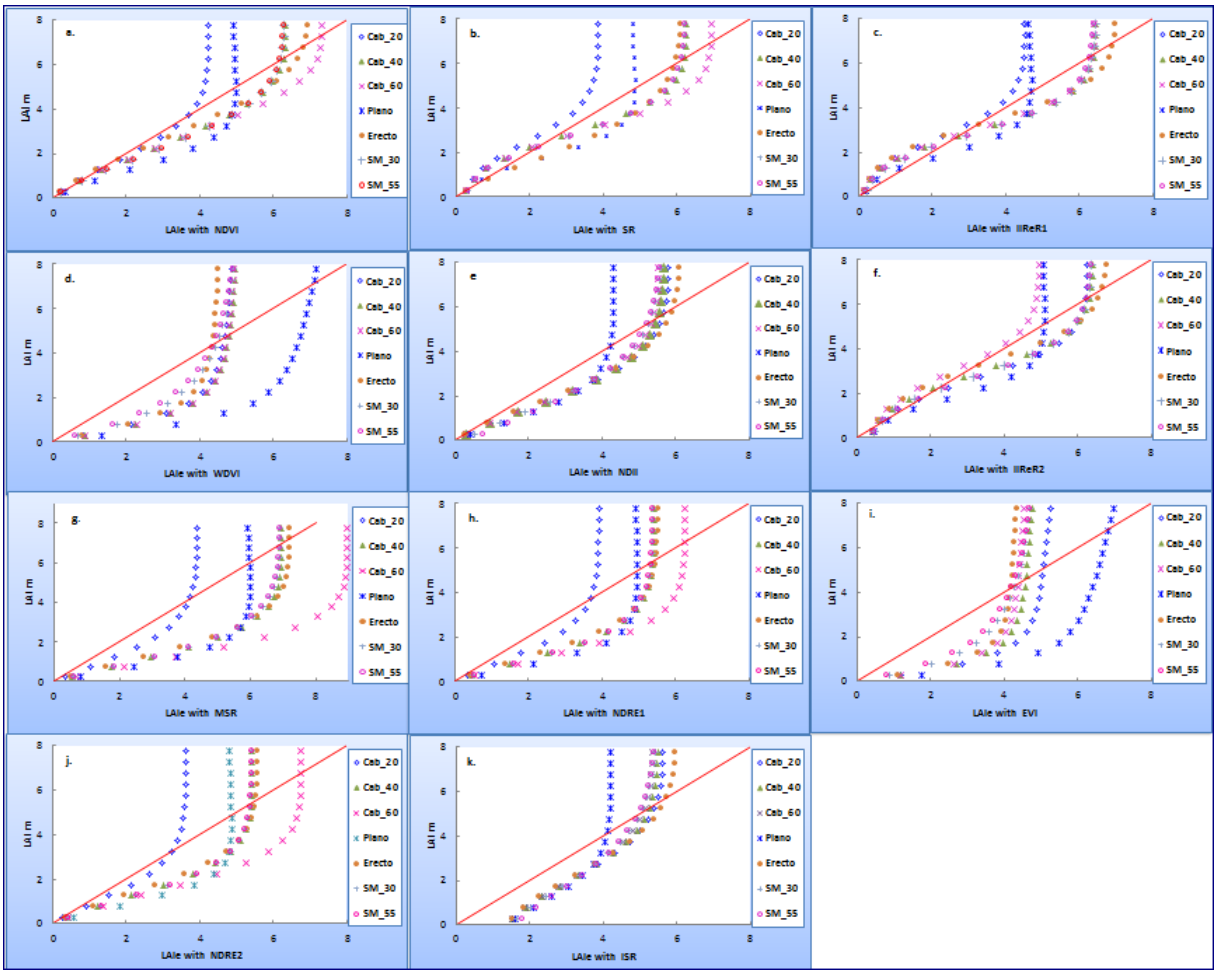

Figure 8. Validation of the performance of SVIs using independent datasets. NDVI (a), SR (b), IIReR1 (c), WDVI (d), NDII (e), IIReR2 (f), MSR (g), NDRE1 (h), EVI (i), NDRE2 (j)and ISR (k) were tested for varying leaf, soil and canopy parameters where the predicted LAI (LAIe) with each index is plotted against the measured or simulated (LAI m). In addition to the information provided in the legend the spherical LADs and bright soil (SM_5%) had the same value with Cab_40 µgcm-2 as these parameters were set to default in all the combinations.

A further analysis of the performance of those SVIs with the different leaf, soil and canopy parameters was performed using the validation datasets based on MSR16R band settings. The result confirmed the graphical illustrations already presented (Figure 8) in that almost all the SVIs showed the highest RMSE values while predicting LAI with planophile LADs (figure 9). Exception to this was the MSR which had similar levels of accuracy, though poor, for the three LADs considered. It can also be seen from the graph (figure 9) that the least RMSE was reported with erectophile LADs followed by spherical LADs where the value for the latter was the same as C_{ab} 40 µgcm^{-2}. One can also see that $IIReR_2$, $IIReR_1$, SR, NDII and NDVI reported the smallest overall RMSE making them suitable for LAI prediction in the same order.

A similar procedure was implemented based on variable leaf Cab levels of 20, 40 and 60 µgcm-2. Parallel to what could be observed from Figure 8 where many of the greenness indices such as NDVI, SR, NDRE1, NDRE2 and MSR showed the poorest performance with low leaf Cab, the highest RMSE was reported with Cab level of 20 µgcm-2 for almost all the SVIs except for MSR. On the other hand, all of those indices excluding MSR had the lowest RMSE with high leaf Cab (60 µgcm-2) followed by intermediate (40 µgcm-2) Cab level. The

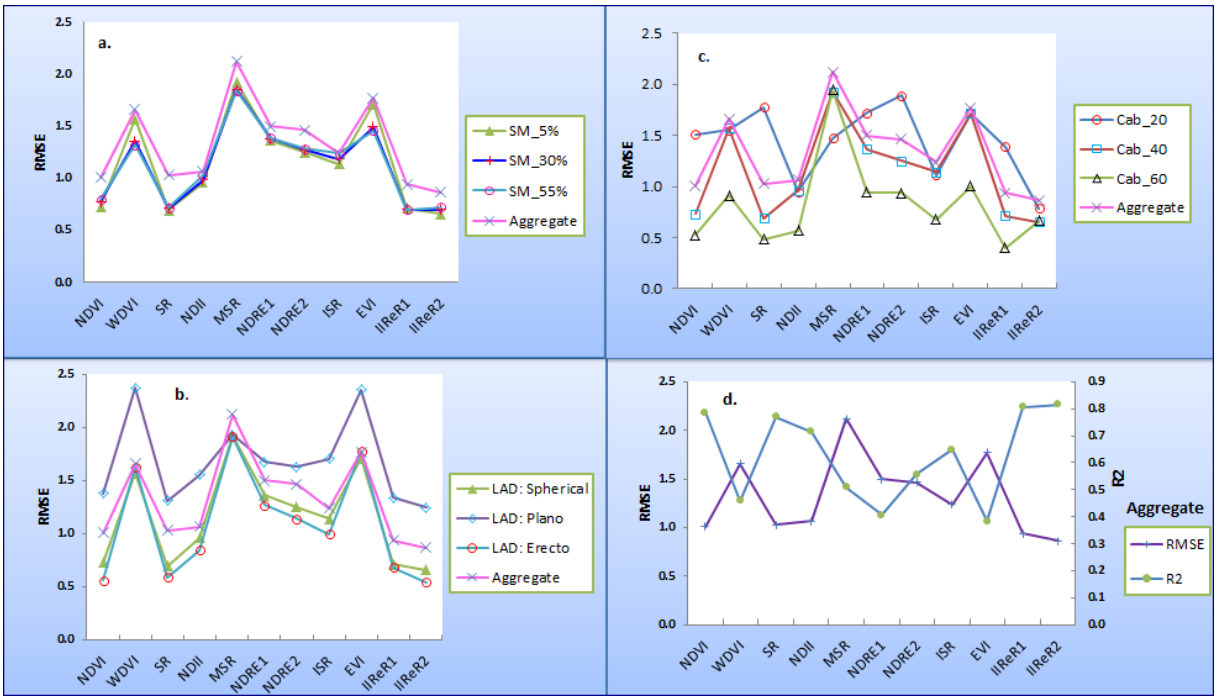

Figure 9. Results on the validation of the performance of SVIs with varying soil moisture levels (a), LADs (b), leaf Cab levels (c) and all parameters combined (d) as simulated based on the MSR16R band settings

gap in the RMSE values appeared to be high for those greenness indices while it was relatively narrow for those SVIs derived partly based on the SWIR bands.

Contrary to expectations, the result showed more consistent performance for almost all the SVIs at varying soil moisture levels. However, there is still a considerable variation among the indices in the level of insensitivity to canopy background effects. IIReR1, IIReR2, SR and NDVI did not only show similar records at the three moisture levels, but also performed well as indicated by their small RMSE values. On the other hand, EVI and MSR showed the poorest performance as was the case with other leaf and canopy parameters. Furthermore, WDVI and EVI showed more sensitivity to bright soil background as compared to the other indices.

4.1.5 Results on sensitivity analysis based on PROSAIL model

The sensitivity functions were computed for each SVI following the SVI - LAI relationships defined based on both bivariate linear regression and non-linear regression models. A comparison was made between the exponential model based on the Beer Lambert's model and the best fitting function defined from the SVI-LAI relationship established based on the simulated data. Hence LAI was regressed as a function of SVI which permits the computation of the proportion of variability of each SVI (dependent variable) in response to a unit of change in the LAI (independent variable). To this end, the inverse of the derivative was taken because the interest in this case was to examine the responsiveness of SVIs to changes in LAI. The ratio of the first derivative of the regression function, (dSVI/dLAI), to the standard error of the estimated LAI, ($\boldsymbol{\sigma}_{\hat{\mathbf{Y}}\mathbf{i}'}$), was used to derive the *S* function across the range of LAI values.

The *S* function depicted in the graph (Figure 10) demonstrates the sensitivity of the SVIs analysed in this study. The analysis was based on the dataset generated based on spherical LAD, bright soil with 5% soil moisture, and leaf Cab level being set at 40µgcm-2. These combinations were chosen for demonstrating the SVI-LAI sensitivity as the LAD and C_{ab}

level chosen were meant to represent the potato crop best with bright soil background. The performance of the SVIs might vary under different circumstances making the knowledge about their sensitivity important for applying the appropriate SVI whenever deemed essential. Moreover, this assessment is based on the band settings of the MSR16R sensor and hence there is no guarantee regarding the consistency of the levels of sensitivity for other sensors, and hence need to be tested.

The result of the analysis indicated overall a high sensitivity at a low vegetation density. After the LAI value reached a value of four all the indices plotted with the exception of SR and IIReR exhibited a quick drop in sensitivity and they eventually became insensitive after the point where the vegetation density reaches an LAI of 4 and beyond (Figure 10). The degree of sensitivity was quite high at low LAI for most of the SVIs for which the best fitting function was exponential. On the other hand, the other SVIs with more or less uniform levels of sensitivity such as SR, $IIReR_1$ and $IIReR_2$ as well as MSR showed better sensitivity than others over a wide range of LAI. These SVIs had a gradually increasing sensitivity with increase in vegetation density, reaching their peak around an LAI value of 4.5 to 5 after which their sensitivity started to decline with a further increase in LAI.

Based on the sensitivity function plotted it is clearly shown that many of the SVIs, such as NDVI, NDII, ISR, NDRE1 and NDRE2, were more sensitive at low LAI values of up to 2, beyond which the sensitivity saw a sharp decline and eventually became insensitive after LAI value of four. More importantly, NDVI saw quite high sensitivity at low LAI ($LAI \leq 2$) while its sensitivity quickly dropped at moderately high LAI eventually becoming insensitive ($LAI \geq 4$). The statistical analysis also indicated that SR, $IIReR_2$, $IIReR_1$, MSR, WDVI, and EVI were sensitive for the full LAI range considered at 95% confidence level. The minimum acceptable sensitivity level beyond which an SVI in considered insensitive as indicated by the solid red line in the graph (figure 10) is 2.042. This corresponds to a t-value at a p-value of 0.05 and a degree of freedom = 30 as the number of observation was 32. Following this, a few indices such as NDVI, NDII, ISR and $NDRE_1$ and $NDRE_2$ became totally insensitive for higher LAI ranges as the sensitivity function crosses the threshold (*S=2.402*) beyond which the corresponding SVI was not sensitive anymore. This indicates that any of these indices could be used for LAI mapping for low vegetation densities making NDVI and NDII most suitable for low vegetation density ($LAI \leq 2$). Similarly, $IIReR_1$, $IIReR_2$, SR and MSR appeared to be suitable for LAI ranges beyond 1.75 through higher vegetation densities. Moreover, they maintain considerable degree of stability in the degree of their sensitivities over a wider range of LAI as opposed to other SVIs which saw a sharp decline with a slight increase in LAI values. Nevertheless, all SVIs might also exhibit varying levels of sensitivity with different models (best fit vs. SRM) as well as with the empirical field data hence demanding the empirical verification on the degree of sensitivities based on the analysis of field measurements. Therefore, the sensitivity of the indices to different disturbance factors will be dealt with in the subsequent sections.

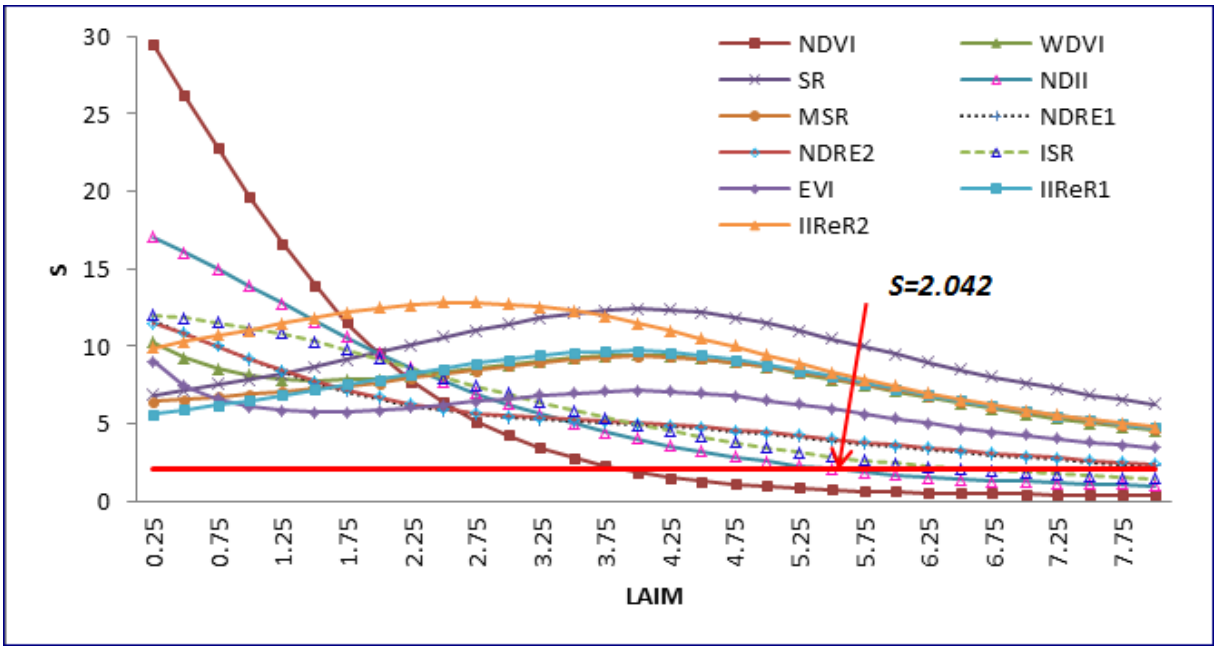

Figure 10. Sensitivity analysis of SVIs based on the exponential model

4.1.5.1 SVIs sensitivity to different leaf Cab levels

The analysis of SVIs based on three different leaf C_{ab} concentrations (20 µgcm^{-2}, 40 µgcm^{-2}, and 60 µgcm^{-2}) showed varying performance levels. Although many of the SVIs performed well with high leaf C_{ab} concentrations, the IIReR2 followed by NDII seem to have been consistent in a low leaf C_{ab} (20 µgcm^{-2}) situation as well. The situation was different for WDVI and MSR where the RMSE value at leaf C_{ab} value of 40 µgcm^{-2} slightly exceeded the corresponding RMSE value at C_{ab} = 20 µgcm^{-2} which implies a lack of clear pattern regarding their performance. Nevertheless, all other SVIs had superior LAI estimation power at high leaf C_{ab} concentrations with *$IIReR_1$, SR, NDVI, NDII, and $IIReR_2$* being among the best performing ones.

Table 8. Sensitivity of SVIs to different leaf Cab levels (P-value < 0.0l for all SVIs)

SVIs	20 µgcm^{-2}		40 µgcm^{-2}		60 µgcm^{-2}	
	R^2	RMSE	R^2	RMSE	R^2	RMSE
NDVI	0.83	1.51	0.91	0.73	0.94	0.53
WDVI	0.67	1.55	0.64	1.57	0.64	0.91
SR	0.88	1.48	0.91	0.69	0.92	0.48
NDII	0.86	0.95	0.85	0.96	0.85	0.57
MSR	0.76	1.47	0.74	1.92	0.73	1.95
$NDRE_1$	0.72	1.72	0.71	1.36	0.71	0.94
$NDRE_2$	0.73	1.89	0.74	1.25	0.77	0.94
ISR	0.90	1.11	0.89	1.14	0.89	0.68
EVI	0.60	1.72	0.58	1.71	0.58	1.00
$IIReR_1$	0.89	1.39	0.91	0.71	0.92	0.40
$IIReR_2$	0.89	0.79	0.92	0.66	0.93	0.67

The analysis of all the three Cab levels using the sensitivity function indicated the presence of a slight difference in the sensitivity levels for the different C_{ab} levels. Figure 11 presents the sensitivity analysis based on leaf Cab of 20, 40 and 60 µgcm-2. In all the three cases spherical LAD and bright soil moisture was assumed constituting similar modelling environment with the previous sensitivity threshold S (Figure 11). This was used to indicate how sensitive each of those SVIs was to the LAI ranges. The result could be compared to the statistical indicators summarized in table 8. Those SVIs with low RMSE values such as SR, IIReR1 and IIReR2 also performed well under the sensitivity analysis as demonstrated by the high sensitivity values at high LAI (LAI > 1.75). Other SVIs such as NDVI, NDRE1, NDRE2, ISR, NDII, and EVI exhibited high sensitivity at low LAI values (LAI < 2) beyond which their sensitivity decayed exponentially and eventually approaching the critical S (S= 1.96) at high LAI values (LAI > 5). The threshold, in this case (S = 1.96), indicates the minimum acceptable *S* value below which any SVI is considered insensitive to LAI. As already introduced, this corresponds to the student's test statistic (t-value) at a chosen P-value (in this case, 0.05 or 95% confidence level) and at the degree of freedom (in this case, 16-2=14). Because the number of observations considered in this analysis contained 16 LAI values for which the corresponding SVI estimations as well as standard error computations were made to derive *S*.

Although the sensitivity function explains the degree of performance of the indices there were contradictions between the RMSE values reported and the sequence in the level of sensitivity. This was the case for NDVI which had a smaller RMSE at least compared to NDRE1, NDRE2, EVI and WDVI (table 9), but reported to be the least sensitive of all the SVIs analysed because it became less sensitive over a wider range of LAI values (LAI > 3) (Figure 11).

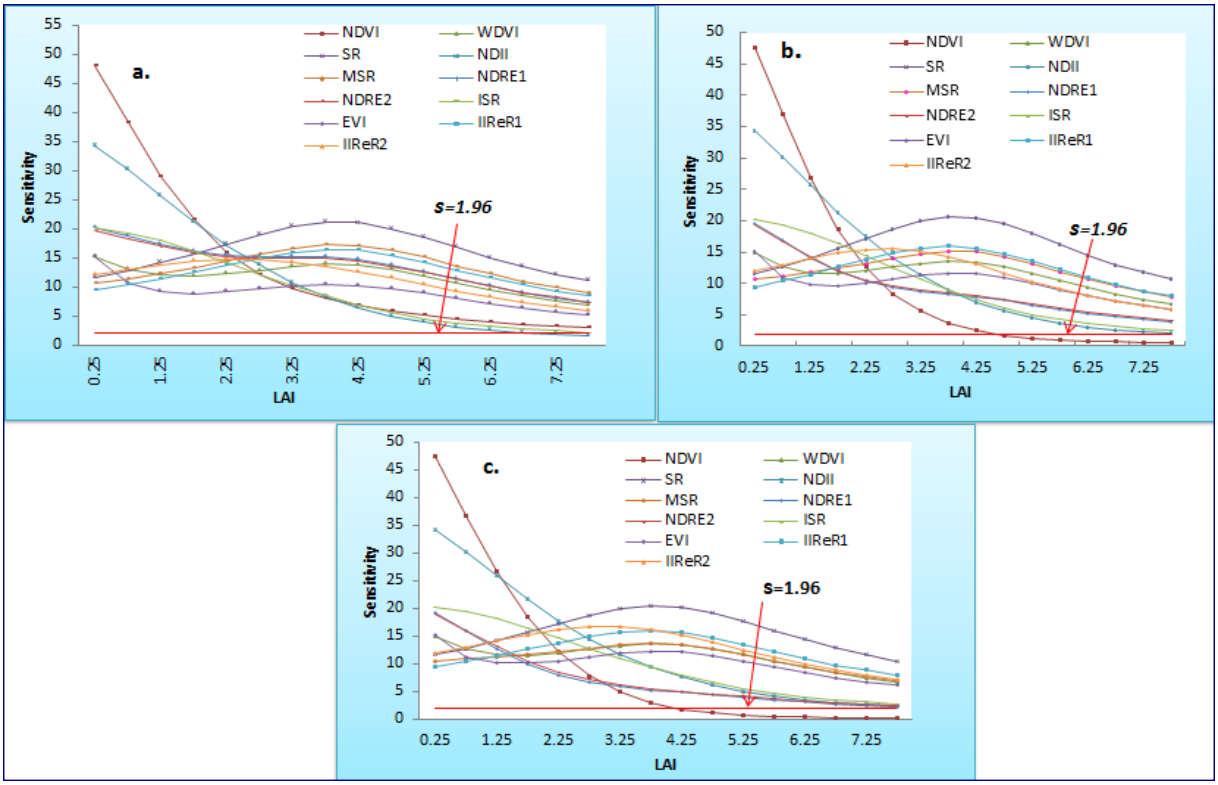

Figure 11. Sensitivity analysis based on the SRM at leaf Cab level of 20 µgcm-2 (a), 40 µgcm-2 (b) and 60 µgcm-2 (c) with Spherical LAD and bright soil background.

Contrary to expectations, there was also lack of consistency regarding the performance of those indices as well. NDVI, despite its relatively low RMSE compared to some other SVIs, saw a quick drop in its sensitivity to a point where it was not sensitive (LAI > 3.75) at 95% level of confidence. However, NDVI sustained an acceptable level of sensitivity over a wider LAI range. NDII also had a similar pattern where it was found to be sensitive up to high LAI (LAI = 5) based on the SRM while it saw a dramatic drop with the best-fit-function because its sensitivity was limited to low LAI (LAI < 2) (Appendix 5A).

4.1.5.2 SVIs sensitivity to canopy background effects

The simulated spectral data with different percentages of soil moisture was also analysed separately. Based on the non-linear regression using the SRM the results for many of the SVIs were consistent across the three different soil moisture levels. The consistency in the performance of the SVIs across the three soil moisture levels showed that the indices are not susceptible to soil moisture. However, the persistent poor performance of some of the SVIs such as MSR, EVI, $NDRE_1$, and WDVI might be attributed to some other factors. The NDVI and SR also proved to be consistently good as illustrated by their lower RMSE values in comparative terms. Contrary to expectations, the result for some SVIs indicated higher RMSE values for high soil moisture levels. The summarized statistical measures regarding the performance of those SVIs were provided in table 9.

The S function was also calculated to see whether the performance of the SVIs could be distinguished and to examine their sensitivities to the different canopy backgrounds as simulated by varying soil moisture levels. The overall sensitivity function revealed similar patterns for the three moisture levels, bright (a), intermediate (b) and moist (c) (Figure 12). Some of the SVIs, which had a better performance as indicated by their low RMSE values, also showed higher sensitivity as demonstrated in the graphs (Figure 12). This holds for SR, $IIReR_1$, and $IIReR_2$ which had a higher sensitivity curve compared to other indices particularly at high LAI values (LAI > 3.25). Contrary to expectations the sensitivity analysis showed high sensitivity for those SVIs which had reported high RMSE values as well. This included MSR, WDVI, $NDRE_1$ and even EVI, which had a relatively high sensitivity for high LAI ranges. Two indices, NDII and NDVI, reported high sensitivity at low LAI (LAI < 3) with NDVI experiencing significant drop eventually becoming insensitive at moderately high LAI (LAI > 4) while NDII maintained a considerable level of sensitivity until it became insensitive at high LAI (LAI > 6).

Table 9. Sensitivity of SVIs to different soil moisture levels (P-value < 0.01 in all SVIs)

SVIs	SM=5%		SM=30%		SM=55%	
	R^2	RMSE	R^2	RMSE	R^2	RMSE
NDVI	0.91	0.73	0.90	0.78	0.90	0.80
WDVI	0.64	1.57	0.79	1.36	0.82	1.32
SR	0.91	0.69	0.91	0.71	0.90	0.72
NDII	0.85	0.96	0.87	0.98	0.88	1.03
MSR	0.74	1.92	0.75	1.86	0.75	1.84
$NDRE_1$	0.71	1.36	0.71	1.38	0.70	1.39
$NDRE_2$	0.74	1.25	0.74	1.27	0.74	1.28
ISR	0.89	1.14	0.91	1.19	0.92	1.24
EVI	0.58	1.71	0.76	1.49	0.79	1.46
$IIReR_1$	0.91	0.71	0.91	0.70	0.91	0.70
$IIReR_2$	0.92	0.66	0.91	0.70	0.91	0.72

Most of the analysed SVIs reported an acceptable level of sensitivity under all soil moisture levels. As can be seen from the graph (Figure 13) the sensitivity function had similar pattern under the three soil moisture levels proving the negligible effect of variation in soil moisture on the performance of those SVIs. Moreover, the sensitivity function for many of the SVIs, with the exception of NDVI, NDII and ISR, was found to be above the critical *S* (s = 1.96) for the entire LAI range showing their acceptable level of sensitivities to LAI. The level of sensitivity was also significant at 95% confidence level (P-value = 0.000) for SR, MSR, $IIReR_1$, WDVI, $IIReR_2$, $NDRE_1$ and $NDRE_2$, in this order of decreasing sensitivities. The graphs presented in figure 12 show the consistency of the sensitivities of the SVIs under the different soil moisture levels.

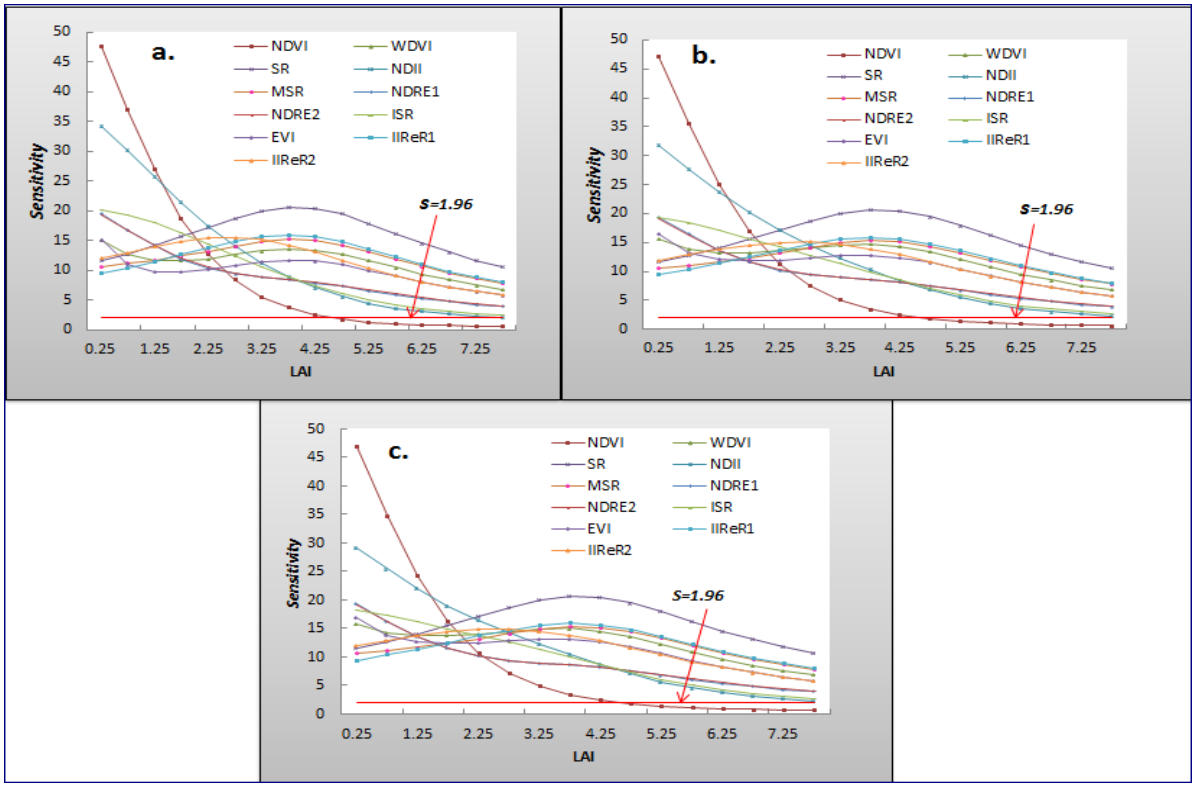

Figure 12. SVIs Sensitivity to LAI under a) bright, b) intermediate and c) moist soil conditions

4.1.5.3 SVIs sensitivity to canopy LADs

The analysis of the SVIs under different leaf orientations showed differences in the performance of those indices. All the indices relatively performed well for the vertical leaf orientations (erectophile) as can be seen from their low RMSE values compared to planophile. This particularly holds for NDVI, WDVI, SR, NDII, ISR, and IIReRs for which the RMSE is twice as low as the corresponding RMSE values for a planophile LAD. On the other hand, MSR, $NDRE_1$ and $NDRE_2$ maintained more or less similar values of RMSE at both leaf angle orientations. The same holds for WDVI, which had an RMSE value of (1.63 *vs.* 2.37), SR (0.59 *vs.* 1.31) and NDII (0.84 *vs.* 1.56), for erectophile and planophile, respectively.

On the other hand both the IIReRs surprisingly had a better RMSE value at a planophile LAD compared to the other SVIs, although they followed the general trend of superior performance with erectophile LAD with the lowest RMSE (0.54 and 0.68). These two indices maintained relatively better LAI estimation margins over the other SVIs analysed. Secondly, the inclusion of the red edge in the derivation of these indices made them relatively resilient to vegetation densities as the amount of light absorbed by photosynthetically active leaves were accounted

Table 10. Sensitivity of SVIs to canopy leaf orientations (P-value <0.01 in all SVIs)

SVIs	*Planophile*		*Spherical*		*Erectophile*	
	R^2	RMSE	R^2	RMSE	R^2	RMSE
NDVI	0.73	1.38	0.91	0.73	0.96	0.56
WDVI	0.48	2.37	0.64	1.57	0.63	1.63
SR	0.76	1.31	0.91	0.69	0.94	0.59
NDII	0.74	1.56	0.85	0.96	0.89	0.84
MSR	0.65	1.93	0.74	1.92	0.93	1.91
NDRE1	0.61	1.68	0.71	1.36	0.75	1.27
NDRE2	0.64	1.63	0.74	1.25	0.79	1.14
ISR	0.77	1.71	0.89	1.14	0.93	1.00
EVI	0.34	2.35	0.58	1.71	0.56	1.78
IIReR1	0.76	1.34	0.91	0.71	0.94	0.68
IIReR2	0.68	1.25	0.92	0.66	0.95	0.54

for. Table 10 presents the statistical measures of the relative performances of those indices under different canopy leaf orientations.

With regard to the sensitivities of the SVIs under different LADs the sensitivity function reported different levels of sensitivities. Most of the SVIs performed well with an erectophile LAD whereas the overall sensitivity level was lower with the planophile LADs. The pattern of sensitivity under spherical LAD was the same with the one discussed under C_{ab} level of 40 μgcm^{-2}, because the spherical LAD was assigned as default PROSAIL model value under varying C_{ab} and soil moisture levels. As a result, the sensitivity result presented in the previous section (Fig.12 b same as Fig.13b) corresponds to the spherical LAD indicating high sensitivity level for NDII and NDVI at low LAI while SR, MSR and $IIReR_1$ had better performance than other SVIs over the higher LAI ranges. Moreover, those indices which had high sensitivity at low LAI saw a quick drop in their sensitivity with increase in LAI whereas SR, $IIReR_1$ and $IIReR_2$ clearly performed well across the higher LAI ranges. The better performance of these SVIs complies with their low RMSE values except for the MSR, which despite its high RMSE value, had a high sensitivity record. The sensitivity function (Fig 13) also indicated a decline in the sensitivity of NDVI, for example, with spherical and erectophile which contradicts with R^2 measures corresponding to theses LADs.

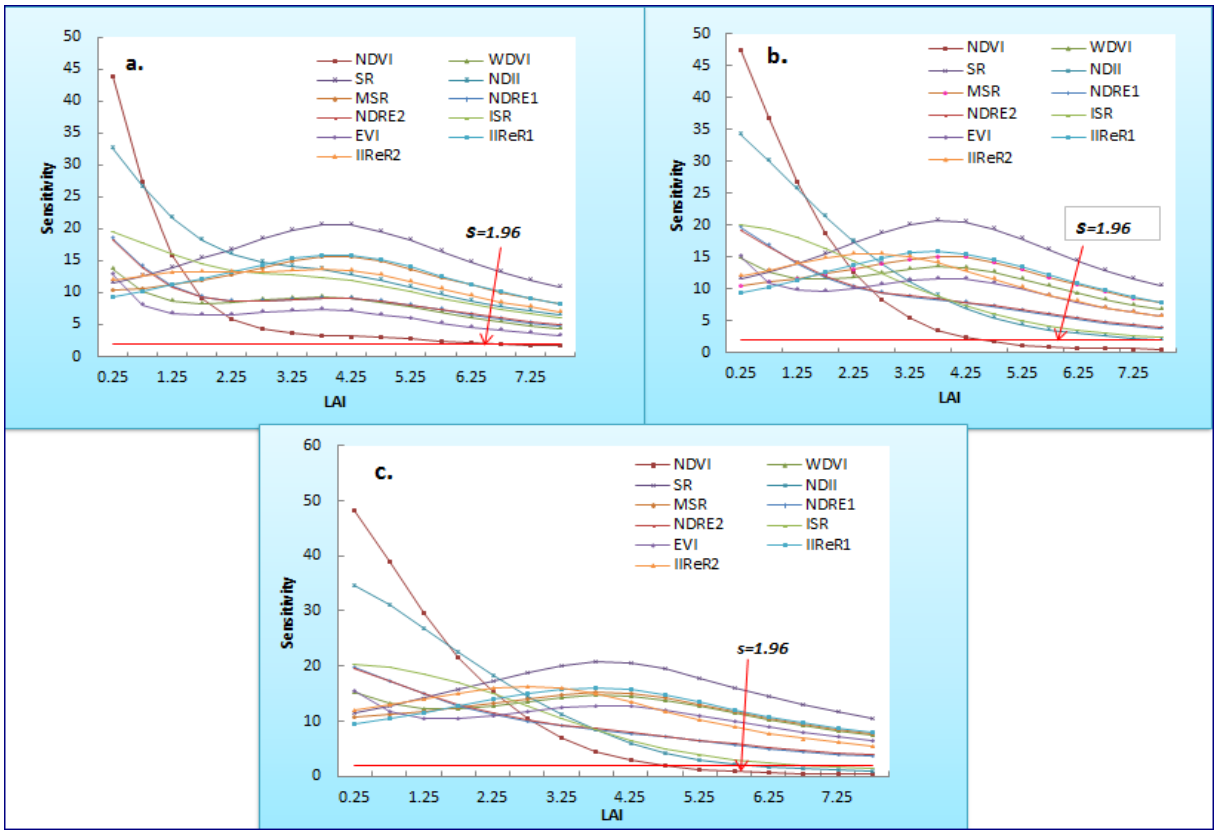

Figure 13. A comparison of sensitivity analysis for planophile (a), spherical (b) and erectophile (c) LADs based on SRM.

Nevertheless, the sensitivities functions (Fig.13) also revealed the highest sensitivity for NDVI and NDII at low LAI for erectophile LADs. The overall assessment showed improved sensitivity of SVIs under the erectophile LAD. This was, for example, demonstrated by NDVI which maintained some degree of sensitivity up to an LAI = 4.5, a point where it lost its sensitivity. NDII also had high sensitivity at low LAI whereas SR, IIReR1 and $IIReR_2$ had better sensitivity than others. In general the SVIs considered were most sensitive for LAI under an erectophile LAD followed by spherical and least sensitive with planophile LADs .

A further comparison of the sensitivity based on the best fit and the exponential function, performed for a planophile LAD also reported some differences between the two methods (Appendix 5B). Almost all the SVIs analyzed using the best-fit had high sensitivity at very low LAI followed by a steep drop of sensitivity for NDVI, EVI, WDVI, $NDRE_1$ and $NDRE_2$ with slight increase in LAI values (LAI > 2). On the contrary, this same LAI level was a point at which the sensitivity saw an upward jump with the exponential model (Appendix 5B). The sensitivity result with the exponential model showed better performance for NDII, ISR, MSR, IIReR1 and IIReR2 in decreasing order. Moreover, most of the SVIs saw an initial raise in their sensitivities with increase in LAI reaching their peak at LAI = 4.25 beyond which they steadily declined. The overall sensitivity for most of the indices were higher with the exponential than what was reported with the best-fit model On the other hand, NDRE1, NDRE2, WDVI and NDVI were found to be less sensitive with NDVI being below the critical *S* level from fairly low LAI (LAI = 3.25) onwards. Moreover, those SVIs derived partly based on the SWIR region of the spectrum performed well with the exponential model.

4.2 Results based on empirical data

4.2.1 Monitoring LAI through the growing seasons

The results from the empirical measurements of LAI for the 12 experimental plots during the 2011 growing season on average showed an increasing trend characterized by quick take-off during the first sampled four weeks (Figure 13). The LAI value on average reached its peak around the 27th June 2011 followed by an abrupt break reaching its dip during 11th of July 2011 from where it started to slightly revive during the next two weeks. This means that the peak LAI was sampled during the 11th week since the planting date was 12th April 2011. The trend showed that the overall LAI value saw a gradual decline starting 18th of July 2011, eventually reaching the lowest value at the last time the measurement was performed. The abrupt break in the LAI value at the 11th of July 2011, which is the feature of all the 12 plots might be attributed to certain climatic factors such as heavy storm which might have led to the wear down of the potato leaves when the measurement was acquired. The magnitude of the break during the 6th week is apparently comparable across the field, which is attributed to the effect of heavy storm on the 28th of June 2011. The gradual decline during the last couple of weeks should however be due to the maturity of the crop and the leaf foliage as the potato crops would not continue to grow anymore (Figure 14). The figure demonstrates the trend in the potato LAI throughout the growing season. With regard to the plot specific records of the LAI acquired, three plots, namely; C, D, and K followed by A, B and L had consistently low records whereas the LAI for the other plots were hardly distinguishable lacking a clear pattern for comparison as shown in figure 14.

4.1.1 The effect of differential nitrogen application on potato LAI

It has been discussed that the plots were subjected to various initial nitrogen fertilizations as well as differential treatments during the growing season (see section 3.1). The results showed differences of various magnitudes particularly between the blocks that received different initial nitrogen application. The analysis of variance between the different set-ups and subsequent LSD analysis showed a statistically significant difference (p-value: 0.000) between the blocks given 0, and the other three with 161, 242 and 322 kg N/ha. However, the difference in the LAI values between those three blocks, which had certain amount of nitrogen, was not statistically significant at 95% level of confidence.

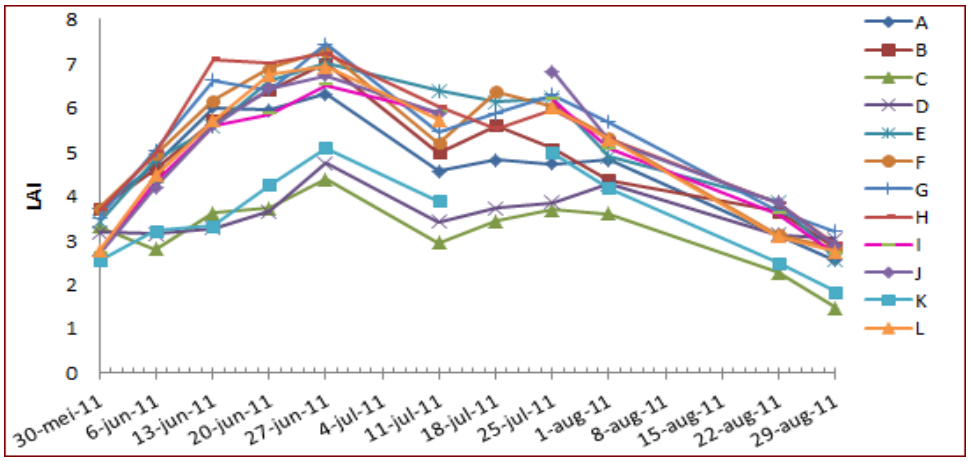

Figure 14. Average LAI per plot for 2011 growing season

This implies that the LAI value for potato depends to a greater extent on the level of initial nitrogen fertilization regardless of treatments made during the growing season. The fact that the LAI for plots C, D and K was consistently low justifies the decisive role of initial fertilizer application. On the other hand, the difference in the average LAI measured between the treatment groups (CL, MB, and TTW) was not statistically significant at 95% level of confidence. It can be seen from the graphs (Figure 14 and Figure 16) that plot given low or no initial fertilization had consistently low LAI records throughout the growing season regardless of the different treatment they received afterwards. Moreover, the interaction effects of initial fertilization and treatment during the growing season appeared to have affected the crop growth (Figure 15a&b). This was however found to be not significant at 95% confidence level. On the other hand, Figure 15 (c) clearly illustrates the difference between the average LAI values based on initial nitrogen application whereas the differences in mean LAI introduced due to treatment during the growing season (CL, MB, and TTW) (Figure 15d) is negligible as was also confirmed by the statistical tests through the analysis of variance (P-value > 0.1) (Appendix 15).

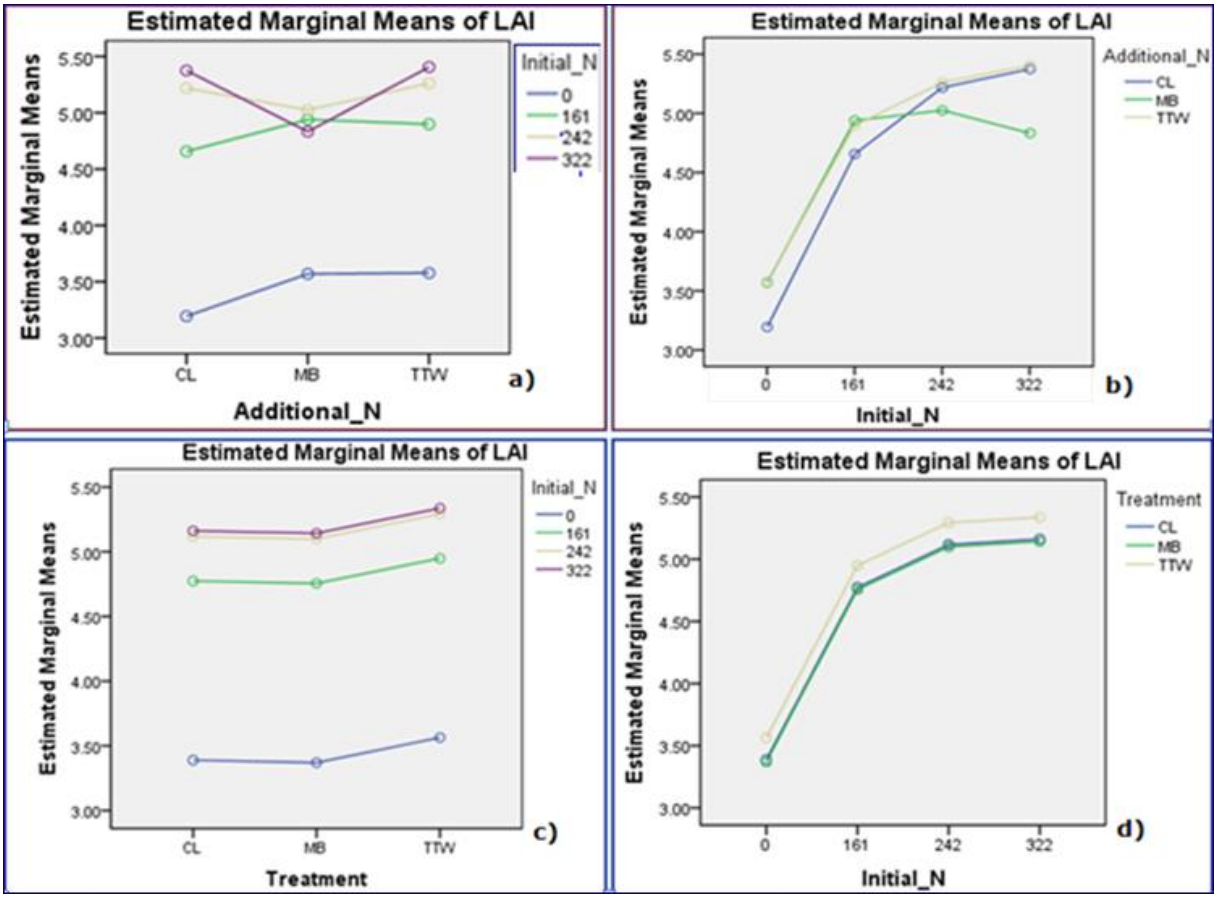

Figure 15. Variation in average LAI based on initial nitrogen application and treatment during the growing season showing the interaction effect for initial nitrogen (a) and treatment (b) and main effects for initial nitrogen (c) and treatment (d).

A further analysis of the effect of differential nitrogen treatment was also compared with the additional nitrogen application during the 2011 growing season. A similar pattern was depicted where plots with no initial nitrogen followed by those with little fertilization consistently had low average LAI throughout the growing season for which samples were taken. The effect of treatment during the growing season still lacked a clearly distinguishable pattern as the curves for the three treatment classes were close if not overlapping for the entire period for which samples were acquired.

Furthermore, the analysis of variance on the average LAI among the four treatment groups was performed to examine the impact of the interventions on the growth of the potato crop for the 2012 growing season based on LAI as measured by LAI-2000. This showed that zero (0) treatment blocks (plots G & H) which were given no fertilizer of any kind had a consistently low record of LAI throughout the growing season followed by treatment blocks 1 (plots A & B) which received the least amount of fertilizer. On the other hand, treatment blocks 3 (plots C & D) and 2 (plots E & F), which received higher doses of fertilizer in the same order reported higher LAI values in their respective order. The ANOVA also revealed a statistically significant difference in the mean LAI between the treatment blocks for the 2012 site (Appendix 16). Accordingly a significant mean difference was revealed between plots without nitrogen and those with higher fertilization levels (117 and 218 $kgha^{-1}$) with P-value of 0.013 and 0.005. In addition the difference in mean LAI was also significant [p-value = 0.033] between plots with 43 $kgha^{-1}$ and those with highest nitrogen, 218 $kgha^{-1}$. As illustrated in Figure 13 the value of LAI had also similar sequence as the amount of fertilizer applications: meaning higher fertilizer application yielding higher LAI values. This pattern, however, did not last for the entire growing season as the LAI value for treatment block 1 became higher than the value for block 2 during the last three weeks of the growing season, the last time the measurement was performed. This might imply that plots, which already received a higher fertilizer doze, grew faster and matured earlier and hence leaf foliage died earlier. On the contrary, under circumstances of sub optimal or low fertilizer application, crops might continue to experience a steady growth hence maintaining their leaves for some time. This in turn might mean a slightly extended growing season due to stunted plant growth in cases of low fertilizer application whereas high fertilizer application enables the potato crop to grow faster during early growing season and hence mature earlier.

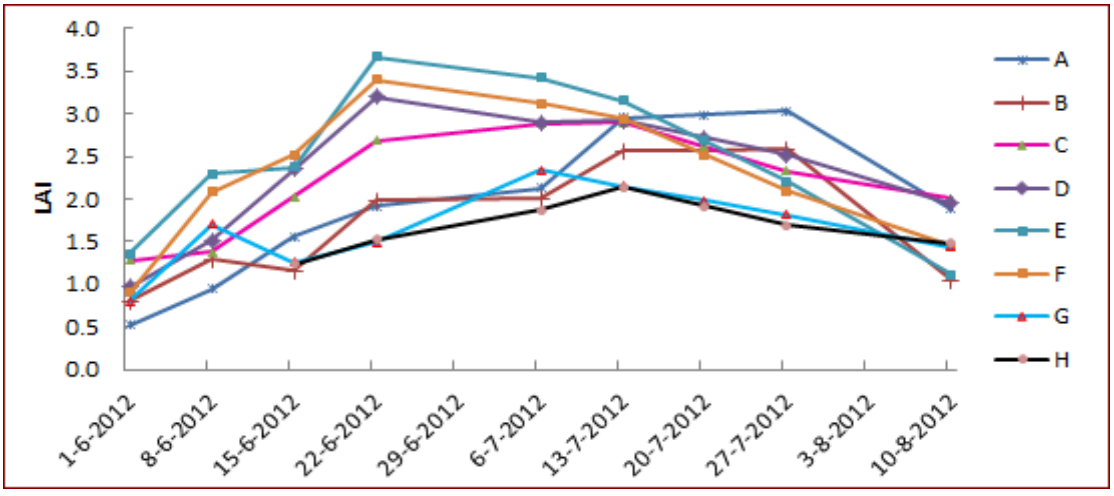

Figure 16. Average LAI per plot based on nitrogen fertilization levels for 2012 growing season

4.1.2 Comparison of weather parameters for 2011 and 2012 growing seasons

A comparison of the LAI curve for the two growing seasons showed significant variations, whereby the LAI measured during 2011 exceeded by far the corresponding values for the 2012 growing season. As already discussed in the previous section, a significant variation in the mean LAI among the treatment blocks in the same growing season was attributed to differential nitrogen treatments. The differences in the amount of fertilizer applied did vary not only among treatment plots in the same year but also varied between the two growing seasons. Accordingly, the amount of nitrogen applied was considerably lower in 2012 than in 2011. Obviously this could be one of the reasons for the high LAI values in 2011, which exceeded the LAI values of 2012 by almost two fold. On the other hand, the overall growth condition of the potato crop in the 2012 growing season also showed a considerable decline, where the maximum LAI was only as high as the minimum LAI value at the sampling dates for 2011. This significant difference in LAI may not only be explained by the amount, nature and timing of fertilizer applied, but also the variability in the elements of weather such as temperature, precipitation and total sun hours might have had a significant contribution to affecting the crop growth.

Apart from the level of fertilizer applied, it is also important to note that the two growing seasons had different physical environments, which had an important role in affecting the growth of crops in general and potato in particular. These include differences in soil conditions because the farms were located at different geographical locations. The soil condition for the 2012 plots being characterized as a poorly developed sandy soil with a thin 'A' horizon might have affected the growth of the potato crop. Moreover, the elements of weather and climate such as precipitation, temperature and total sun hours were also different which might have contributed to the differences in the growth level of the potato crop between the two sites and growing seasons. The analysis of meteorological data showed more favourable weather for the 2011 growing season with higher total temperature and more sun hours as compared to the 2012 growing season (Figure 17). On the other hand the total rainfall amount was higher during the 2012 growing season. A statistical analysis using a paired t-test also indicated a significant mean difference (p-value = 0.000) in the amount of rainfall, temperature and sun hours between the two growing seasons (Appendix 7). However, the fact that the 2012 growing season was characterized by lower cumulative temperature and less sun hours compared to its 2011 counterpart was not favourable for the optimal growth of crops in general and potato in particular.

These weather parameters as well as soil conditions coupled with the overall low nitrogen application during the 2012 growing season resulted in the stunted growth of the potato crop and hence low LAI compared to the 2011 site, which had more favourable weather, well developed soil as well as high nitrogen application. The cumulative values of those weather parameters as depicted in Figure 17 illustrate the trend through the growing season for the two years. Figure 17 indicates the cumulative values for the three weather parameters T (temperature in degree Celsius), SH (sun hour duration in hours), and RF (rain fall in mm) for the 2011 and 2012 calendar years. The computation of those parameters started at the calendar dates which correspond to the planting dates (12^{th} and 14^{th} of April 2011/2012) of the potato crop for the two growing seasons.

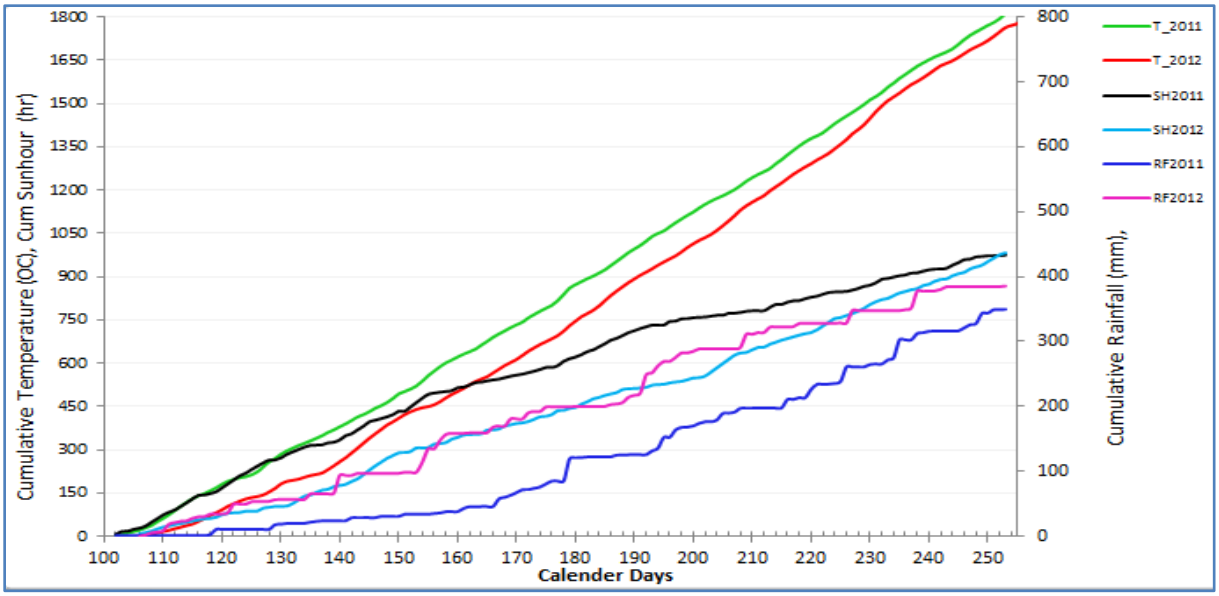

Figure 17. Cumulative weather parameters during the 2011 and 2012 growing seasons

4.1.3 Relationships between LAI and biomass

An analysis of the relationship between fresh above ground biomass and LAI for the two sites was performed. The result showed better relationship for the 2011 site (with Pseudo $R^2 = 0.66$) compared to 2012 (Pseudo $R^2 = 0.51$). The relationship was examined across the plots as well as through the growing season based on the date of data acquisition. The plots with more nitrogen tended to show better linearity between LAI and biomass for both sites. A graphical illustration of such relationships by plots for the two sites was also appended (Appendix 12). Moreover, the scatter plots demonstrated that high LAI during the 2011 growing season showed sharp increase in biomass after moderately high LAI was reached (LAI > 4). On the other hand, the magnitude and value range in the LAI acquired during the 2012 growing season was lower than four below which no clear pattern could be distinguished even in the 2011 site. This suggest that higher LAI ranges result in higher R^2 value.

In addition, the analysis of the LAI-biomass relationship through the growing season produced a more clear insight into understanding the pattern. The lowest biomass was measured on 30th of May and 1st of June for the 2011 and 2012 seasons, respectively, whereas the highest was measured on 20th June and 22nd of June in the same order. This coincides with the period of peak LAI for both sites making LAI a key indicator of biomass. Furthermore, the LAI declined after the peak as the crop matures and so does the biomass as can be seen from the graph (Figure 18). Therefore, the potato leaf constitutes a considerable proportion of the overall biomass. Nevertheless, it is not clear whether the underground biomass continues to mature gaining more weight after the potato crop already reached its peak in terms of LAI.

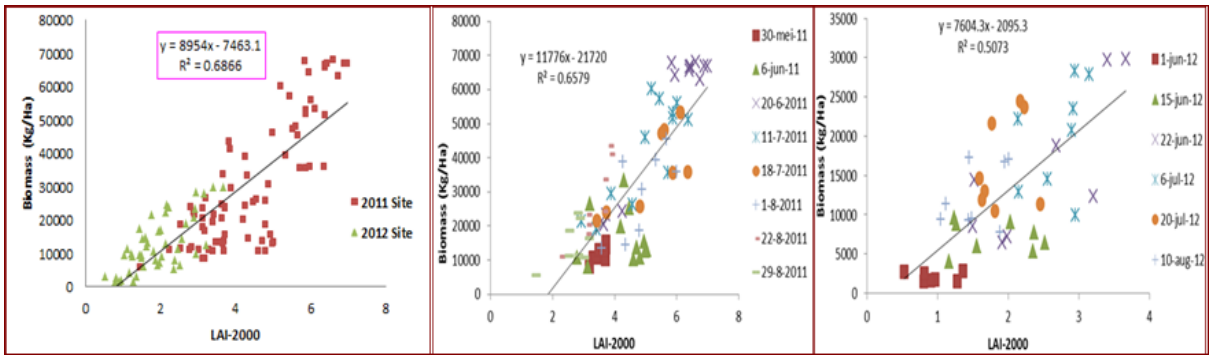

Figure 18. LAI and aboveground biomass relationships for 2011 and 2012

4.1.4 Results on SVI-LAI relationships

4.1.4.1 SVI-LAI relationships based on MSR16R and LAI-2000

Different SVIs tested with the simulated datasets were also analysed using the spectral datasets acquired for a potato field over the 2011 and 2012 growing seasons using the MSR16R instrument. Once those SVIs were computed, the corresponding LAI was estimated based on the model tested using the simulated dataset. The result of the analysis of the MSR16R spectral data using the selected SVIs indicated that some of the SVIs, which performed well with the simulated data, also maintained a comparable degree of relationships with LAI (Appendix 9). However, there was no consistency regarding the performance of the SVIs for the two growing seasons. For instance, $IIReR_2$, SR and NDVI had better relationships with LAI as measured with LAI-2000. Some SVIs such as $NDRE_2$ even performed better with the empirical field data from the 2011 growing season than it did with the simulated spectra. Some other indices such as $IIReR_2$, SR and $IIReR_1$ had consistent performances between the simulated and the empirical data for the 2011 growing season. These SVIs also had better sensitivity for high vegetation density as demonstrated in the sensitivity analysis using the sensitivity function. However, most of the SVIs showed inferior LAI prediction power based on the 2012 empirical data. Exceptions to these were the $NDRE_1$, NDII and ISR, which all had a better performance in the 2012 growing season as indicated by the pseudo-R^2 values. The Psuedo-R^2 values increased from 0.61 (2011) to 0.65 (2012) for $NDRE_1$, 0.44 (2011) to 0.64 (2012) for NDII and 0.59 (2011) to 0.65 (2012) for ISR.

A comparison of the performance of the best performing SVIs for the two growing seasons alongside the corresponding performance of the same SVI in the other year is presented in Figure 19 for ease of comparison. There was a large deterioration in the relationship between LAI and NDRE2 where the Pseudo-R^2 dropped from 0.82 (2011) to 0.13 (2012). This value also saw a considerable drop for $IIReR_2$ from 0.8 (2011) to 0.60 (2012). On the other hand, NDRE1 and ISR improved their relationship from 0.58 and 0.57 in 2011 to 0.61 and 0.60 in 2012, respectively. A detailed graphical illustration of the performances of the SVIs for the 2012 growing season is also appended (Appendix 10).

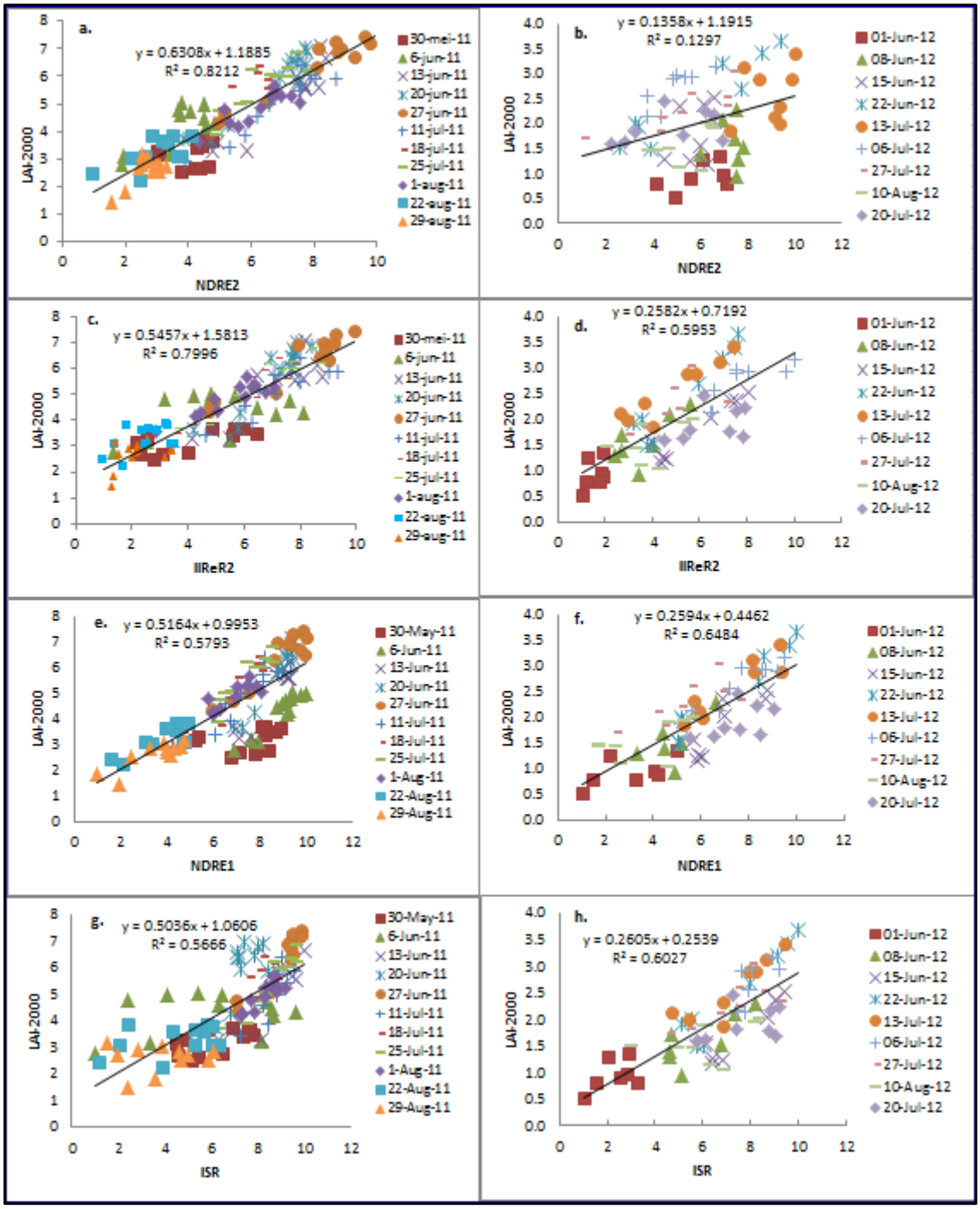

Figure 19. The relationship between selected SVIs and LAI-2000 for 2011(a, c, e and g) and 2012 (b, d, f and h) growing seasons.

The lack of consistency in the performance of those SVIs could be attributed to differences in the disturbance factors, mainly soil background effect. Moreover, the difference in the sensitivity levels of the different SVIs might also contribute to such inconsistency under different vegetation densities. This was partly because the 2011 growing season was a year of good harvest with high nitrogen application for the growth of potato so that it had a high LAI compared to 2012. Moreover, those indices which had better relationship with LAI-2000 in the 2012 growing season were found to be more sensitive to LAI at low vegetation density as discussed under the sensitivity analysis based on the simulated dataset. For example NDII and ISR had high sensitivities only next to NDVI at low LAI. Yet NDVI, which had always been

most sensitive at low LAI, did not show better performance in 2012 compared to 2011. Nonetheless, those SVIs which were reported to have high sensitivity to an open canopy, maintained more or less the same relationship for the two growing seasons, whereas those SVIs which did well with high LAI, as was the case for 2011, had poor performance under low LAI in 2012. Nevertheless, this was not always the case as there were some SVIs which had reported high sensitivity but poorly performed under both low as well as high vegetation densities. MSR had the poorest relationship with LAI-2000 despite its relatively high sensitivity record from the sensitivity analysis.

This implies that the performance of SVIs vary under different circumstances and so did their sensitivity as was analysed with the sensitivity function. However, the sensitivity function might not be always a useful indicator of how good an index might be, although it can still be a useful technique to map the general pattern of various SVIs. Despite the inconsistencies reported in relation to the performances of SVIs, there is a possibility to synergize the performance of SVIs by combining two or more indices for LAI mapping as opposed to the conventional use of single SVIs for LAI mapping. This could be done by employing different SVIs for predicting different LAI ranges based on their sensitivity function on the condition that one has enough information about the vegetation condition to be mapped.

Furthermore, a comparison of the performance of SVIs based on the combination of the datasets of the two growing seasons shows clear distinction of the point clouds. It can be seen from Figure 20 that the SVI-LAI relationships were low even for those SVIs which demonstrated high performance based on the 2011 growing season. NDRE2 and $IIReR_2$ were the SVIs with the best relationship with LAI-2000 based on the 2011 dataset whose Pseudo R^2 dropped from 0.80 and 0.82 to 0.16 and 0.64, in the same order. And yet $IIReR_2$ followed by WDVI and SR had the best relationship with LAI-2000 with the datasets of the two sites combined.

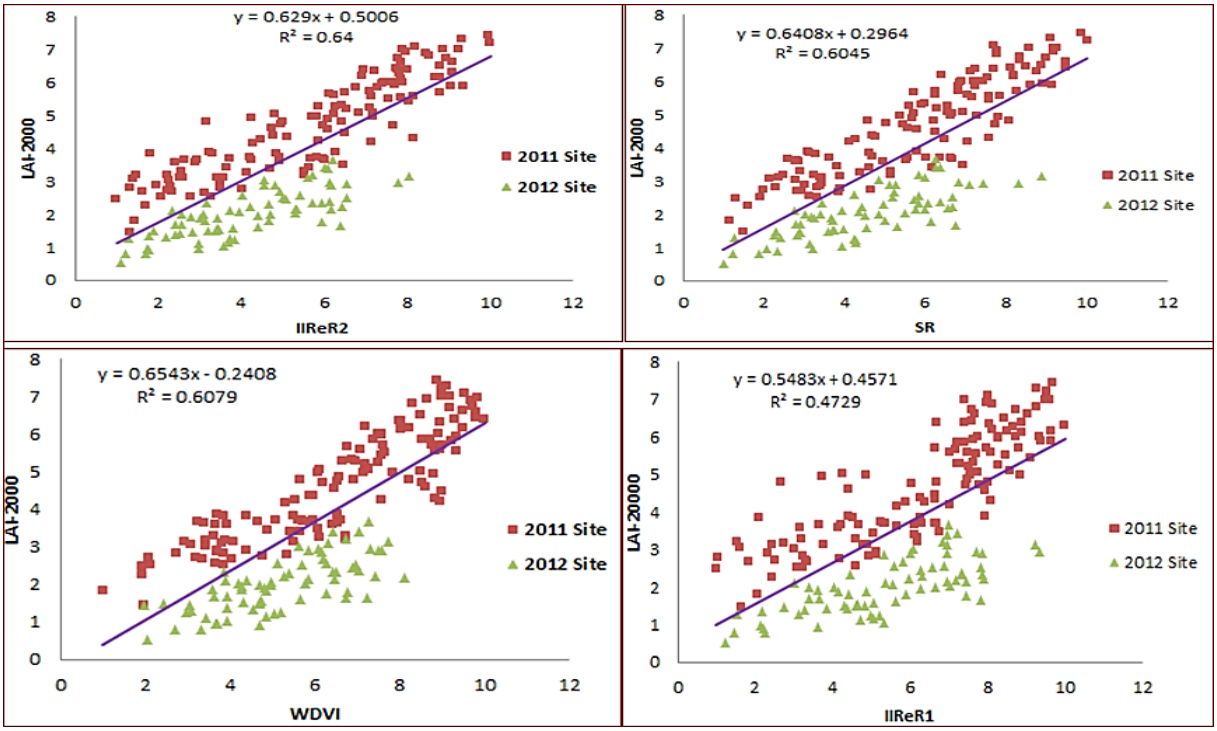

Figure 20. Comparison of SVI-LAI relationships based on the combined data for the two growing seasons

4.1.4.2 SVI-LAI relationships based on APEX imagery

SVIs selected on the basis of the sensitivity analysis were analysed using the APEX imagery acquired during the 27th June 2011 flight mission. The imagery was used to test the performance of those SVIs based not only on APEX but also adjusted for the ESA's upcoming space systems (S-2 and VENµS) as well as Landsat TM band settings. The fitted linear regression based on all the datasets of SVI values derived from those sensors and LAI-2000 indicated strong linear relationships. All the SVIs considered for broad and narrow band sensors, except EVI and MSR which were excluded owing to their poor performance as evaluated with MSR16R, showed consistency across the sensors. NDVI, WDVI, SR, NDII and ISR showed some degree of consistency (Appendix 11). It was also found that SR, WDVI, NDVI and IIReR1 maintained a considerable degree of consistency in their performance. The first two also showed a better relationship across the broad band and narrow band sensors both with pseudo R^2 = 0.86 and 0.87, respectively (Figure 22). The overlapping point measurements for the corresponding sensors indicate high consistency. The result was in agreement with the relationship established based on the simulated data where the SVIs showed consistency across the different sensors.

Similar results were reported for the other SVIs. Figure 21 demonstrates the two SVIs (SR and WDVI) which had the best relationships with the LAI-2000. NDVI, ISR and NDII computed based on APEX, MSR16R, S-2 and Landsat TM had less consistency. Although they had pseudo R^2 values of 0.84, 0.84 and 0.83, respectively, there were deviations among the derived values for the different sensors. The R^2 values presented here, however, represent the goodness of fit of all the point clouds based on all the sensors for an index while the overlapping points imply the extent of consistency in the values of an index based on those sensors.

Moreover, the results indicated that SR, WDVI, and NDVI were also consistent across the narrow band sensors themselves as the overlapping points for APEX, S-2, VENµS and MSR16R demonstrate. However, the extent of the overlap as well as clustering of points seem to depend on the similarity of the band settings of sensors. For instance, the overlap between APEX and VENµS complies with this fact. Yet, the derived values based on MSR16R deviated more than the corresponding values for the Landsat TM do with reference to APEX, S-2 and VENµS, whose values overlap more often than others. The situation was even clearer with NDII and ISR.

In addition to the SVIs already mentioned, other indices such as $NDRE_1$, $NDRE_2$, $IIReR_1$ and $IIReR_2$ were computed for other sensors except the Landsat TM, which lacks the specific band settings required for their computation. These indices were used to assess the performance of ESA's upcoming hyperspectral spaceborne systems based on their red edge bands. The result showed that the narrowly positioned red edge bands of S-2 and VENµS could be used and compared to indices derived based on the broad bands of TM, for example.

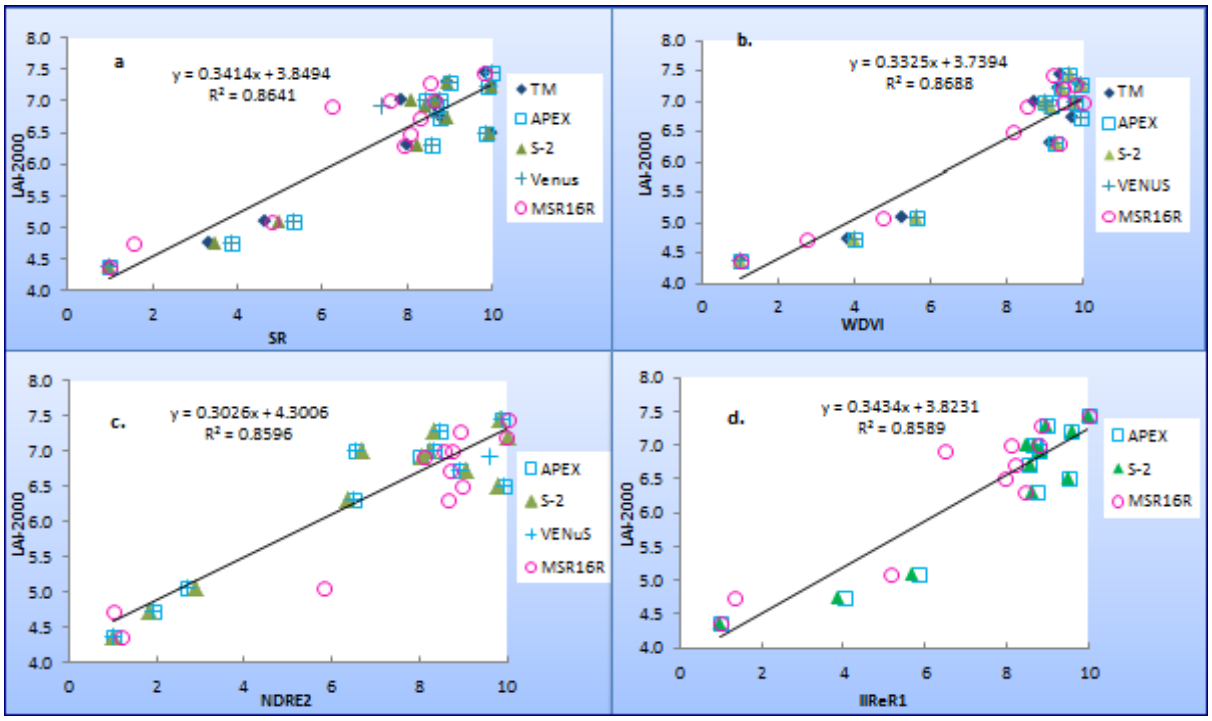

Figure 21. A comparison of the SVI-LAI relationship for a) SR and b) WDVI c) NDRE2 and d) IIReR1 across the different sensors. The fitted regression line is based on whole datasets from the sensors compared.

4.1.5 Results on validation of SVI-LAI relationships

4.1.5.1 Validation of MSR16R-LAI-2000 relationships

The prediction of LAI was performed using the SRM whose parameters, the coefficient of light extinction α and the asymptotically limiting factor SVI_{∞}, were estimated based on the simulated dataset. This was done after the SVI values were normalized by rescaling to the same value range of 1 to 10 to be later used for sensitivity analysis. The R^2, RMSE and RPD values were computed for each SVI after the LAI was predicted for both sites (table 11). The result confirmed that those SVIs with a better relationship maintained superior LAI prediction power with $IIReR_1$ (R^2=0.81, RMSE= 0.41) and SR (R^2=0.79, RMSE= 0.44) being the most suitable SVIs based on the 2011 growing season. $IIReR_2$ had also demonstrated superior performance as tested with the simulated dataset. Moreover, both $IIReR_2$ and SR had shown high sensitivity to high vegetation density as demonstrated under the sensitivity analysis.

Table 11. LAI prediction for MSR16R using SRM from the simulated data and validation results based on the LAI-2000

SVI	LAI=f(SVI)	2011 Site			2012 Site		
		R^2	RMSE	RPD	R^2	RMSE	RPD
NDVI	-1/0.727*LN(1-NDVI/10.044)	0.76	0.51	2.84	0.51	0.26	2.77
WDVI	-1/0.191*LN(1-WDVI/13.448)	0.77	0.48	3.02	0.49	0.27	2.67
SR	-1/0.016*LN(1-SR/97.699)	0.79	0.44	3.30	0.58	0.22	3.28
NDII	-1/0.461*LN(1-NDII/11)	0.57	0.91	1.59	0.62	0.20	3.61
ISR	-1/0.343*LN(1-ISR/12)	0.63	0.79	1.84	0.63	0.20	3.66
$NDRE_1$	-1/0.328*LN(1-$NDRE_1$/11.135)	0.58	0.89	1.63	0.67	0.17	4.15
$NDRE_2$	-1/0.319*LN(1-$NDRE_2$/11.236)	0.76	0.50	2.90	0.17	0.44	1.64
$IIReR_1$	-1/0.029*LN(1-$IIReR_1$/54.667)	0.81	0.41	3.54	0.54	0.25	2.94
$IIReR_2$	-1/0.12*LN(1-$IIReR_2$/17.52)	0.70	0.63	2.30	0.58	0.22	3.23
MSR	-1/0.068*LN(1-MSR/26.68)	0.54	0.97	1.21	0.59	0.22	3.31

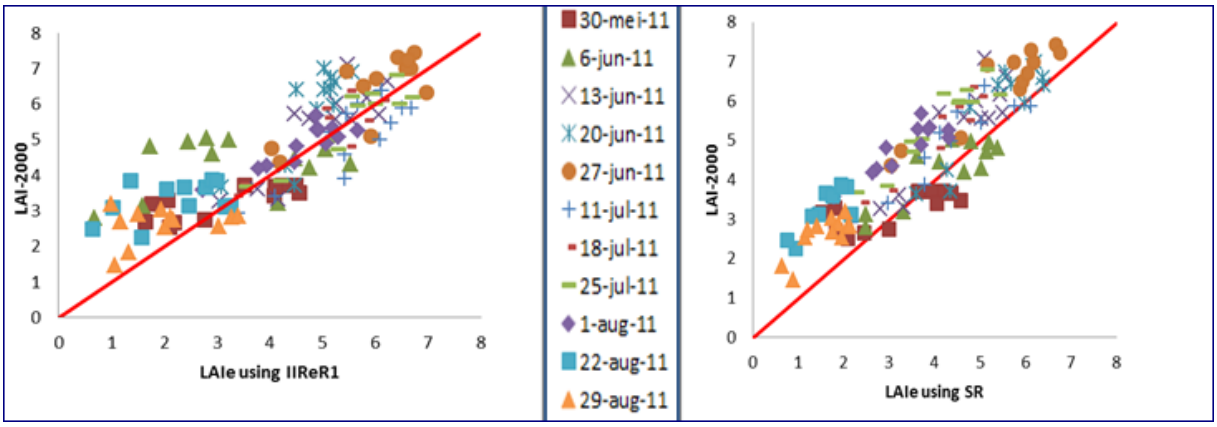

Figure 22. Validation of LAI prediction for the 2011 site using LAI-2000

The RMSE values, however, yielded smaller values for 2012 than in 2011 mainly because of the differences in the value range of the two datasets. A cross site comparison using RMSE was therefore found to be misleading (table 11). As a result, the RPD was calculated to standardize for differences in data range. The values could indicated the relative performance of the SVIs next to the R^2 values although it often lacked consistency with the R^2 values.

The same procedure was followed for the 2012 site measurements where the validation result followed a similar pattern as the relationship the SVIs had with LAI-2000 measurements. However, most of the SVIs had inferior performance compared to the 2011 site (table 12). A few exceptions to this include NDII and $NDRE_1$ which showed improvements for the 2012 dataset as indicated by their higher RPD and R^2 values of 0.62 and 0.67, respectively. The other SVIs had either lower performances or maintained the same level for the two sites. The RMSE values presented in the same table should be taken with caution as direct comparison between the two sites might be misleading. This was because of the difference in the magnitude of value ranges for LAI for the two sites. The 2011 site had values with larger magnitudes where the maximum LAI for 2011 and 2012 was about 7.5 and 3.5, respectively. This made a cross-site comparison of the performance of the SVIs using the RMSE impractical. As a result, only the R^2 values, not the RMSE computed for the two growing seasons should be used for a cross-site comparison of the performance of SVIs. This shortcoming of the use of RMSE was also confirmed by (Ji and Peters 2007).

A graphical display of the predicted LAI against LAI-2000 measurement also confirmed how well the SVIs could predict LAI for the two sites. Figure 22 presents the best performing SVIs ($IIReR_1$ and SR) where the predicted LAI throughout the growing season was plotted against the corresponding LAI-2000 measured data for the 2011. The graphs showed that both $IIReR_1$ and SR predicted well between the LAI range of 3 and 6 as more points either overlapped or aggregated around the equality line through the origin. On the other hand, the points are relatively further away from the line around the origin implying less accurate predictions at low vegetation densities. This complies with the sensitivity result where the two indices were found to be less sensitive at low LAI. However, their high sensitivity over the wider LAI ranges particularly at high LAI allowed them to make better predictions of LAI as tested with the 2011 site. It can also be seen from Figure 23 that SR underestimated the LAI compared to IIReR1. A summary of the validation results with other SVIs across the two sites can be found in the Appendix 14.

4.1.5.2 Validation of SVI-LAI-2000 relationships based on APEX imagery and MSR16R

Relationships between MSR16R, APEX, S-2 and VENµS based SVIs and LAI-2000 were established to evaluate the added value of the red edge bands of ESA's upcoming spaceborne systems (Table 13). Moreover, the consistency or lack of SVI-LAI relationships across broad and narrow bands were evaluated. The LAI prediction was performed based on the SVIs derived using APEX imagery while the algorithms were adjusted for the sensor specific band settings. The result of LAI prediction based on the SRM reported that $IIReR_1$, WDVI and SR yielded highly consistent relationships with LAI as explained by their corresponding R^2 values. The WDVI, IIReR1 and SR maintained the same degree of performance for all the sensors whereas $IIReR_1$ could be computed only for three sensors (APEX, MSR16R and S-2). NDII and ISR also demonstrated a comparable degree of consistency among the four sensors (excluding VENµS as it lacks SWIR bands). The other SVIs derived from APEX, MSR16R, S-2 and VENµS were $NDRE_1$ and $NDRE_2$ and they did not show high consistency across those sensors. For instance, $NDRE_1$ had an R^2 value as high as 0.88 with MSR16R and as low as 0.51 with VENµS, whereas the corresponding value for $NDRE_2$ being 0.88 and 0.70 (table 12).

Some of the SVIs analysed such as WDVI, SR, NDII, ISR, $IIReR_1$ and $IIReR_2$ revealed consistent performances with S-2 and VENµS. The red edge indices such as $NDRE_1$ and $NDRE_2$ did not show consistency across the narrow band sensors nor had they superior performances. However, they both performed well with MSR16R (both $R^2 = 0.88$). On the other hand, those SVIs based partly on the SWIR bands maintained a considerable degree of consistency both within the narrow band sensors as well as with the broad band sensor. The newly proposed indices, $IIReR_1$ and $IIReR_2$, also had comparable performances among APEX, MSR16R and S-2. The former consistently showed high performances (R^2=0.88), whereas the latter had lower performances (R^2=0.52). A demonstration of the performance of IIReR1at image level using the hyperspectral APEX image is also presented, which distinguishes well between different N fertilization levels as shown with LAI mapping (see Appendix 19).

Table 12. Comparison of the performance of SVIs across sensors based on SRM (p-value <0.01 for all SVIs).

SVIs	MSR16R		APEX		S-2		VENµS		TM	
	R^2	RMSE	R^2	RMSE	R^2	RMSE	R^2	RMSE	R^2	RMSE
WDVI	0.88	0.15	0.87	0.16	0.87	0.16	0.87	0.16	0.87	0.17
NDRE1	0.88	0.15	0.74	0.31	0.75	0.31	0.51	0.61	-	-
NDRE2	0.88	0.15	0.68	0.39	0.70	0.37	0.70	0.37	-	-
SR	0.87	0.16	0.88	0.15	0.88	0.15	0.85	0.18	0.89	0.14
IIReR1	0.87	0.16	0.88	0.15	0.88	0.14	-	-	-	-
NDII	0.72	0.35	0.90	0.12	0.88	0.15	-	-	0.90	0.12
IIReR2	0.60	0.49	0.55	0.55	0.52	0.60	-	-	-	-
NDVI	0.59	0.50	0.66	0.43	0.40	0.74	0.62	0.47	0.54	0.56
ISR	0.59	0.51	0.91	0.11	0.89	0.14	-	-	0.91	0.12

4.1.6 Results on sensitivity analysis based on empirical data

The sensitivity analysis performed on the basis of SVIs derived from MSR16R spectral data and LAI values acquired with LAI-2000 during the 2011 and 2012 growing season gave the following results (Figure 23). The sensitivity values were averaged for every five consecutive LAI values after the LAI-values were sorted in increasing order. This was done to smooth the sensitivity curve for ease of visualization as the actual number of observation for LAI measurements were 128, too large to visualize making the plots hardly informative. This procedure does not affect the sensitivity function. Regardless of the jumps observed with the *S* function at different LAI values the overall sensitivity pattern indicated the relative position of the different SVIs. NDVI, $NDRE_2$, ISR and NDII demonstrated high sensitivity for low LAI ranges (LAI < 4) beyond which some of these indices, particularly NDVI and NDII, showed a considerable drop in their sensitivities.

The overall sensitivity indicated that all the SVIs considered were sensitive across the entire LAI range of as high as 7.5. However, NDVI appeared to be the least sensitive beyond an LAI of six (6) and eventually losing its sensitivity as it crosses the critical sensitivity value of 1.96, which is a t-value below which the SVIs lose sensitivity at 95% level of confidence. Compared to many other SVIs, the sensitivity curve was found to be smoother than others for SR, $IIReR_2$, $IIReR_1$ as well as $NDRE_2$. These same indices also had better LAI prediction power than others as tested with the same dataset. For instance, $IIReR_1$ and SR had superior performance (R^2 = 0.81 and 0.79, respectively) followed by WDVI (R^2 = 0.77), $NDRE_2$ and NDVI (0.76 each). The first two indices also had a higher and more stable sensitivity function across the wider LAI ranges particularly at high LAI values. This also complies with the low sensitivity curve at low LAIs (LAI < 3) (figure 23a). On the other hand, those SVIs, which had low prediction power such as MSR, $NDRE_1$, NDII and ISR, also performed poorly with their sensitivity function.

Similarly, the result for the 2012 site showed high sensitivity for NDVI, NDII, ISR, $NDRE_1$ and $NDRE_2$ at low LAI (LAI < 2) beyond which it declined. $IIReR_1$ and $IIReR_2$ on the other hand had low sensitivity records for 2012, whereas these same indices reported high sensitivity particularly at high LAI ranges. Regardless of the varying sensitivity levels for the different indices, all the SVIs analysed reported a statistically significant sensitivity to LAI at 95% confidence level.

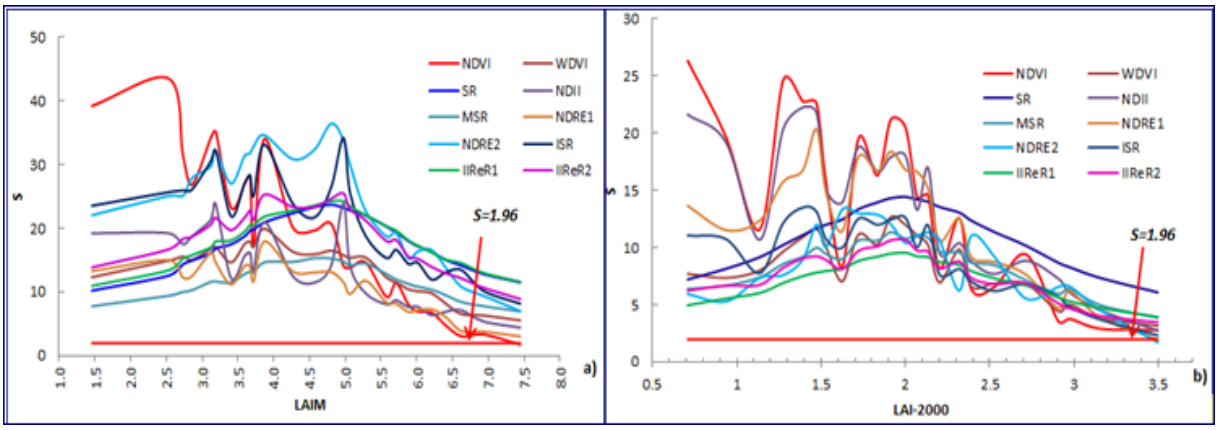

Figure 23. Sensitivity analysis based on MSR16R and LAI-2000 measurements during a) 2011 and b) 2012 growing seasons

5. Discussion

5.1 Results based on PROSAIL Model

5.1.1 Sensitivity of spectral regions to canopy background effects

The result on the sensitivity analysis of the spectral regions to canopy background effects across LAI ranges based on the PROSAIL simulated data showed that the effect of canopy background was high at low vegetation density for individual spectral regions. As demonstrated through variable soil moisture levels (Figure 4) the effect is clearly visible in the analysed spectral regions, namely NIR, SWIR, red-edge and red bands in decreasing order. The reflectance was the highest for a bright soil followed by medium and the least for moist soil backgrounds. This is mainly because dry soil reflects more than moist soil for an open canopy, which was also confirmed by previous findings (Brown, Chen et al. 2000; Gonsamo and Pellikka 2012). The NIR reflectance showed not only high sensitivity to varying soil moisture levels but was also responsive over a wider range of vegetation densities. This confirms the assertion of Houborg and Boegh (2008) that efficient correction for background effect would yield a better NIR-LAI relationship. It also complies with Clevers (1989) who based the derivation of WDVI mainly on the correction for canopy background effects. On the other hand, the reflectance in the SWIR also showed high sensitivity to soil moisture over a considerably wider LAI range as compared to the red edge and red. The contrast between bright and moist soil reflectance for SWIR makes this spectral region more suitable for efficient correction for background effects (Gonsamo and Pellikka 2012), even compared to the commonly used red bands where this reflectance gap is relatively low. Moreover, the reflectance in the SWIR followed by red-edge region continues to respond to background effects while the corresponding spectra for the red become insensitive at relatively lower LAI values (Figure 4). This coincides with (Lee, Cohen et al. 2004) who concluded that the red edge and SWIR bands contain more information useful for LAI retrieval even compared to the NIR region.

More important is that SWIR reflectance continues to decline as a function of LAI for a bright soil which confirms what previous studies revealed (Brown, Chen et al. 2000; Cohen, Maiersperger et al. 2003; Lee, Cohen et al. 2004; Schlerf, Atzberger et al. 2005; Gonsamo and Pellikka 2012). However, the SWIR reflectance slightly rises for moist soil at high LAI (LAI > 5) which is also in agreement with what Gonsamo and Pellikka (2012) found. This makes SWIR an important spectral region for possible corrections for background effects especially at bright soil conditions. Furthermore, the SWIR region is insensitive to variations in C_{ab} levels making it potentially suitable to enhance the SVI-LAI relationship with increased resilience to variations in C_{ab} levels as well as soil moisture levels.

In addition, the spectral reflectance at 670 nm also maintains some stability in variable leaf C_{ab} levels whereas the red-edge region distinguishes better between different LAI values. This region, however, showed considerable sensitivities to variations in C*ab* as compared to SWIR and Red around 670 nm. The Red edge as suggested by Lee, Cohen et al. (2004) has therefore an added-value of distinguishing between LAI ranges while its sensitivity to variations in C_{ab} levels is compensated for by SWIR and Red bands. These features therefore suggest the potential for improving SVIs-LAI relationship based on the integration of those four regions of the spectrum.

5.1.2 SVI-LAI relationships based on PROSAIL model

Based on the results of the SVI-LAI relationship, where the different leaf, canopy and background soil effects were combined, it was found that SVIs showed different degrees of

relationship with LAI. SVIs such as IIReR1, IIReR2 and SR had strong relation with LAI based on the exponential function (Fig. 5). Most of the SVIs also showed a logarithmic relationship with LAI while regressing LAI with SVI. Contrary to the exponential function used in Clevers (1988) and Baret and Guyot (1991) a linear relationship was reported for a few indices such as IIReR1, IIReR2 and SR. These SVIs with linear relationship with LAI also had strong performance based on their R^2 values (Figure 5). The linearity of the relations for some indices was also revealed by previous studies (Broge and Mortensen 2002; Schlerf, Atzberger et al. 2005; Darvishzadeh, Skidmore et al. 2008), which showed the linearity of SVI-LAI relationships based on the exponential function. Some indices also showed large difference between the best-fi and exponential function. This was mainly because the exponential function forces the curve through the origin while the SVI value starts at a value of 1 or more showing deviation from the exponential function around the origin.

The analysed SVIs showed different levels of sensitivity to leaf, soil and canopy parameters. Almost all of the SVIs were found to be highly sensitive to low C_{ab} and planophile LADs, whereas they showed less sensitivity to high C_{ab} and erectophile LADs. However, the effect of canopy background was reported to be negligible as the indices revealed less variability in their performances under the three soil moisture levels. The degree of sensitivity always varied among those indices. Those SVIs based on the red edge bands, namely NDRE1, NDRE2, SR and IIReR1 showed high sensitivity to low leaf C_{ab} levels with early saturation levels (LAI < 3). This could be due to the use of either red edge or chlorophyll absorption bands which led to lower values for the indices at low C_{ab} level as the red reflectance [the denominator] would have a higher value than otherwise. This effect of the red edge was also reported in previous studies (Broge and Mortensen 2002; Darvishzadeh, Skidmore et al. 2008; Houborg and Boegh 2008; Clevers and Gitelson 2013) making it more suitable for chlorophyll estimation than for LAI. On the other hand, those SVIs based partly on the SWIR region, namely, NDII, ISR and $IIReR_2$, showed better sensitivity to LAI with low leaf C_{ab} (C_{ab} 20 μgcm^{-2}). This upports the idea of Lee, Cohen et al. (2004) who showed that the red edge and SWIR bands contain more useful information about canopy LAI than the NIR region.This could be explained by the less sensitivity of SWIR bands to leaf C_{ab} levels. On the other hand, the red-edge around 710 nm for $IIReR_2$ yielded higher reflectance with low C_{ab} (as the red edge shifts to the left), which was also comfirmed by others (Danson and Plummer 1995; Clevers and Kooistra 2012).

The analysis of the SVI-LAI relationships based on different LADs also indicated overall poor performance with planophile LADs. However, there was variation in the level of sensitivity across the LAI ranges. This was particularly the case with $IIReR_1$, $IIReR_2$, ISR, SR and NDII, which showed high sensitivity to low LAI values (LAI < 4) with a planophile LAD. These SVI values saturate earlier for planophile LAD, while it still continued to increase with spherical and erectophile LADs. This higher sensitivity with planophile LADs at low LAI could be explained by a relatively high exposure of planophile LAD and hence higher absorption of red reflectance which in turn yields higher values for the SVIs. The effect was soon reversed at higher LAI (LAI > 4) possibly because spherical and erectophile LADs, with better exposure to illumination source, would have the same effect on red reflectance as was the case with a planophile LAD at low LAI. With planophile LADs the leaf layers have a shadowing effect overlaying each other and hence relatively higher red reflectance and subsequent saturation effect with increasing vegetation density was noticed.

A further analysis of the SVI-LAI relationships based on variable soil moisture revealed consistent patterns. This showed that soil moisture did have a negligible effect on the performance of the analyzed SVIs. However, this does not mean that all the SVIs efficiently

corrected for background effects because the soil reflectance was fixed to 50% in the PROSAIL model.

5.1.3 Performance of SVI with broad and narrow band sensors

Based on the PROSAIL model it was found that the SVIs derived from the broad and narrow band sensors, namely WDVI, NDVI, EVI, NDII, ISR and SR, were strongly consistent across the sensors (Figure 7). The result of the correlation of the LAI estimated by those SVIs with measured LAIs also reported statistically significant values ($P<0.01$) (Table 7). This is in agreement with previous studies in that strong correlation was reported for NDVI and REIP based on continuous and VENµS bands (Herrmann, Karnieli et al. 2010). There were, however, contradicting reports regarding the contribution of narrow bands in relation to LAI retrieval. Some studies revealed a better performance of hyperspectral data than multispectral sensors for LAI prediction (Lee, Cohen et al. 2004; Schlerf, Atzberger et al. 2005; Liu, Pattey et al. 2012), whereas other studies found that hyperspectral sensors did not show better performance than broad band sensors (Broge and Mortensen 2002; Liu, Pattey et al. 2012). Lee, Cohen et al. (2004) showed that the spectral properties of MODIS did not have any inherent advantage over those of ETM+ for predicting LAI. They also showed that models based on actual ETM+ bands were generally stronger than those based on simulated data indicating that ETM+ data suffer no penalty for having lower radiometric quality than AVIRIS simulated ETM+ data for predicting LAI. Broge and Leblanc (2001) also concluded, based on simulated data analysis that the hyperspectral narrow bands were not better than the classical broad band SVIs for LAI estimation. These authors added that the broad band spectra are even less vulnerable to external disturbance factor, compared to the 10 nm wide narrow bands. Nonetheless, the high performance of the red edge for chlorophyll estimation was widely acknowledged (Broge and Mortensen 2002; Clevers and Gitelson 2013).

As presented in Figure 7, NDII and ISR showed strong linearity between S-2, APEX and TM, while both indices showed slight deviation for MSR16R. The LAI estimation using NDII and ISR based on MSR16R band settings tended to be higher than the corresponding estimation from TM at low LAI ($LAI<5$) and drops below TM based estimation afterwards. This is mainly due to the disproportionately higher values for both NDII and ISR at low LAI for MSR16R than it was for TM. Because the NIR band used for MSR16R is narrow enough to yield a high ratio although the SWIR band width, the denominator, is comparable for both sensors. This is in agreement with previous findings on the sensitivity of the SWIR region (Brown, Chen et al. 2000; Gonsamo and Pellikka 2012). The result also revealed a deviation of LAIe from the narrow bands using the SR from that of Landsat TM. This could be due to the NIR bands, which are narrow enough to yield high NIR reflectance coupled with the choice of narrow red absorption bands for narrow band sensors compared to the broad bands from TM. The SR value for the narrow bands was therefore higher than that of TM and subsequently yielded higher LAIe values for the former. Regardless of the slight deviations for those few indices the results revealed consistent performances for all the SVIs considered, which complies with what previous studies revealed (Broge and Leblanc 2001; Broge and Mortensen 2002; Lee, Cohen et al. 2004; Herrmann, Pimstein et al. 2011). Moreover, Herrmann, Pimstein et al. (2011) found no added value of using continuous bands over the narrow bands of VENµS for LAI retrieval. These suggest that SVIs derived from the narrow bands of APEX, MSR16R or ESA's upcoming sensors could be comparable with the broad bands of Landsat ETM+ for LAI estimation.

5.1.4 Sensitivity analysis based on PROSAIL Model

The sensitivity analysis based on the PROSAIL model indicated that SVIs had varying performances with varying leaf, soil and canopy parameters. Most of the SVIs analysed had poor performances under low leaf C_{ab} (Table 9), which was particularly worse for greenness indices such as NDVI, NDRE1, NDRE2 and EVI, as compared to their performance with high leaf C_{ab}. This is in agreement with (Liu, Pattey et al. 2012) who reported high sensitivity of greenness indices such as NDVI to C_{ab} level. Other indices such as IIReR1, IIReR2, NDII and ISR showed less variation in their sensitivity to C_{ab} levels although they had high RMSE values at lower C_{ab} level. These indices are partly based on SWIR bands which improved their insensitivity to variations in C_{ab} levels. On the other hand, the result of the sensitivity function for the SVIs analysed showed an overall high sensitivity at low LAI values (LAI < 3) for many of the SVIs. This is because of the steep rise in the slope of the exponentially fitted functions, hence making them highly sensitive at low LAIs. After moderately high LAI value is reached, the S value drops asymptotically approaching zero values for these indices. This was the case for NDVI, which loses its sensitivity to LAI earlier than other indices. This was in agreement with what Herrmann, Karnieli (2010) reported where NDVI reached a saturation point at fairly low LAI values. The fact that the sensitivity of NDVI drops so quickly could be attributed to the use of red bands, which not only decrease with small increase in LAI but also stabilize when the canopy closes up (LAI > 3) (Figure 4). On the other hand, NDII uses the spectral information from the SWIR region instead of the red bands to normalize for canopy background effects. The SWIR continues to respond to soil moisture levels as was confirmed by previous studies (Brown, Chen et al. 2000; Lee, Cohen et al. 2004; Gonsamo and Pellikka 2012).

Moreover, the analysis of the performance of SVIs based on different LADs also distinguished between SVIs (Table 11). The effect of different leaf orientation varied across the indices depending on the extent to which those indices correct for either soil background effects or /and leaf C_{ab} concentrations. This could be the reason why NDVI, for instance, did well with an erectophile LAD, because the effect of C_{ab} is emphasized as the leaves have high exposure to sun light boosting the performance of NDVI. The large effect of LAD on the performance of SVI especially at low to moderate LAI values is well documented (Liu, Pattey et al. 2012). The $IIReR_1$ and $IIReR_2$ reported high sensitivity at high LAI values. This could be explained by reduced soil background effect and partly by the C_{ab} neutrality of the SWIR region. In doing so the effect of soil background in open canopies was minimized because of high reflectance of SWIR in open canopies, particularly for bright soil which continues to decrease as the canopy closes. Similar results were also found by (Brown, Chen et al. 2000; Gonsamo and Pellikka 2012). The sensitivity result based on varying soil moisture, however, revealed consistent performances of SVIs. There were some deviations observed with WDVI based on the three moisture levels, which might be explained by the assumption of fixed soil reflectance of 50% in the PROSAIL model. The soil spectra were, however, subjected to variations in response to changes in soil moisture levels. Contrary to expectations, the result also showed decreasing performance of some of the greenness indices with increasing soil moisture. This could be due to the overestimation of those indices with decreasing red reflectance for moist soil. The consistently high RMSE values for SVIs, however, suggest the negligible effect of variation in soil moisture levels and not that the indices efficiently corrected for canopy background effects.

The use of a normalized sensitivity function showed a general trend of high sensitivity at low LAI which decreases with increasing vegetation density. This complies with previous findings (Ji and Peters 2007; Wu, Wang et al. 2007; Gonsamo and Pellikka 2012) that showed a

decrease in sensitivity at exponentially decaying rate with increasing vegetation density. Despite its capability to indicate the relative sensitivity of multiple SVIs across vegetation densities, the S function could not yield consistent performances with other statistical measures such as R^2 and RMSE (Table 9 & fig.11). For instance, NDVI, as was the case for other SVIs, showed improved performance with high C_{ab} level although the sensitivity function showed deteriorating *S* values with higher C_{ab} levels. Similarly, Gonsamo and Pellikka (2012) also reported the lack of consistency in the performance of the sensitivity function as SVIs tested with empirical data based on their sensitivity function could not reproduce similar performance. Moreover, the normalized sensitivity function revealed inconsistent results based on the use of the best fit and exponential function with a quick drop of sensitivity for the former (Appendix 5A&B) although they both followed a decreasing pattern at high LAI values. Gonsamo and Pellikka (2012) also found similar results where the sensitivity records varied with the best-fit and exponential functions although in both cases the sensitivity decreased at exponentially decaying rate. Similarly, Wu, Wang et al. (2007), who used the first derivative of the slope of the fitted regression line as a measure of sensitivity, reported varying sensitivity of NDVI, for example, for wheat and potato crops. Nevertheless, the *S* function is a useful technique to visualize the SVI-LAI sensitivity at different vegetation densities.

5.2 Results based on empirical data

5.2.1 The effect of differential nitrogen treatments on the LAI of potato crop

The LAI curve throughout the growing season showed a steep rise during the first 6 sampled weeks, meaning reaching its peak in the 13th and 14th week since the planting date for 2011 and 2012, respectively. The dip noticed around 11th of July 2011 was due to heavy storm on 28th June (Fig. 14). This LAI curve coincides with what Zhao, Xiong et al. (2012) reported showing that LAI reached its peak around 110 days after sowing in their study of potato for different mulching and watering environments. The variable rate application of N fertilizer showed significant differences in the potato crop growth as indicated by their LAI values for both 2011 (Fig. 14) and 2012 (Fig. 16) growing seasons. Those plots, which had low LAI throughout the growing season were given little or no fertilizer (Table 3 and Table 4). For instance, regarding the 2011 site plots C, D & K had no initial fertilization, whereas K and D had additional fertilizer on May 18 and June 21, 2011, respectively. These had quick effect on the potato growth for those plots as the LAI values acquired in the subsequent weeks increased for plots D & K over plot C, for example (see Appendix 7 for treatment levels). This shows that the effect of additional nitrogen application quickly manifested itself through increased LAI values acquired shortly following the fertilization dates. Ziadi, Zebarth et al. (2012) reported that potato crops usually requires high N fertilizer (125-200 kg/ha) based on soil conditions. Bélanger, Walsh et al. (2001) also revealed a significant effect of differential N fertilizer and supplemental irrigation on potato biomass. However, the effect of N level was only significant between the non-fertilized or low N and the fertilized plots and not within the fertilized plots. As (Ziadi, Zebarth et al. 2012) also reported the optimal N level was between 125 and 200 kg/ha and any additions of N would only extend the crop growth. This suggests that additional N on plots with already considerable fertilization does not have much effect on the crop growth.

The similarity of the pattern for both sites indicated that the significant difference was between plots without nitrogen and the one with highest nitrogen. However, the 2012 site also reported a significant difference in LAI between plots with 43 $kgha^{-1}$ and those with the highest nitrogen of 218 $kgha^{-1}$. The fact that there was no significant difference between those plots with different fertilization rates for 2011 may be explained by the negligible marginal

effect of additional nitrogen on the crop growth for plots with already some N fertilizer. Regardless of the magnitude of difference in N level the LAI values showed a similar sequence as the amount of fertilizer application; meaning higher fertilizer application yielding higher LAI values. Apart from the level of fertilizer applied, the unfavourable weather conditions (Fig. 17) and poor soil conditions for the 2012 site contributed to the poor growth of the potato (O'Brien, Allen et al. 1983; Allen and O'Brien 1986; Mazurczyk, Lutomirska et al. 2003). Nevertheless, the trends in the LAI values were found to be similar in both cases with a steep rise at the onset of the growing season. Effects of weather parameters such as temperature were also confirmed by previous studies (Chirkov 1965; Hoogenboom 2000; Mazurczyk, Lutomirska et al. 2003). Wang, Li et al. (2005) also found that mulching increased soil temperature and moisture, which in turn resulted in high biomass and tuber yield. This suggests that the unfavourable weather parameters as well as poor soil conditions coupled with the overall low nitrogen application during the 2012 growing season resulted in the stunted growth of the potato crop and hence low LAI and low biomass compared to the 2011 site which had more favourable weather, well developed soil as well as high nitrogen application.

5.2.2 SVI-LAI relationships based on empirical data

The result of the analysis of the MSR16R spectral data using the selected SVIs indicated that some of the SVIs, which performed well with the simulated data, also proved to be better predictors of LAI than other SVIs. However, there was no consistency regarding the performance of the SVIs with the two growing seasons (fig. 19). For instance, $IIReR_1$, SR and NDVI had better relationships with LAI-2000 measurements. Some SVIs, such as $NDRE_2$, even performed better with the empirical field data from the 2011 growing season compared to its performance with the simulated spectra. This could be due to the fact that the simulated spectra contained wide ranges of parameter values while in the actual field data the variation was minimal. Hence, the sensitivity of $NDRE_2$ to C_{ab} levels dropped while improving its sensitivity to LAI. This complies with the strong effect of LAD and C_{ab} (Liu, Pattey et al. 2012). The lack of consistency in the performance of those SVIs in general and the overall deterioration in the performance of SVIs for the 2012 site in particular could be attributed to differences in N application, soil conditions as well as weather parameters which affect the efficiency of an index as suggested by (Broge and Leblanc 2001). The 2011 site had high N fertilizer and subsequently high C_{ab} levels. A sensitivity analysis based on the PROSAIL model also confirmed that the SVIs demonstrated good relationships with LAI at high C_{ab} level as well as erectophile LADs, whereas they performed poorly at low C_{ab} level and planophile LADs. The performance of NDII and ISR, which either improved or maintained the same level of relationship with LAI for 2012, could be justified by the fact that NDII and ISR are less sensitive to C_{ab} levels as they are based partly on SWIR bands. On the other hand, $NDRE_1$ had better performance in 2012 than in 2011, which could be explained by the less C_{ab} sensitivity of the NIR band as compared to the red-edge bands used by $NDRE_2$ where the latter are more sensitive to C_{ab}. Given the low LAI for 2012, the canopy background effect might also explain the overall poor performance of the SVIs.

Furthermore, those indices derived based on MSR16R and which had a better relationship with LAI-2000 in the 2012 growing season were found to be more sensitive to LAI at low vegetation density as discussed under the sensitivity analysis based on the simulated dataset. For example, NDII and ISR had high sensitivities only next to NDVI at low LAI. Yet NDVI, which had always been most sensitive at low LAI, did not show better performance in 2012 compared to 2011. Nonetheless, those SVIs, which were reported to have high sensitivity to low LAI (open canopy), maintained more or less the same relationship for the two growing

seasons, whereas those SVIs which did well with high LAI as was the case for 2011 had poor performance with low LAI in 2012. That is why SWIR based indices, such as NDII and ISR, had comparable performances for both sites due partly to their less sensitivity to C_{ab} and partly to efficient correction for canopy background effects. As a result, it can be said that the choice of an index for LAI prediction depends to some extent on a *priori* knowledge about the condition of the crop. This confirms the assertion of Broge and Leblanc (2001) who concluded that the choice of SVI should depend on a priori knowledge of the variation of external parameters affecting the spectral reflectance of the canopy and the range of parameters to be estimated. As a result, $IIReR_1$, SR and WDVI could be used with high vegetation density whereas NDII and ISR might be preferable for LAI mapping at an open canopy with a low C_{ab} situation.

Nevertheless, the sensitivity function did not show consistency with other statistical indicators on the performance of SVIs. Despite these inconsistencies, it could still be a useful technique to map the general pattern of the performance of various SVIs to synergize their performance by integrating two or more indices for LAI mapping as opposed to the conventional use of single SVIs. This could be done by employing different SVIs for predicting different LAI ranges based on their sensitivity function on the condition that prior knowledge is available about the vegetation condition to be mapped.

5.2.3 SVI-LAI relationships based on APEX imagery

Based on the results from the SVI-LAI relationships derived from APEX imagery all the SVIs had strong linear relationships with LAI-2000. A cross-sensor comparison of the relationships also revealed strong consistency among APEX, VENμS, S-2 and Landsat TM band settings. This is in agreement with a comparable LAI prediction power revealed between MODIS and ETM+ (Broge and Leblanc 2001; Lee, Cohen et al. 2004). However, slight deviations were noticed between SVIs derived from APEX and MSR16R (Appendix 11). This might be explained by the different parameters affecting the spectral characteristics of the two sensors. These include the height from which the data were acquired which is 4600m for APEX whereas the MSR16R measurement is performed at a close range of maximum 3m height. This might be one factor for higher values of SVIs derived from MSR16R data. The other possible justification could be the spatial resolution of the two sensors being 0.6 m radius and 2.5m * 2.9m for MSR16R and APEX, respectively. The relatively low spatial resolution for APEX might be more vulnerable to measuring soil spectra, which might subsequently reduce the spectral values compared to the MSR16R where the potato crop is targeted at fine scale yielding higher spectral data. This effect might be more pronounced in this case as the potato was planted on 0.75 m wide rows with soil background effect being high in between rows unless the LAI is high enough for the canopy to close. Similar effect of the in between row was reported by Herrmann, Pimstein et al. (2011), where the higher RMSE for potato than wheat was attributed to the wider opening in between potato rows. Nevertheless, the LAI was large enough for the canopy to close on the date the APEX flight was acquired and hence the differences due to soil background effect were less likely. Moreover, the temporal aspect might also be an important factor as far as the time of data acquisition coupled with the relative position of the sun is particularly essential for APEX although MSR16R is not sensitive to cloud cover as well as the source of illumination.

5.2.4 Validation of SVI-LAI relationships based on MSR16R and APEX

Based on the MSR16R data the SVIs did not show consistency across sites and most of them had inferior LAI prediction power for the 2012 site as judged by the R^2 values (Table 11). The lower RMSE values for 2012 do not mean an improved prediction power but a bias

introduced by the lower LAI value range in 2012 than 2011. This made a cross-site comparison of the performance of the SVIs using the RMSE misleading. As a result, only the R^2 values, not the RMSE computed for the two growing seasons should be used for a cross-site comparison of the performance of SVIs. This shortcoming of the use of RMSE was also confirmed by (Ji and Peters 2007). The RPD was computed to overcome the problem as it standardizes for differences in the data range and the results showed a better evaluation of the performance of SVI than RMSE. Yet, RPD was also found to depend on the nature of datasets and was influenced by the differences in the distribution of the data for the two years (fig. 20) where the 2012 dataset had less dispersions than the 2011. This suggests that the use of these statistical measures depends on the nature of datasets being compared.

Most of the SVIs analysed revealed comparable performances across the narrow band sensors and broad bands of ETM+ as simulated by APEX data (table 13). This suggests that the ESA's upcoming space systems could be compared with either hyperspectral sensors such as APEX or broad band ETM+. This again complies with (Broge and Leblanc 2001) and (Lee, Cohen et al. 2004) who showed a comparable performance of hyperspectral and ETM+ bands. Unlike many of the SVIs, the red edge indices such as $NDRE_1$ and $NDRE_2$, however, did not yield consistent results across those sensors nor had they superior performances. This could partly be attributed to the reason that the data for the other sensors was a common airborne APEX image, whereas MSR16R data was acquired in a close range. On the other hand, those SVIs based partly on the SWIR bands maintained a considerable degree of consistency both within the narrow band sensors as well as with the broad band ones. In general, results of the use of the red edge bands of S-2 and VENµS were comparable to the broad bands of TM as well as to other narrow band sensors. The performances of the different indices also varied for the ESA's upcoming space borne systems as they did vary with other sensors. Hence, the narrowly positioned red edge bands of those sensors could be used instead of the broad bands.

A comparison of the performance of those SVIs based on the PROSAIL model and empirical data also showed a lack of consistency with most of the indices while only few demonstrated a similar level of performances across sensors. Some indices such as WDVI and NDRE2 showed big improvement with the empirical data. This could be due to the diverse disturbance factors assumed with the simulated data, whereas the empirical data was free from many of these variables such as wide range of C_{ab} levels, different soil moisture levels and LADs.

Furthermore, the sensitivity function indicated high sensitivities for best performing SVIs, for instance, $IIReR_1$ and SR which had superior performance (R^2 = 0.81 and 0.79, respectively) for the 2011 site. Moreover, as the validation graph (Figure 23) suggested both indices, particularly $IIReR_1$, had less accurate LAI prediction as the points were found scattered further away from the equality line (x = y). This also complies with the low sensitivity at low LAIs (LAI < 3). However, there were inconsistencies between the *S* record and the performance of some indices such as WDVI, which had low sensitivity (fig. 24) despite its high LAI prediction power (R^2=0.77) (table 12). This inconsistent performance of the S function was also reported by Gonsamo and Pellikka (2012). The *S* function based on empirical data also showed more fluctuations as compared to the PROSAIL model. This is because the field measurements in terms of both LAI-2000 as well as MSR16R might be prone to disturbances unlike the simulated data where every parameter value was virtually subjected to manipulation. Nonetheless, the S function for both 2011 and 2012 showed a similar pattern with the simulated data, which revealed a high sensitivity at low LAI and a decrease with increasing LAI.

6. Conclusions and recommendations

Based on the analysis of the sensitivity of selected spectral regions to LAI for different soil moisture levels, the NIR followed by SWIR and red-edge bands showed high sensitivity to LAI, while responding differently to canopy background effects compared to the red bands. These spectral regions can be used to improve the SVI-LAI relationships based on NIR. The Integrated Infrared and Red edge Ratio (both IIReR1 and IIReR2), which have been evaluated in this study, demonstrated better sensitivity to LAI than other SVIs based on the PROSAIL data. Moreover, IIReR1, which maintained superior performance with empirical data for potatoes from 2011, was found to be the best for LAI prediction. Hence, the integration of SWIR and red edge bands with the widely used NIR and red bands can improve the SVI-LAI relationship.

Based on the sensitivity analysis using a normalized sensitivity function and the commonly used statistical measures, R^2 and RMSE, it was found that SVIs were highly sensitive to canopy LADs and leaf C_{ab} levels. They showed the poorest performance for planophile LAD and low leaf C_{ab} levels, while SVI-LAI relationships improved at high leaf C_{ab} as well as with erectophile LADs. The effect was more pronounced with greenness indices such as NDVI, $NDRE_1$, $NDRE_2$, WDVI and SR whereas indices partly based on SWIR bands, such as $IIReR_1$, $IIReR_2$, ISR and NDII, showed more resilience though they followed a similar pattern. However, all the SVIs considered showed less sensitivity to varying soil moisture levels. This does not mean that the SVIs minimize the background effect, because the inconsistency in their performance based on empirical data could be partly explained by the soil background effect evident from the 2012 site. The use of a sensitivity function (*S*) for comparing multiple SVIs showed high performance of SVIs at low LAI values while indicating different levels of *S* at various LAI ranges with a general decline in *S* with increasing LAI. Despite the significant sensitivity level of SVIs-LAI relations, the S function does not necessarily indicate the suitability of an index for LAI mapping as few SVIs with high *S* record reported an insignificant relation with LAI based on empirical data.

From the analysis of SVIs across broad and narrow band sensors based on both PROSAIL and empirical data, all the SVIs considered demonstrated strongly consistent performance. Moreover, the broad bands of Landsat TM as simulated using APEX data yielded comparable results with the narrow bands of MSR16R, APEX, S-2 and VENµS. Hence, it could be concluded that broad ETM+ bands suffer no poor performance for its lower spectral resolution than the narrow band multispectral or hyperspectral sensors. However, it should be noted that the broad band sensors do not offer the opportunities to derive narrow band indices which, unlike the conventional broad band indices, are based on multiple spectral regions.

A further validation of the performance of SVIs for LAI prediction across the two growing seasons did not yield consistent performance. Most of the SVIs had better prediction power in 2011 than in 2012, which implies that most of the indices had strong relation with LAI for high canopy. The high performance of IIReR1, SR and WDVI throughout the 2011 growing season indicated consistent performance through crop phenological stages. However, these SVIs were not consistent across different management practices as evident from the poor performance for 2012. Based on the different performance records of SVIs between the two sites the choice of an index should be based on the range of parameter to be estimated and the *priori* knowledge about the factors affecting its estimation in the region of interest. $IIReR_1$, SR and WDVI appear to be suitable for high LAI, whereas NDII and ISR might be preferred for low vegetation density or open canopies characterized by low C_{ab} and bright soil background.

Recommendations:

Based on the above conclusions the following recommendations can be drawn:

- The $IIReR_1$ index was found to be suitable for LAI retrieval among the SVIs considered based on the 2011 site. However, a further validation with empirical field data might be useful to test the robustness of the index.
- The sensitivity function needs to be tested further for its capability to suggest SVIs suitable at certain LAI range. This could be tested with field data to examine the possibility to combine multiple SVIs for LAI mapping particularly for crop monitoring throughout the growing seasons.
- The consistent performance of SVIs across different sensors allows for the possibility to combine spectral information to enhance the temporal resolution for crop monitoring. Yet, further comparison of hyperspectral narrow band and broad band sensors could be essential to investigate the advantage of the spectral properties of the former over the latter for LAI estimation for different crops.
- The application of additional nitrogen did not have significant effect on LAI between fertilized plots. Further research in to the matter could be helpful to gain understanding on the effect of N levels by controlling for extraneous factors such as soil conditions and weather parameters.

References

Allen, E. J. and P. J. O'Brien (1986). "The practical significance of accumulated day-degrees as a measure of physiological age of seed potato tubers." Field Crops Research **14**(0): 141-151.

Asner, G. P., J. M. O. Scurlock, et al. (2003). "Global synthesis of leaf area index observations: implications for ecological and remote sensing studies." Global Ecology and Biogeography **12**(3): 191-205.

Baret, F. and G. Guyot (1991). "Potentials and limits of vegetation indices for LAI and APAR assessment." Remote Sensing of Environment **35**(2–3): 161-173.

Becker, F. and B. J. Choudhury (1988). "Relative sensitivity of normalized difference vegetation Index (NDVI) and microwave polarization difference Index (MPDI) for vegetation and desertification monitoring." Remote Sensing of Environment **24**(2): 297-311.

Beeri, O. and A. Peled (2009). "Geographical model for precise agriculture monitoring with real-time remote sensing." ISPRS Journal of Photogrammetry and Remote Sensing **64**(1): 47-54.

Bélanger, G., J. Walsh, et al. (2001). "Tuber growth and biomass partitioning of two potato cultivars grown under different N fertilization rates with and without irrigation." American journal of potato research **78**(2): 109-117.

Bishop, T. F. A. and A. B. McBratney (2002). "Creating Field Extent Digital Elevation Models for Precision Agriculture." **3**(1): 37-46.

Brantley, S. T., J. C. Zinnert, et al. (2011). "Application of hyperspectral vegetation indices to detect variations in high leaf area index temperate shrub thicket canopies." Remote Sensing of Environment **115**(2): 514-523.

Broge, N. H. and E. Leblanc (2001). "Comparing prediction power and stability of broadband and hyperspectral vegetation indices for estimation of green leaf area index and canopy chlorophyll density." Remote Sensing of Environment **76**(2): 156-172.

Broge, N. H. and J. V. Mortensen (2002). "Deriving green crop area index and canopy chlorophyll density of winter wheat from spectral reflectance data." Remote Sensing of Environment **81**(1): 45-57.

Brown, L., J. M. Chen, et al. (2000). "A Shortwave Infrared Modification to the Simple Ratio for LAI Retrieval in Boreal Forests: An Image and Model Analysis." Remote Sensing of Environment **71**(1): 16-25.

Canisius, F., R. Fernandes, et al. (2010). "Comparison and evaluation of Medium Resolution Imaging Spectrometer leaf area index products across a range of land use." Remote Sensing of Environment **114**(5): 950-960.

Chirkov, Y. I. (1965). "Agrometeorological indices in the development and formation of maize crops." Agricultural Meteorology **2**(2): 121-126.

Clevers, J. G. P. W. (1988). "The derivation of a simplified reflectance model for the estimation of leaf area index." Remote Sensing of Environment **25**(1): 53-69.

Clevers, J. G. P. W. (1989). "Application of a weighted infrared-red vegetation index for estimating leaf Area Index by Correcting for Soil Moisture." Remote Sensing of Environment **29**(1): 25-37.

Clevers, J. G. P. W., C. Büker, et al. (1994). "A framework for monitoring crop growth by combining directional and spectral remote sensing information." Remote Sensing of Environment **50**(2): 161-170.

Clevers, J. G. P. W. and A. A. Gitelson (2013). "Remote estimation of crop and grass chlorophyll and nitrogen content using red-edge bands on Sentinel-2 and -3." International Journal of Applied Earth Observation and Geoinformation **23**(0): 344-351.

Clevers, J. G. P. W. and L. Kooistra (2012). "Using hyperspectral remote sensing data for retrieving canopy chlorophyll and nitrogen content." Selected Topics in Applied Earth Observations and Remote Sensing, IEEE Journal of **5**(2): 574-583.

Clevers, J. G. P. W. and H. J. C. van Leeuwen (1996). "Combined use of optical and microwave remote sensing data for crop growth monitoring." Remote Sensing of Environment **56**(1): 42-51.

Cohen, W. B., T. K. Maiersperger, et al. (2003). "An improved strategy for regression of biophysical variables and Landsat ETM+ data." Remote Sensing of Environment **84**(4): 561-571.
Cox, S. (2002). "Information technology: the global key to precision agriculture and sustainability." Computers and Electronics in Agriculture **36**(2–3): 93-111.
Danson, F. and S. Plummer (1995). "Red-edge response to forest leaf area index." Remote Sensing **16**(1): 183-188.
Darvishzadeh, R., C. Atzberger, et al. (2009). "Leaf Area Index derivation from hyperspectral vegetation indicesand the red edge position." International Journal of Remote Sensing **30**(23): 6199-6218.
Darvishzadeh, R., A. Skidmore, et al. (2008). "LAI and chlorophyll estimation for a heterogeneous grassland using hyperspectral measurements." ISPRS Journal of Photogrammetry and Remote Sensing **63**(4): 409-426.
Demarty, J., F. Chevallier, et al. (2007). "Assimilation of global MODIS leaf area index retrievals within a terrestrial biosphere model." Geophysical Research Letters **34**(15).
Dente, L., G. Satalino, et al. (2008). "Assimilation of leaf area index derived from ASAR and MERIS data into CERES-Wheat model to map wheat yield." Remote Sensing of Environment **112**(4): 1395-1407.
Fernandes, R., C. Butson, et al. (2003). "Landsat-5 TM and Landsat-7 ETM+ based accuracy assessment of leaf area index products for Canada derived from SPOT-4 VEGETATION data." Canadian Journal of Remote Sensing **29**(2): 241-258.
Gitelson, A. A. (2004). "Wide Dynamic Range Vegetation Index for Remote Quantification of Biophysical Characteristics of Vegetation." Journal of Plant Physiology **161**(2): 165-173.
Gitelson, A. A. and M. N. Merzlyak (2003). "Relationships between leaf chlorophyll content and spectral reflectance and algorithms for non-destructive chlorophyll assessment in higher plant leaves." Journal of Plant Physiology **160**(3): 271-282.
Gonsamo, A. (2011). "Normalized sensitivity measures for leaf area index estimation using three-band spectral vegetation indices." International Journal of Remote Sensing **32**(7): 2069-2080.
Gonsamo, A. and P. Pellikka (2012). "The sensitivity based estimation of leaf area index from spectral vegetation indices." ISPRS Journal of Photogrammetry and Remote Sensing **70**: 15-25.
González-Sanpedro, M. C., T. Le Toan, et al. (2008). "Seasonal variations of leaf area index of agricultural fields retrieved from Landsat data." Remote Sensing of Environment **112**(3): 810-824.
Haboudane, D., J. R. Miller, et al. (2002). "Integrated narrow-band vegetation indices for prediction of crop chlorophyll content for application to precision agriculture." Remote Sensing of Environment **81**(2): 416-426.
Hardisky, M., V. Klemas, et al. (1983). "The influence of soil salinity, growth form, and leaf moisture on the spectral radiance of Spartina alterniflora canopies." Photogrammetric Engineering and Remote Sensing **49**: 77-83.
Hatfield, J. L. and J. H. Prueger (2010). "Value of using different vegetative indices to quantify agricultural crop characteristics at different growth stages under varying management practices." Remote Sensing **2**(2): 562-578.
Herrmann, I., A. Karnieli, et al. (2010). Assessment of field crops leaf area index by the red-edge inflection point derived from venμs bands. 10 th International Conference on Precision Agriculture. CD-ROM.
Herrmann, I., A. Pimstein, et al. (2011). "LAI assessment of wheat and potato crops by VENμS and Sentinel-2 bands." Remote Sensing of Environment **115**(8): 2141-2151.
Hoogenboom, G. (2000). "Contribution of agrometeorology to the simulation of crop production and its applications." Agricultural and Forest Meteorology **103**(1–2): 137-157.
Houborg, R. and E. Boegh (2008). "Mapping leaf chlorophyll and leaf area index using inverse and forward canopy reflectance modeling and SPOT reflectance data." Remote Sensing of Environment **112**(1): 186-202.
Huete, A., C. Justice, et al. (1994). "Development of vegetation and soil indices for MODIS-EOS." Remote Sensing of Environment **49**(3): 224-234.

Jacquemoud, S., C. Bacour, et al. (2000). "Comparison of Four Radiative Transfer Models to Simulate Plant Canopies Reflectance: Direct and Inverse Mode." Remote Sensing of Environment **74**(3): 471-481.
Jacquemoud, S. and F. Baret (1990). "PROSPECT: A model of leaf optical properties spectra." Remote Sensing of Environment **34**(2): 75-91.
Jacquemoud, S., F. Baret, et al. (1995). "Extraction of vegetation biophysical parameters by inversion of the PROSPECT+ SAIL models on sugar beet canopy reflectance data. Application to TM and AVIRIS sensors." Remote Sensing of Environment **52**(3): 163-172.
Ji, L. and A. J. Peters (2007). "Performance evaluation of spectral vegetation indices using a statistical sensitivity function." Remote Sensing of Environment **106**(1): 59-65.
Kooistra, L., E. Beza, et al. (2012) "Integrating remote-, close range-and in-situ sensing for high-frequency observation of crop status to support precision agriculture."
Lee, K.-S., W. B. Cohen, et al. (2004). "Hyperspectral versus multispectral data for estimating leaf area index in four different biomes." Remote Sensing of Environment **91**(3–4): 508-520.
Liu, J., E. Pattey, et al. (2012). "Assessment of vegetation indices for regional crop green LAI estimation from Landsat images over multiple growing seasons." Remote Sensing of Environment **123**(0): 347-358.
López-Granados, F., M. Jurado-Expósito, et al. (2005). "Using geostatistical and remote sensing approaches for mapping soil properties." European Journal of Agronomy **23**(3): 279-289.
Mazurczyk, W., B. Lutomirska, et al. (2003). "Relation between air temperature and length of vegetation period of potato crops." Agricultural and Forest Meteorology **118**(3–4): 169-172.
McBratney, A., B. Whelan, et al. (2005). "Future Directions of Precision Agriculture." **6**(1): 7-23.
Moreenthaler, G. W., N. Khatib, et al. (2003). "Incorporating a constrained optimization algorithm into remote sensing/precision agriculture methodology." Acta Astronautica **53**(4–10): 429-437.
O'Brien, P. J., E. J. Allen, et al. (1983). "Accumulated day-degrees as a measure of physiological age and the relationships with growth and yield in early potato varieties." The Journal of Agricultural Science **101**(03): 613-631.
Palacios-Orueta, A. and S. L. Ustin (1998). "Remote Sensing of Soil Properties in the Santa Monica Mountains I. Spectral Analysis." Remote Sensing of Environment **65**(2): 170-183.
Pearson, R. L. and L. D. Miller (1972). Remote mapping of standing crop biomass for estimation of the productivity of the shortgrass prairie.
Richter, K., C. Atzberger, et al. (2009). "Experimental assessment of the Sentinel-2 band setting for RTM-based LAI retrieval of sugar beet and maize." Canadian Journal of Remote Sensing **35**(3): 230-247.
Rouse Jr, J., R. Haas, et al. (1974). "Monitoring the vernal advancement and retrogradation (green wave effect) of natural vegetation."
Schaepman, M. Jehle, et al. (2012). "The 4th generation imaging spectrometer APEX and its application in Earth observation." IEEE Transactions on Geoscience and Remote Sensing.
Schellberg, J., M. J. Hill, et al. (2008). "Precision agriculture on grassland: Applications, perspectives and constraints." European Journal of Agronomy **29**(2–3): 59-71.
Schlerf, M., C. Atzberger, et al. (2005). "Remote sensing of forest biophysical variables using HyMap imaging spectrometer data." Remote Sensing of Environment **95**(2): 177-194.
Seelan, S. K., S. Laguette, et al. (2003). "Remote sensing applications for precision agriculture: A learning community approach." Remote Sensing of Environment **88**(1–2): 157-169.
Shafri, H. Z. M., M. A. M. Salleh, et al. (2006). "Hyperspectral remote sensing of vegetation using red edge position techniques." American Journal of Applied Sciences **3**(6): 1864-1871.
Si, Y., M. Schlerf, et al. (2012). "Mapping spatio-temporal variation of grassland quantity and quality using MERIS data and the PROSAIL model." Remote Sensing of Environment **121**(0): 415-425.
Stroppiana, D., M. Boschetti, et al. (2006). "Evaluation of LAI-2000 for leaf area index monitoring in paddy rice." Field Crops Research **99**(2–3): 167-170.
Tian, Y., R. Dickinson, et al. (2004). "Comparison of seasonal and spatial variations of leaf area index and fraction of absorbed photosynthetically active radiation from Moderate Resolution

Imaging Spectroradiometer (MODIS) and Common Land Model." Journal of Geophysical Research: Atmospheres (1984–2012) **109**(D1).
Verhoef, W. (1985). "Earth observation modeling based on layer scattering matrices." Remote Sensing of Environment **17**(2): 165-178.
Vickers, D. and P. Rees (2007). "Creating the UK National Statistics 2001 output area classification." Journal of the Royal Statistical Society: Series A (Statistics in Society) **170**(2): 379-403.
Wang, F. M., J. F. Huang, et al. (2007). "New vegetation index and its application in estimating leaf area index of rice." Rice Science **14**(3): 195-203.
Wang, L., J. J. Qu, et al. (2008). "Sensitivity studies of the moisture effects on MODIS SWIR reflectance and vegetation water indices." International Journal of Remote Sensing **29**(24): 7065-7075.
Wang, X.-L., F.-M. Li, et al. (2005). "Increasing potato yields with additional water and increased soil temperature." Agricultural Water Management **78**(3): 181-194.
Wiegand, C. L., S. J. Maas, et al. (1992). "Multisite analyses of spectral-biophysical data for wheat." Remote Sensing of Environment **42**(1): 1-21.
Wu, C., Z. Niu, et al. (2008). "Estimating chlorophyll content from hyperspectral vegetation indices: Modeling and validation." agricultural and forest meteorology **148**(8): 1230-1241.
Wu, J., D. Wang, et al. (2007). "Assessing broadband vegetation indices and QuickBird data in estimating leaf area index of corn and potato canopies." Field Crops Research **102**(1): 33-42.
Xiao, Z., S. Liang, et al. (2011). "Real-time retrieval of Leaf Area Index from MODIS time series data." Remote Sensing of Environment **115**(1): 97-106.
Xiao, Z., S. Liang, et al. (2009). "A temporally integrated inversion method for estimating leaf area index from MODIS data." Geoscience and Remote Sensing, IEEE Transactions on **47**(8): 2536-2545.
Xu, X., W. Fan, et al. (2009). "The spatial scaling effect of continuous canopy Leaves Area Index retrieved by remote sensing." Science in China Series D: Earth Sciences **52**(3): 393-401.
Yao, Y., Q. Liu, et al. (2008). "LAI retrieval and uncertainty evaluations for typical row-planted crops at different growth stages." Remote Sensing of Environment **112**(1): 94-106.
Yuping, M., W. Shili, et al. (2008). "Monitoring winter wheat growth in North China by combining a crop model and remote sensing data." International Journal of Applied Earth Observation and Geoinformation **10**(4): 426-437.
Zhang, N., M. Wang, et al. (2002). "Precision agriculture—a worldwide overview." Computers and Electronics in Agriculture **36**(2): 113-132.
Zhao, D., T. Yang, et al. (2012). "Effects of crop residue cover resulting from tillage practices on LAI estimation of wheat canopies using remote sensing." International Journal of Applied Earth Observation and Geoinformation **14**(1): 169-177.
Zhao, H., Y.-C. Xiong, et al. (2012). "Plastic film mulch for half growing-season maximized WUE and yield of potato via moisture-temperature improvement in a semi-arid agroecosystem." Agricultural Water Management **104**(0): 68-78.
Zheng, G. and L. M. Moskal (2009). "Retrieving Leaf Area Index (LAI) Using Remote Sensing: Theories, Methods and Sensors." Sensors **9**(4): 2719-2745.
Ziadi, N., B. Zebarth, et al. (2012). Soil and Plant Tests to Optimize Fertilizer Nitrogen Management of Potatoes. Sustainable Potato Production: Global Case Studies. Z. He, R. Larkin and W. Honeycutt, Springer Netherlands**:** 187-207.

APPENDICES

Appendix 1: Variability of the red and red-edge spectra across different leaf Cab levels. The graph presents the reflectance at 710 and 670 at LAI values of 1, 2, 3 and 4 beyond which the reflectance saturates for 670 nm while it still continues to drop for 710 with negligible effect of LAI.

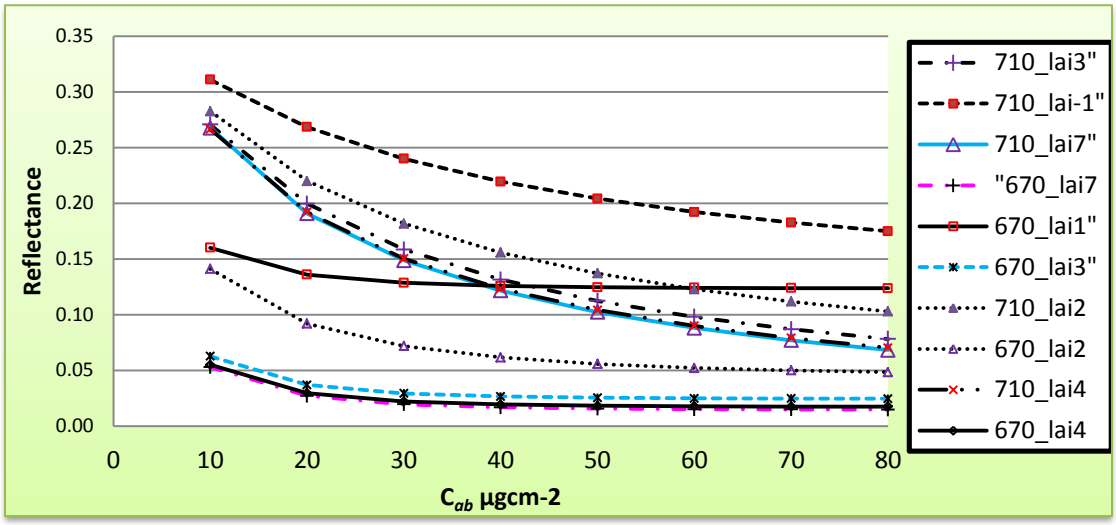

Appendix 2: SV-LAI Relationships based on different soil moisture levels for NDVI (a), WDVI (b), IIReR1 (c), SR (d), NDII (e), IIReR2 (f), MSR (g), NDRE1 (h), EVI (i), NDRE2 (j) and ISR (k).

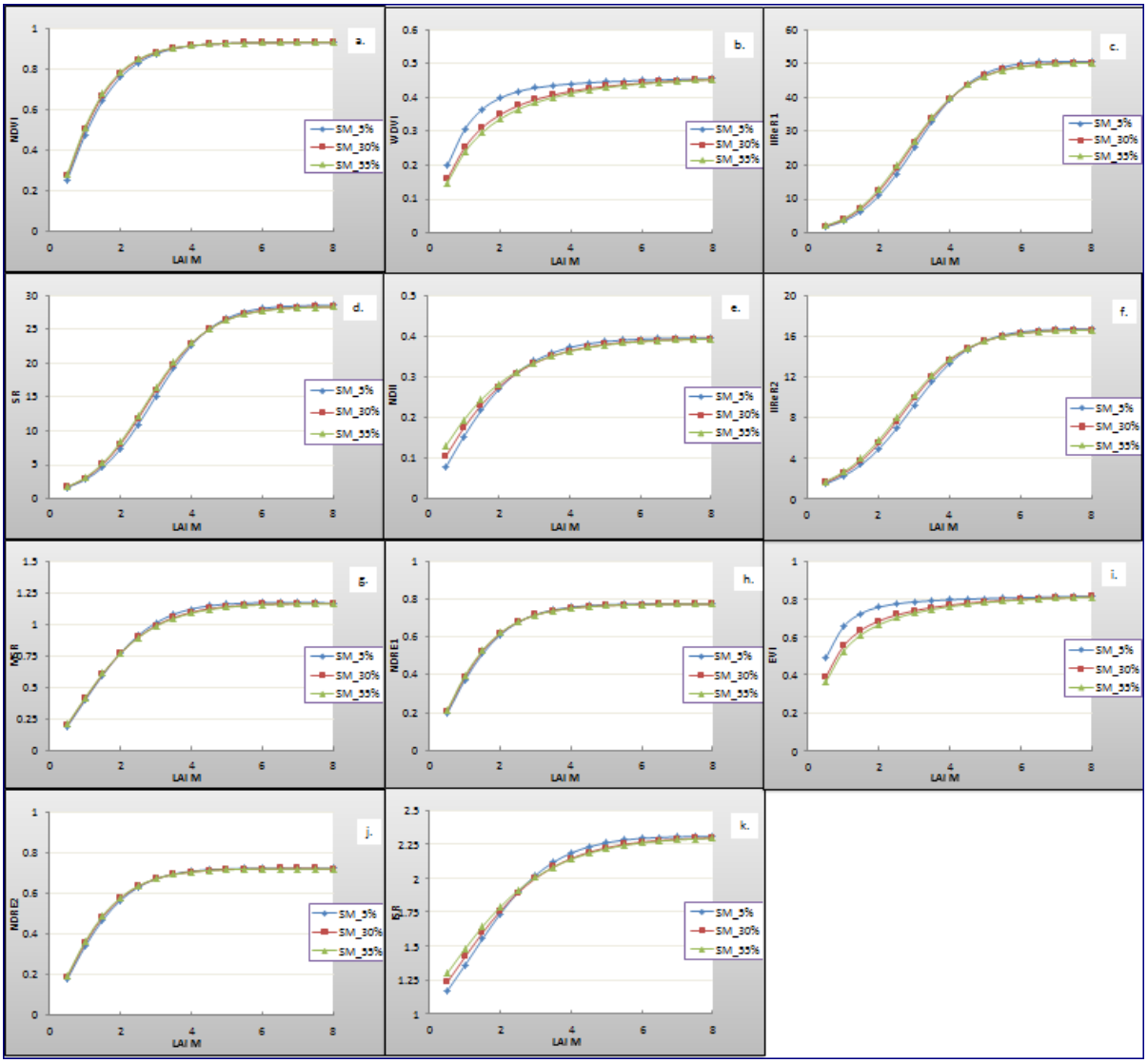

Appendix 3: SVI-LAI relationships based on Planophile, spherical and Erectophile LADs for NDVI (a), WDVI (b), IIReR1 (c), SR (d), NDII (e), IIReR2 (f), MSR (g), NDRE1 (h), EVI (i), NDRE2 (j) and ISR (k).

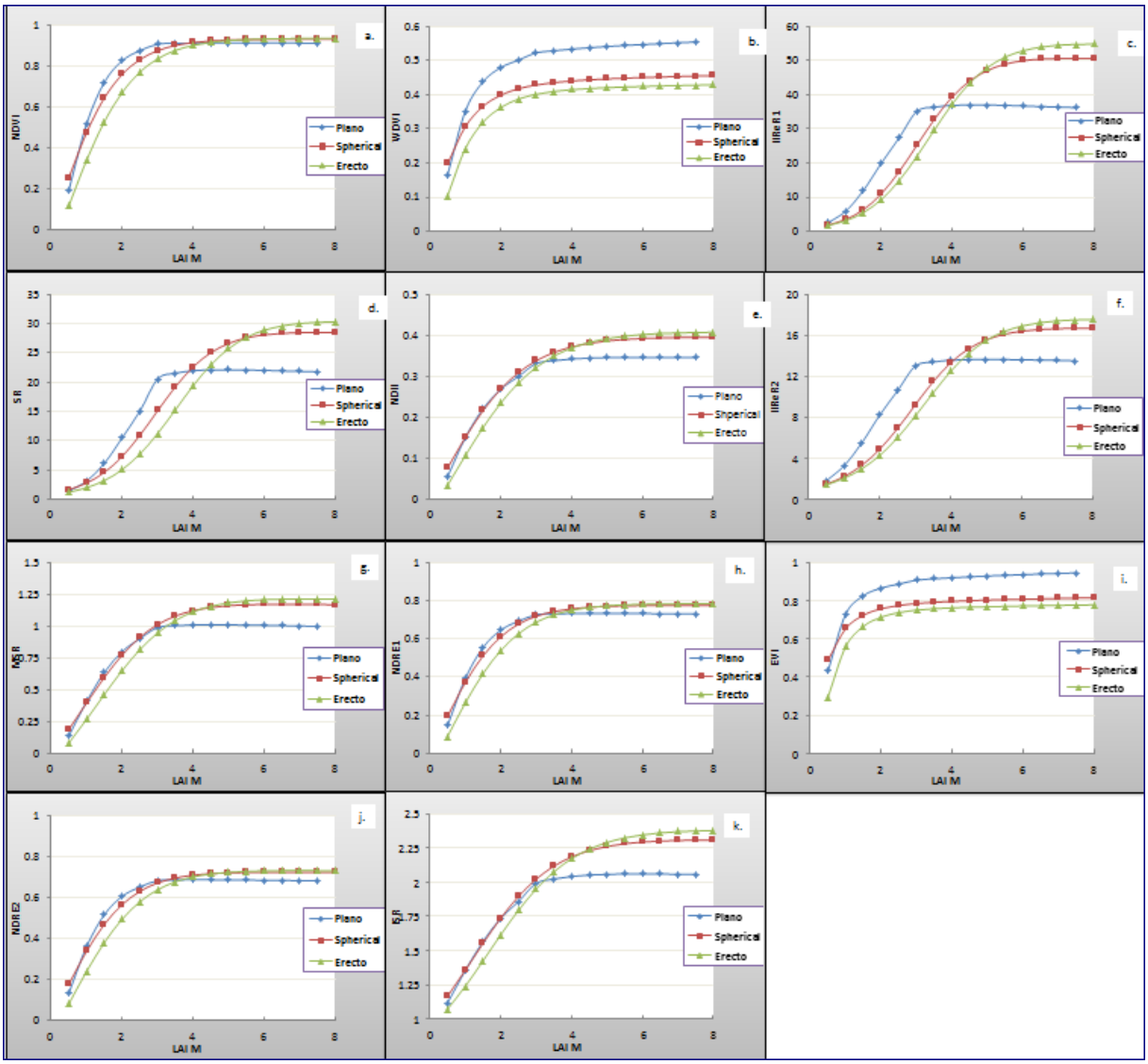

Appendix 4: SVI-LAI Relationship based on different leaf Cab levels (20µgcm-2, 40µgcm-2, and 60µgcm-2) for NDVI (a), WDVI (b), IIReR1 (c), SR (d), NDII (e), IIReR2 (f), MSR (g), NDRE1 (h), EVI (i), NDRE2 (j) and ISR (k).

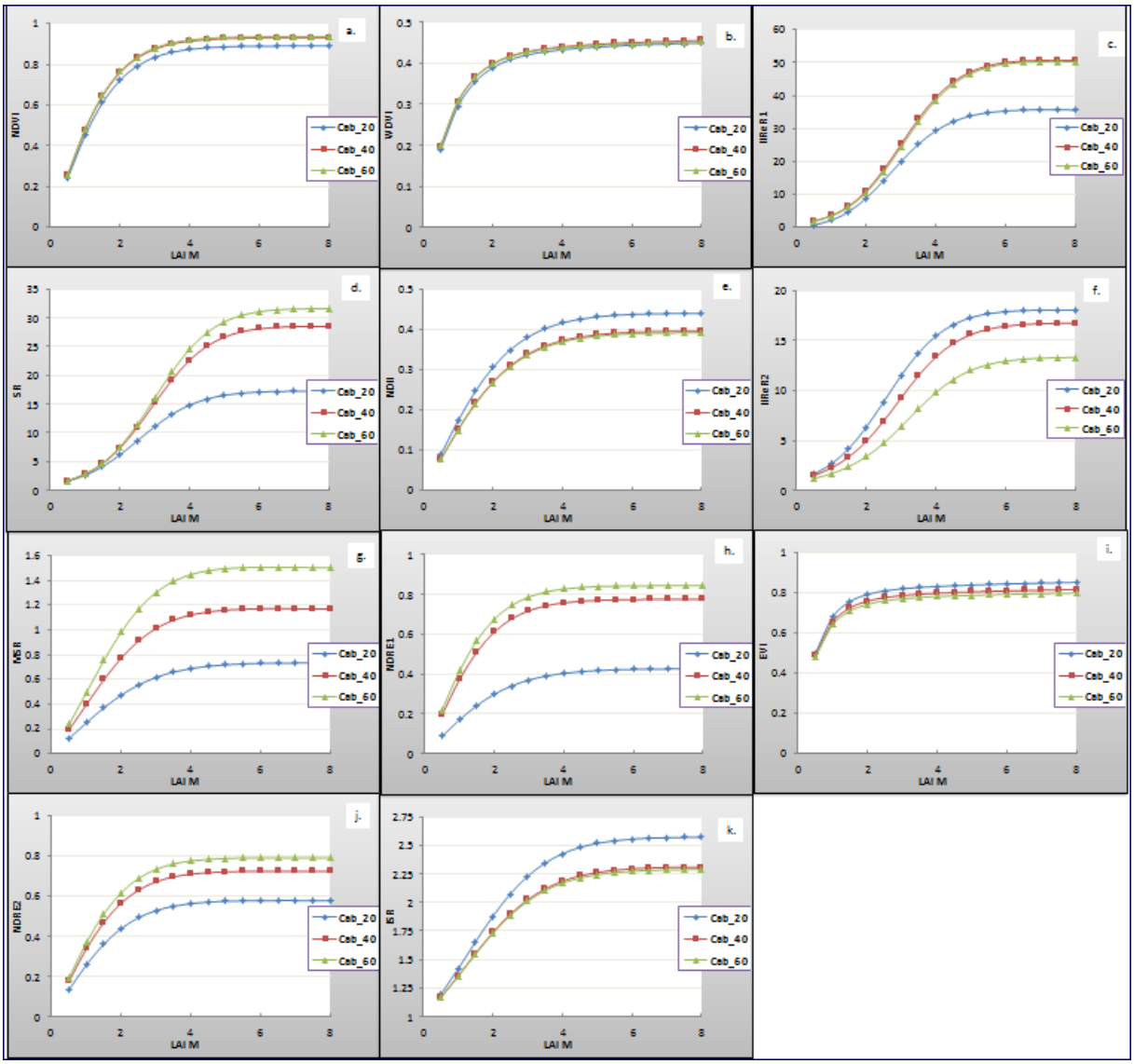

Appendix 5: Sensitivity analysis using a sensitivity function (S).

A) Sensitivity analysis based on a) the best-fit-function and b) the exponential model at leaf C_{ab} level of 40 µgcm-2, spherical LAD and bright soil background.

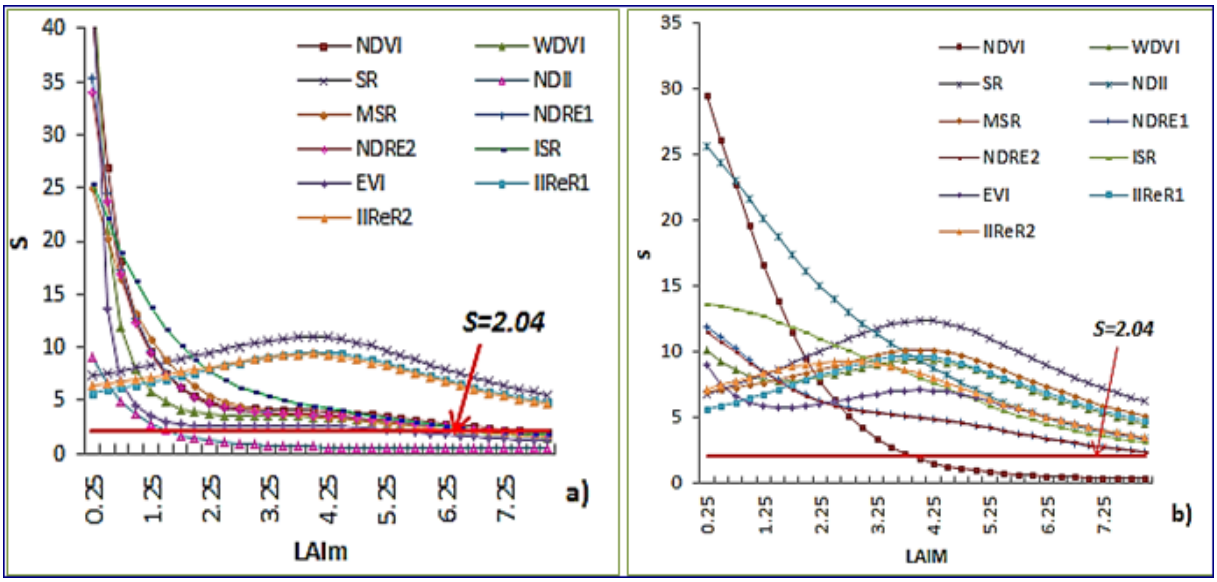

B) Sensitivity analysis of SVIs to LAI based on planophile LAD using best fit (a) and SRM (b) with NDVI and NDII showing high sensitivity at low vegetation under both models with the former showing high sensitivity at low LAI.

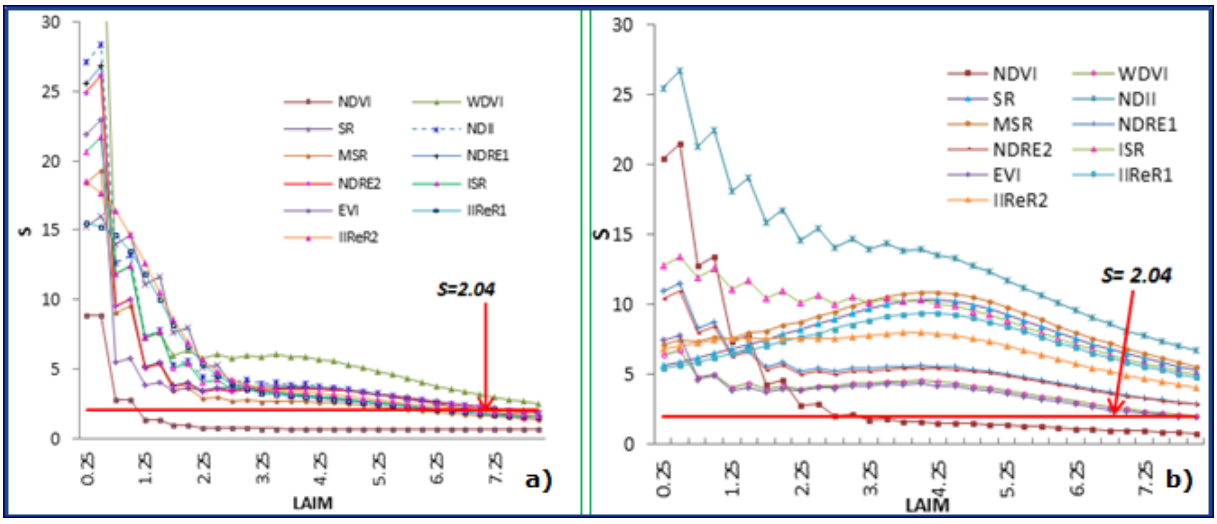

Appendix 6: Initial fertilization levels and additional nitrogen application during the growing seasons for 2011 sites

Plot	Initial Organic N kg/ha	Treatment Type	Additional Nitrogen Fertilization during the growing season								
			May 18		June 21		July 7		July 20		
			Advised	Applied	Advised	Applied	Advised	Applied	Advised	Advised	Total
A	**23**	**CL**									**165**
B	**23**	**TTW**			**15**	**13.5**			**15**	**13.5**	**192**
C	**0**	**CL**									**38**
D	**0**	**TTW**			**50**	**54**			**50**	**54**	**146**
E	34	**CL**									**229**
F	34	**TTW**									**229**
G	46	**CL**									**292**
H	46	**TTW**									**292**
I	46	**MB**					**49**	**54**			**346**
J	34	**MB**					**28**	**27**			**256**
K	**0**	**MB**		**54**			**0**	**54**			**146**
L	23	**MB**	**48**	**54**			**59**	**54**			**321**

Appendix 7. Comparison of mean difference between the weather parameters for 2011 and 2012 growing seasons using a paired samples t-test

		Paired Differences					t	df	Sig. (2-tailed)
		Mean	Std. Deviation	Std. Error Mean	95% Confidence Interval of the Difference				
					Lower	Upper			
Pair 1	CumT_2011 - CumT_2012	41.301	28.060	2.276	36.805	45.80	18.15	151	.000
Pair 2	CumRF2011 - CumRF2012	-84.961	37.573	3.048	-90.982	-78.94	-27.88	151	.000
Pair 3	CumSH2011 - CumSH2012	101.505	60.147	4.879	91.866	111.14	20.81	151	.000

Appendix 8. Average LAI based on nitrogen treatment levels through 2011 (a & b) and 2012 (c) growing seasons.

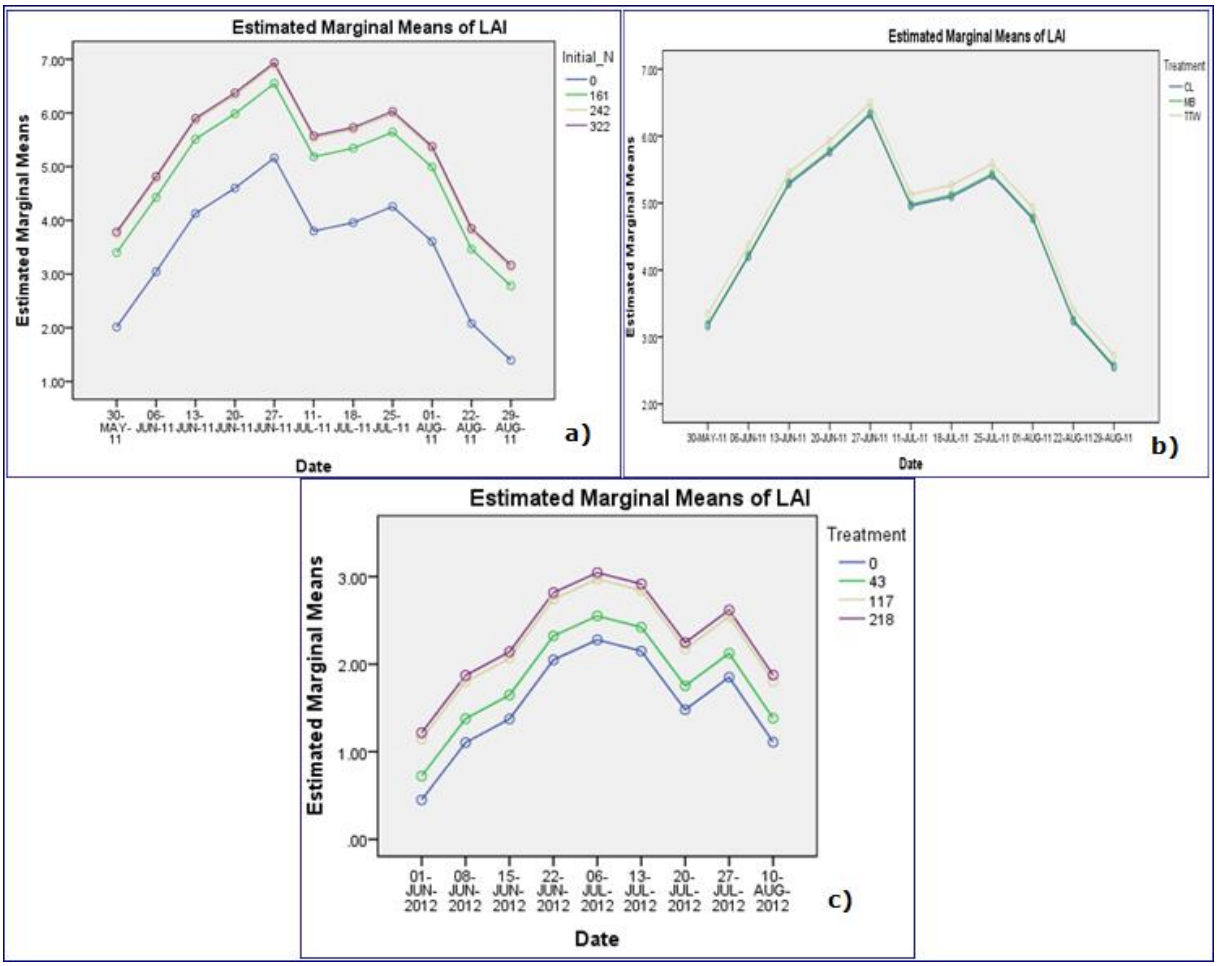

Appendix 9: SVI-LAI relationships for the 2011 growing season. Note that the values for all the SVIs were normalized to the same value range of 1 to 10.

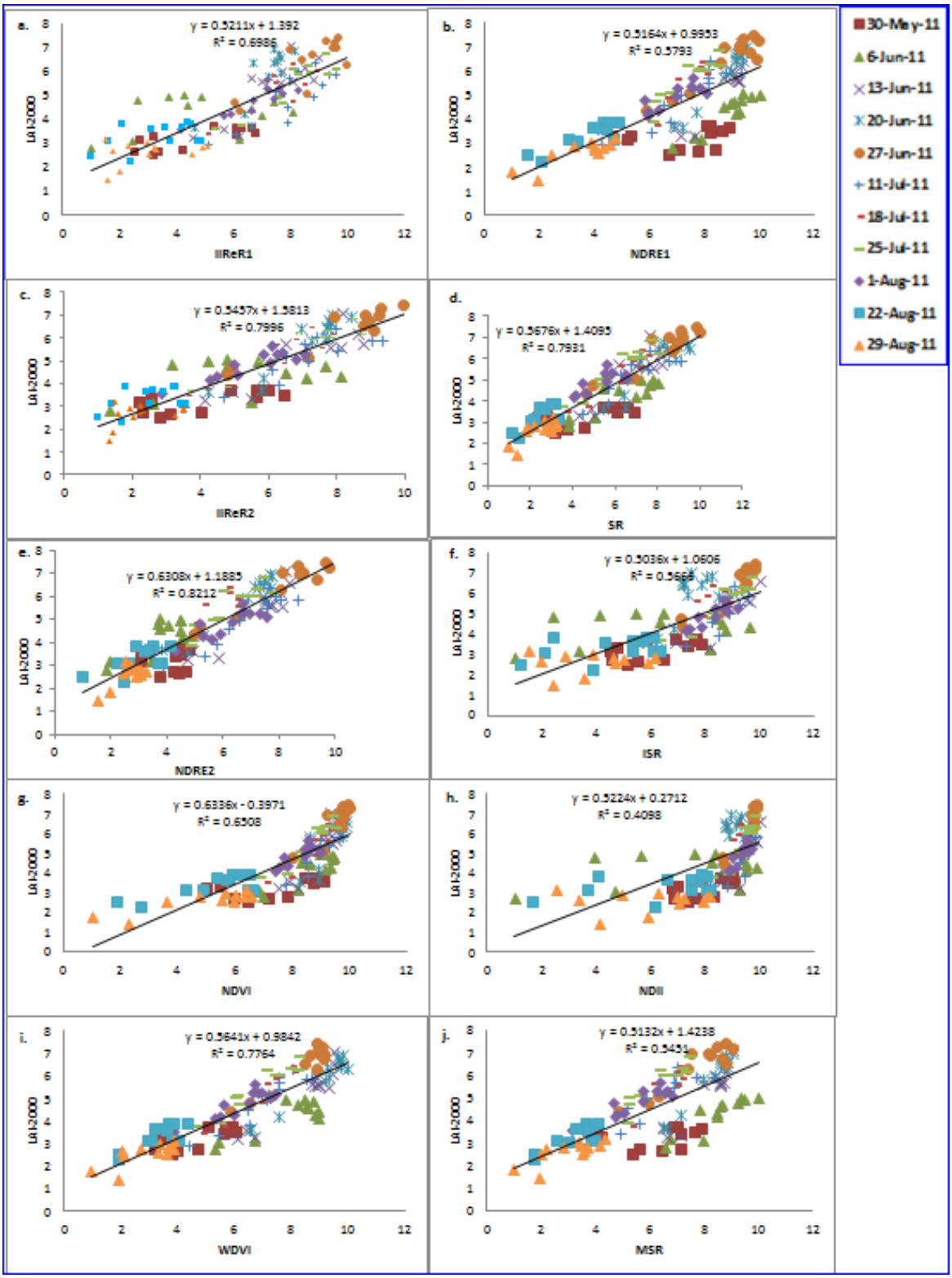

Appendix 10: SVI-LAI Relationships for the 2012 growing season for IIReR1 (a), IIReR2 (b), WDVI (c), NDVI (d), NDII (e), NDRE2 (f), ISR (g), NDRE1 (h), SR (i) and MDR(j). The value ranges for SVIs as already mentioned were normalized to a value range of 1 to 10.

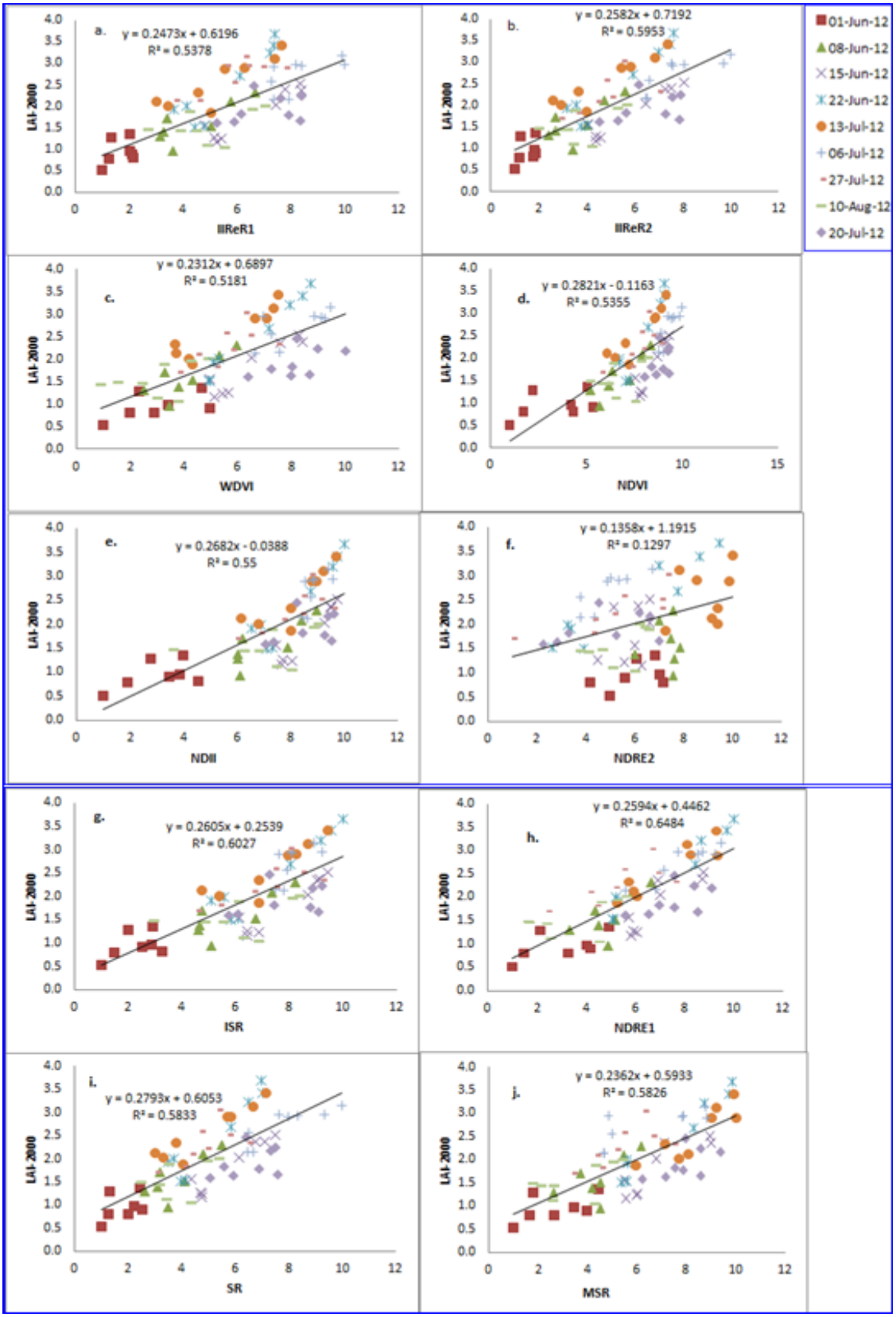

Appendix 11. SVI-LAI relationships based on APEX imagery indicating strong linear relationships for SR(a), WDVI (b), NDRE2 (c), IIReR1(d), NDVI (e), NDRE1 (f), ISR (g), NDII (h) and IIReR1 (i)

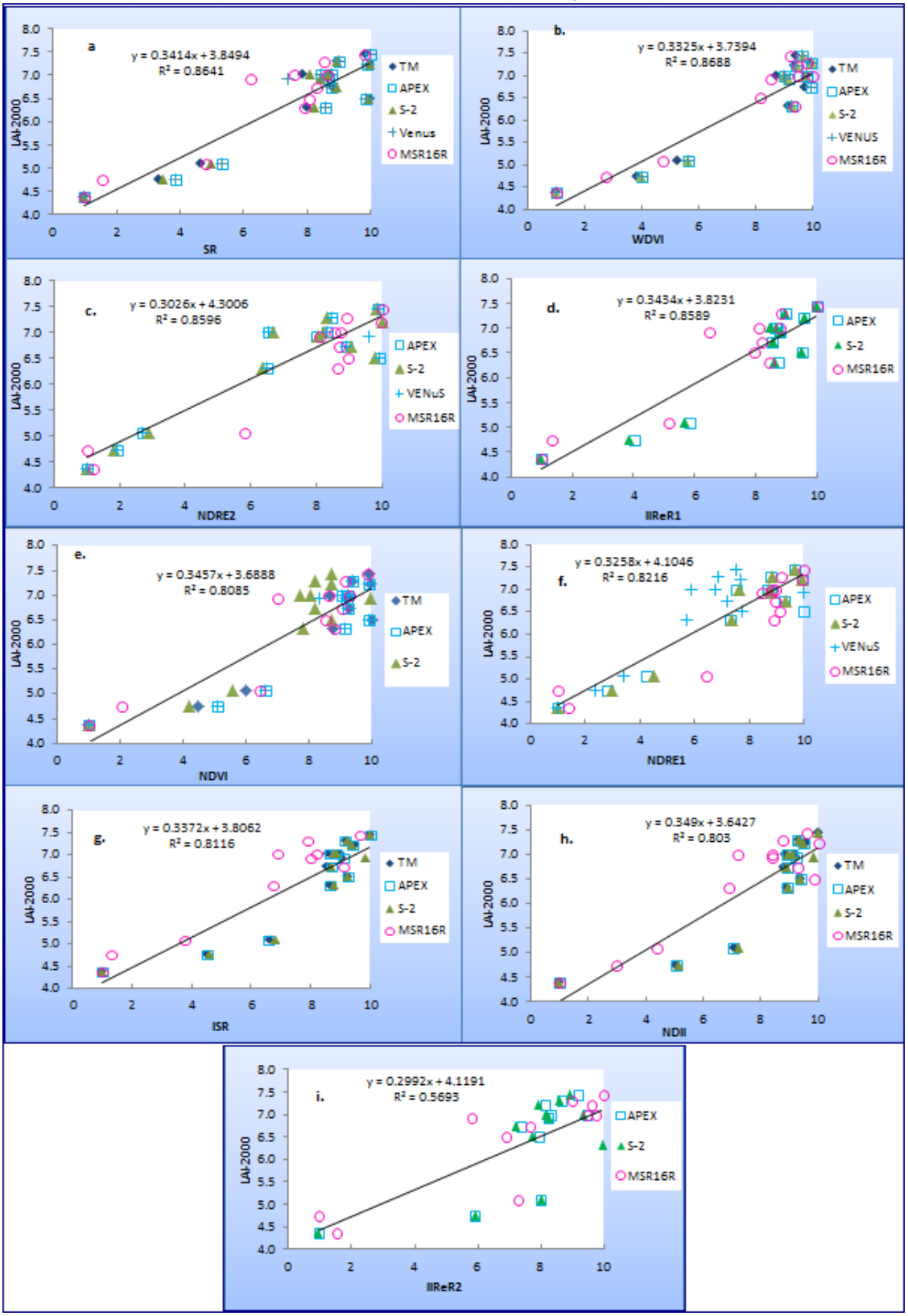

Appendix 12: LAI-Biomass relationships for the 2011 and 2012 sites. The legends indicate the closest (for 2012 site) or exact dates on which both biomass and LAI data were acquired.

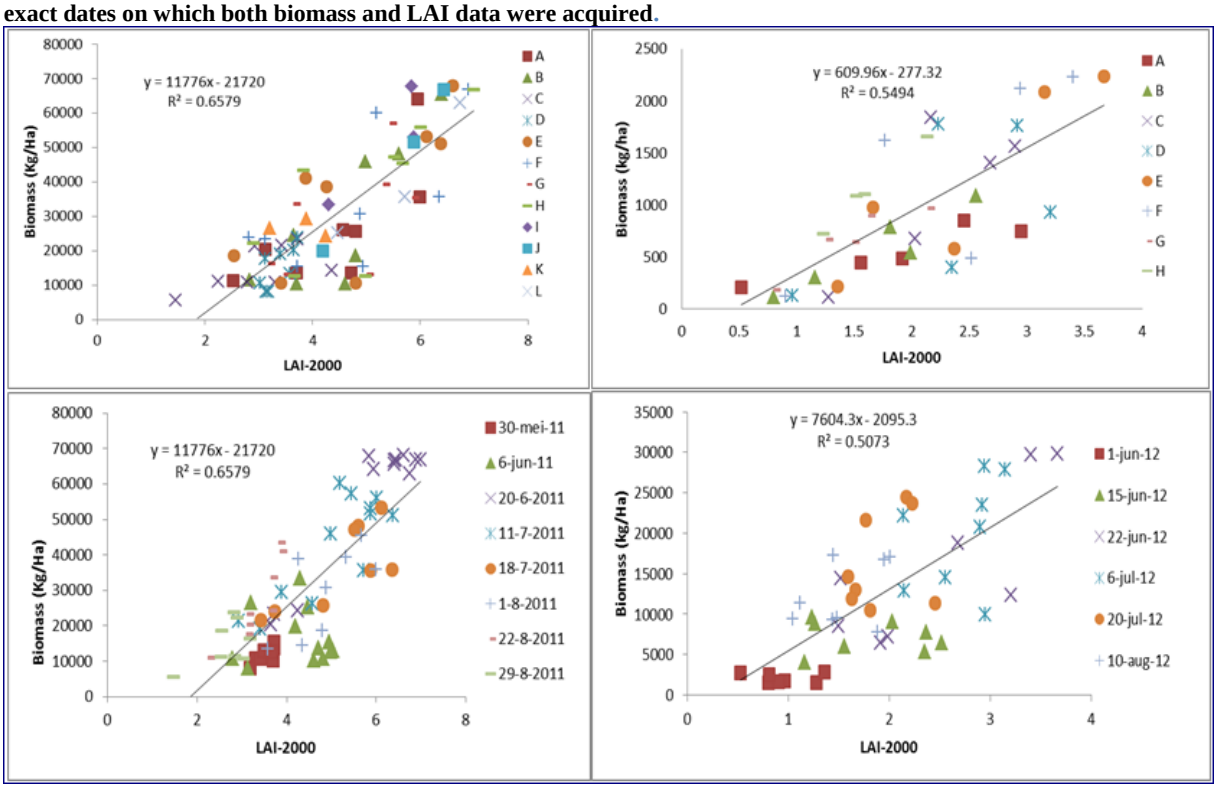

Appendix13. SVI-LAI relationships based 2011 and 2012 sites indicating clearly different patterns corresponding to the differences in the biophysical parameters of the potato crop which was poor in 2012 than in 2011. The point cloud for 2012 is more condensed with small value range compared to the 2011.

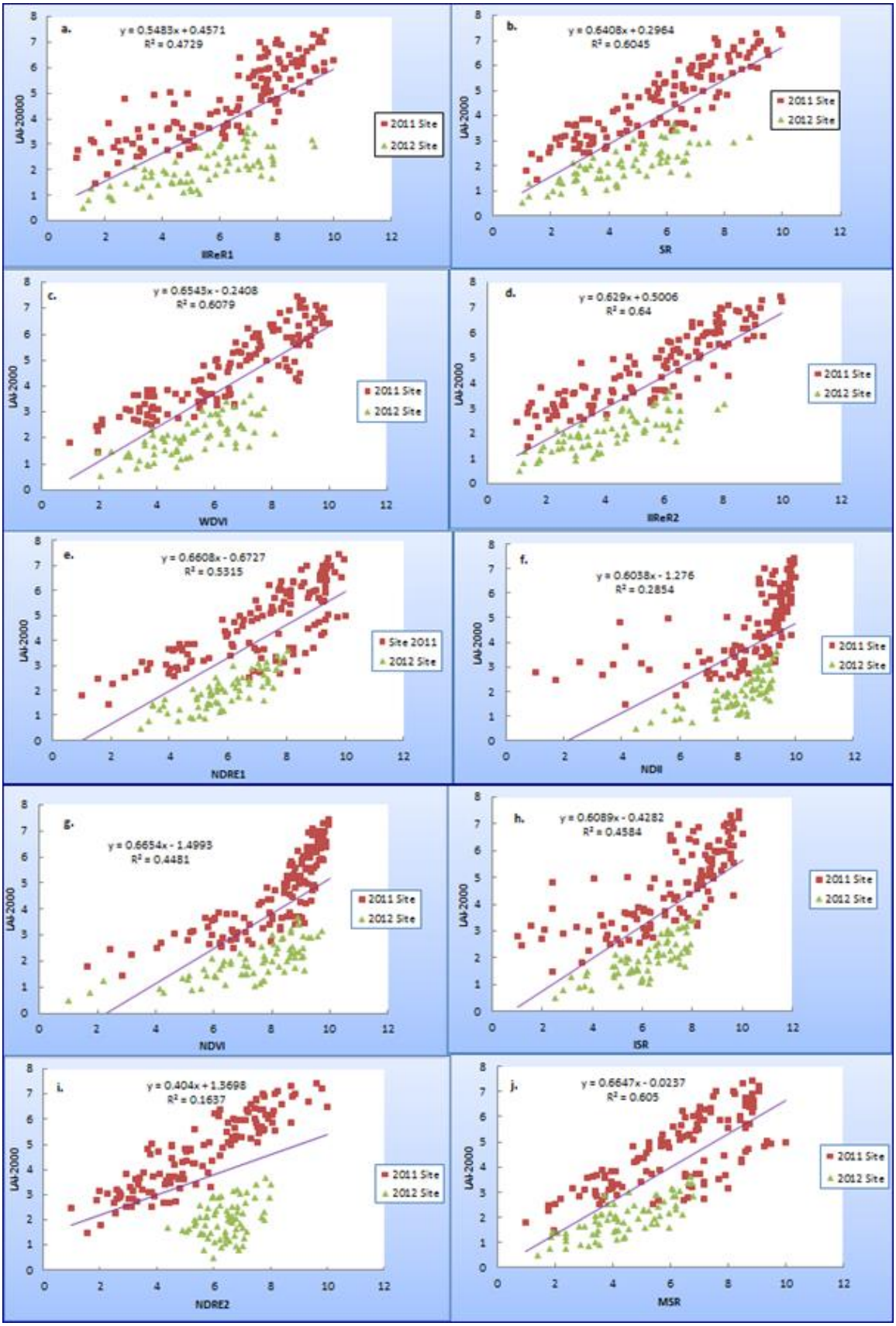

Appendix 14: Results on the validation of SVI-LAI relationships based on 2011 site for IIReR1 (a), SR (b), IIReR2 (c), WDVI (d), NDVI (e), ISR (f), NDII (g), NDRE1 (h), MSR (i) and NDRE2 (j). The legend stands for the date of data acquisition throughout the growing season and is valid for all the graphs.

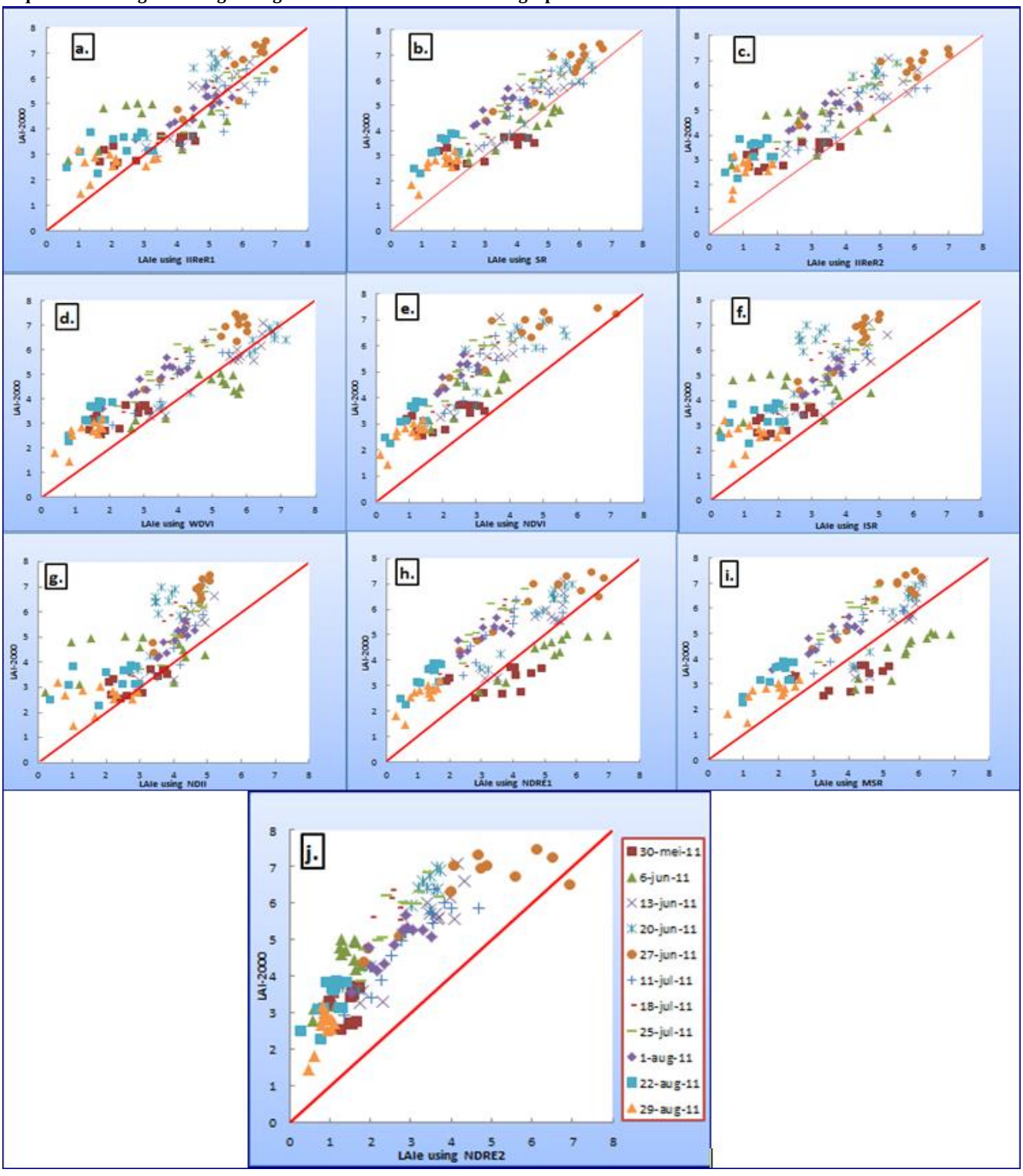

Appendix 15. Results from ANOVA showing significant effect of nitrogen treatment on LAI for 2011 site

a) Results from ANOVA

Source	Type III Sum of Squares	df	Mean Square	F	Sig.
Corrected Model	66.560[a]	3	22.187	13.723	.000
Intercept	2785.402	1	2785.402	1722.868	.000
Initial_N	66.560	3	22.187	13.723	.000
Error	200.474	124	1.617		
Total	3052.435	128			
Corrected Total	267.033	127			

a. R Squared = .249 (Adjusted R Squared = .231)

b) A pair-wise comparison of the effect of different fertilization levels on LAI using the LSD

(I) Initial_N	(J) Initial_N	Mean Difference (I-J)	Std. Error	Sig.	95% Confidence Interval	
					Lower Bound	Upper Bound
0	161	-1.3852*	.31788	.000	-2.0143	-.7560
	242	-1.7290*	.31788	.000	-2.3582	-1.0998
	322	-1.7725*	.31788	.000	-2.4017	-1.1433
161	0	1.3852*	.31788	.000	.7560	2.0143
	242	-.3438	.31788	.282	-.9730	.2853
	322	-.3873	.31788	.225	-1.0165	.2418
242	0	1.7290*	.31788	.000	1.0998	2.3582
	161	.3438	.31788	.282	-.2853	.9730
	322	-.0435	.31788	.891	-.6727	.5857
322	0	1.7725*	.31788	.000	1.1433	2.4017
	161	.3873	.31788	.225	-.2418	1.0165
	242	.0435	.31788	.891	-.5857	.6727

Based on observed means.

The error term is Mean Square(Error) = 1.617.

*. The mean difference is significant at the 0.05 level.

Appendix 16. Results from ANOVA and LSD test for significance of the effect of nitrogen treatment on LAI for 2012 site

a)Results from ANOVA

Source	Type III Sum of Squares	df	Mean Square	F	Sig.
Corrected Model	5.440[a]	3	1.813	3.929	.012
Intercept	278.144	1	278.144	602.616	.000
Treatment	5.440	3	1.813	3.929	.012
Error	30.463	66	.462		
Total	317.671	70			
Corrected Total	35.903	69			

b). A pair-wise comparison of the effect of different fertilization levels on LAI using the LSD

(I) Treatment	(J) Treatment	Mean Difference (I-J)	Std. Error	Sig.	95% Confidence Interval	
					Lower Bound	Upper Bound
0	43	-.1778	.23343	.449	-.6439	.2882
	117	-.5990*	.23343	.013	-1.0651	-.1330
	218	-.6719*	.23343	.005	-1.1380	-.2059
43	0	.1778	.23343	.449	-.2882	.6439
	117	-.4212	.22646	.067	-.8733	.0310
	218	-.4941*	.22646	.033	-.9462	-.0420
117	0	.5990*	.23343	.013	.1330	1.0651
	43	.4212	.22646	.067	-.0310	.8733
	218	-.0729	.22646	.748	-.5251	.3792
218	0	.6719*	.23343	.005	.2059	1.1380
	43	.4941*	.22646	.033	.0420	.9462
	117	.0729	.22646	.748	-.3792	.5251

Based on observed means.

The error term is Mean Square(Error) = .462.

*. The mean difference is significant at the 0.05 level.

Appendix 17. Specifications of the CROPSACAN MSR16R system

Spectral band position (nm)	Band width (nm)
490	7.3
530	8.5
550	9.2
570	9.7
670	11
700	12
710	12
740	13
750	13
780	11
870	12
940	13
950	13
1000	15
1050	15
1650	200

Appendix 18. A correlation of predicted LAI (LAIe) using narrow band sensors with LAIe from Landsat TM (broad band) based on NDVI, NDII, ISR, SR, EVI and WDVI. The correlation is strong for all the indices indicating their consistent performance across sensors.

SVI	MSR16R		APEX		S-2		VENµS	
	R	P-value	R	P-value	R	P-value	R	P-value
NDVI	0.99	0.00	0.99	0.00	0.99	0.00	0.99	0.00
NDII	0.98	0.00	0.99	0.00	1.00	0.00	-	-
ISR	0.98	0.00	0.99	0.00	1.00	0.00	-	-
SR	0.99	0.00	0.99	0.00	0.99	0.00	0.98	0.00
EVI	0.99	0.00	0.99	0.00	0.94	0.00	0.99	0.00
WDVI	0.99	0.00	0.99	0.00	0.99	0.00	0.99	0.00

Appendix 19. LAI Map using IIReR1 based on APEX image. The values indicate the LAI range which is the lowest for those plots with little or no fertilization while those regions with high N fertilizer showed high LAI values demonstrating the suitability of IIReR1 for LAI mapping at image level.